Dissertation

submitted to the

Combined Faculties for the Natural Sciences and for Mathematics

of the Ruperto-Carola University of Heidelberg, Germany

for the degree of

Doctor of Natural Sciences

presented by

Diplom- Biologist Maria Paola Santini

Born in : Rome (Italy)

Oral Examination:

mIGF-1 regulates heart physiology and induces complete regeneration of infarcted myocardial tissue

Referees: Prof. Dr. Werner W. Franke

Prof. Dr. Claus Nerlov

INDEX

ACKNOWLEDGMENTS

I would like to thank all the people who make possible this work.
This work was possible thanks to Nadia who allows me to express my attitudes and my ideas, who teaches me the patience to dial with different people in different environments, and the strength to never give up in the most difficult situations.
All the members of the lab were amazingly stimulating and a great landmark for scientific discussion.
My special gratitude is going to Esfir for her constant and precise help with mice colony management and for her patience to dial with an impatient person like me.
My gratitude is going to Nadine who was always ready during these years to share with me the bad and the good of this job and of life.

All this work and whatever I did and I will do in future is dedicated to my family that helped me to stand again when I fell.

PART I

INTRODUCTION

ZUSASMMENFASSUNG

Das Säugetier Herz reagiert besonders empfindlich auf traumatische Verletzungen oder andauernde Herz-Kreislaufkrankheiten. Narbenbildung und Schwächung des Gewebes führt zu einem Verlust der kontraktilen Funktion des Herzens und damit zu einer Verschlechterung des Gesundheitszustandes insgesamt. Der Versuch Herzverletzungen oder Schädigungen vorzubeugen oder die verheerenden Folgen derselben zu beheben waren bisher wenig erfolgreich, was unter anderem auf die begrenzten regenerativen Fähigkeit des Herzens zurückzuführen ist.

In der vorliegenden Arbeit wurde die regenerierende Fähigkeit einer lokal agierenden Isoform des Insulin-ähnlichen Wachstumsfaktors-I (mIGF-1) auf verletztes Herzmuskelgewebe untersucht, indem die Expression des mIGF-1 Transgens auf das Myocardium des Mausherzens beschränkt wurde. Durch die Herz-spezifische Expression des Transgens können endokrine Effekte auf andere Organe ausgeschlossen werden.

Die Herzen, die das Transgen tragen zeigten beschleunigtes postnatales Wachstum, wobei die Größe des Herzens nicht über die Normalgröße von erwachsenen Wildtyp-Herzen hinausging.

Das frühe hypertrophe Wachstum der transgenen Herzen wurde begleitet von einer kurzzeitigen Aktivierung von MAP-Kinasen, einer erhöhten Funktion der translationalen Maschinerie und einer moderaten Erhöhung von Hypertrophie Markern, wobei die Herzfunktion unverändert war. Es ist hervorzuheben, dass Akt, einer der Haupteffektoren von IGF-1, nicht aktiv war, was darauf hindeutet, dass eine andere Kinase als Effektor von IGF-1 agiert.

Die Fähigkeit von IGF-1 die Regeneration des Mausherzens zu stimulieren, wurde auf zwei Wegen untersucht. Wir nutzen LAD-Ligation oder direkte Injektionen von Cardiotoxin (CTX) in das linke Ventrikel von erwachsenen Mäusen, um eine Verletzung des Herzgewebes herbeizuführen. Die Verletzung von Wildtyp und transgenen Mäusen war reproduzierbar und führte zu lokalen Infarkten, verbunden mit frühem Zelltod und ausgeprägter Entzündung der betroffenen Bereiche. Im Gegensatz zu der charakteristischen Narbenformierung in Wildtyp Herzen, fanden wir, dass mIGF-1 in den transgenen Herzen innerhalb eines Monats eine komplette Wiederherstellung des verletzten Gewebes herbeiführte, ohne Narben zu bilden.

Die Regenerierung des Gewebes ging einher mit einer ausgeprägten Erniedrigung von Entzündungsstimulierenden Zytokinen und einer Erhöhung von Entzündungshemmenden Zytokinen. Diese Ergebnisse deuten darauf hin, dass mIGF-1 seine regenerierende Funktion teilweise durch Modulierung des Entzündungsprozesses ausübt. Die transgenen Herzen zeigte ausserdem erhöhte proliferative Aktivität in Infarktnähe und konnten die normale Herztätigkeit wieder herstellen.

Durch die Wiederherstellung des Herzgewebes nach einer Verletzung, scheint mIGF-1 die evolutionären Einschränkungen der Regenerierung von Säugetier Herzen zu umgehen.

Die Verbesserung kardialer Regeneration durch die lokale Expression dieses Wachstumsfaktors verspricht neue klinische und therapeutische Strategien zur Eindämmung von Entzündungsreaktionen und Wiederherstellung von verletztem Herzgewebe.

ABSTRACT

The mammalian heart is particularly susceptible to traumatic injury or sustained disease, suffering tissue deterioration, scarring and loss of contractile function. Clinical interventions to prevent or reverse the devastating effects of cardiac damage have met with limited success, presumably due to restricted cardiac regenerative potential. We tested the ability of a locally acting mIGF-1 isoform to regenerate the injured heart, restricting expression of a mIGF-1 transgene to the mouse myocardium to exclude endocrine effects on other tissues. Transgenic mIGF-1 hearts displayed accelerated postnatal cardiac growth that never exceeded the wild-type adult cardiac size. Early remodelling of the transgenic hearts was accompanied by transient activation of MAPKs and increased function of the translational machinery, without perturbing cardiac performance, and by modest upregulation of hypertrophic markers at one and two months. Notably, AKT the downstream effector of IGF-1 signalling was not activated in the hearts of transgenic mIGF-1 animals, indicating that a different kinase regulates mIGF-1 downstream signalling in the heart.

The regenerative capacity of mIGF-1 was analyzed either by LAD ligation or by direct cardiotoxin (CTX) injection into the ventricles of adult mice. Injury to both wild-type and transgenic mIGF-1 hearts produced reproducible and localized infarctions coupled with early cell death and marked inflammation. In contrast to the characteristic progression of scar formation in wild-type hearts, transgenic mIGF-1 hearts induced complete repair of the injured tissue after 1 month, without scar formation. mIGF-1-induced regeneration was associated with a marked decrease in pro-inflammatory cytokines and an increase in anti-inflammatory cytokines, indicating that mIGF-1 drives regeneration in part by modulating the inflammatory response in pathological conditions. At later stages, mIGF-1 transgenic hearts displayed increased proliferative activity proximal to the infarct, and restored cardiac functionality. By enabling myocardial reconstruction following injury, the mIGF-1 isoform appears to bypass the evolutionary restrictions on mammalian regeneration. The enhancement of cardiac regeneration by localized expression of this growth factor suggests novel and clinically feasible therapeutic strategies to decrease inflammation and increase cell replacement after tissue damage.

PROJECT AIMS

Two important aspects prompted us to investigate IGF-1 signalling in the heart: the regenerative properties of IGF-1, and the complete absence of a regenerative program in most of the adult tissues, such as the myocardium. Our principle aim was to analyze whether overexpression of IGF-1 in the heart could overcome the barrier of tissue deterioration, normally occurring in case of extended injury, and restore heart functionality following severe damage.

The regenerative properties of the mIGF-1 isoform have been previously documented in skeletal muscle. In regenerating transgenic mouse muscle, overexpression of the mIGF-1 isoform under a muscle-specific promoter, enhanced myogenic progenitors, maintaining tissue integrity during exercise and aging, countered muscle decline in degenerative disease and cachexia, and promoted healing following injury (*1, 2*). These results define a mechanism, enhanced at every level by supplementary mIGF-1, whereby injury stimulates local regenerative signals to rebuild damaged tissue.

Empirically, complete regeneration of complex organs in mammals is characteristically precluded by inadequate tissue replacement and fibrotic reactions, leading to scar formation. The mammalian heart is particularly susceptible to traumatic injury or sustained disease, suffering irreversible tissue deterioration, scarring and loss of contractile function. Although cell hypertrophy can increase cardiac mass in response to stress, organ function is compromised by tissue loss during myocardial infarction and ischemia-reperfusion. Interventions to prevent or reverse the devastating effects of human heart attacks have met with limited success, presumably due to the restricted regenerative potential of the heart.

Based on these considerations and the data mentioned above, we tested the ability of the locally acting IGF-1 isoform, mIGF-1, to regenerate the injured heart. We generated transgenic mice with a rat mIGF-1 cDNA driven by the mouse cardiac myosin heavy chain (α-MHC) promoter to restrict expression of mIGF-1 to the mouse myocardium. Our analysis addressed the physiological and the pathological features of mIGF-1 overexpression.

- In physiological conditions, postnatal transgenic mIGF-1 hearts displayed accelerated cardiomyocyte hypertrophy, precociously attaining wild-type adult heart size. We found a significant increase in the size of cardiomyocytes in transgenic hearts compared to wild-type hearts, induction of the hypertrophic marker ANP and a sustained activation of the translational machinery, mediated through PDK1 signaling. Measurement of cardiac function by echocardiography and electrocardiography showed that mIGF-1 induced a transient 20% concentric left ventricular hypertrophy, and a mild impairment in systolic and diastolic components of cardiac function. Transgenic mIGF-1 did not otherwise affect cardiac output and blood pressure, which were maintained at normal levels.
- The regenerative capacity of mIGF-1 was analysed by direct cardiotoxin (CTX) injection into the ventricles of four months old mice. CTX injection in both wild-type and transgenic mIGF-1 hearts produced a reproducible, titratable and localized infarction with evident cell death and marked inflammation. In contrast to the characteristic progression of scar formation in wild-type hearts, transgenic mIGF-1 induced repair of the injured tissue after one month, without scar formation. Down-regulation of specific inflammatory cytokines suggests that mGF-1 improves cardiac regeneration in part by modulation of the inflammatory response. Moreover, transgenic mIGF-1 hearts contained dramatically increased numbers of proliferative cells in the area of damage after one month, suggesting that the regeneration program, following an earlier survival/repair program, is activated as a later step in response to mIGF-1. Cardiac functionality, measured by echocardiography, showed normal cardiac parameters and restoration of the posterior wall thickness and contractility.

Our results need further analyses to cover the intracellular signaling activated by mIGF-1 and to exhaustively explain the remarkable regenerating capacity of this isoform, but the study clearly demonstrated that tissue-specific supplementary mIGF-1 expression is an effective and potentially powerful approach to counter a number of prevalent and life-threatening cardiovascular pathologies. Our data further suggest that the enhancement of cardiac regeneration by localized expression of this growth factor can be the basis for novel and clinically feasible therapeutic strategies to decrease inflammation and increase cell replacement after tissue damage.

THESIS ORGANIZATION

A helpful guide throughout the thesis is meant to connect the different parts of this work. I divided the thesis in two parts. The first part contains the Introduction, while the second part describes Materials and Methods, Results and Discussion.

Part I:

The Introduction consists of three different Chapters. Each Chapter analyzes in details the most important findings in the field of heart development, IGF-1 and regeneration. Chapter I covers the past and recent discoveries of pre- and post-natal heart development; Chapter II is entirely dedicated to IGF-1 gene structure and tissue specific function, and Chapter III analyzes the major aspects of tissue and organ regeneration. In the latter two Chapters, the most important discoveries that connect IGF-1 signaling and regeneration are discussed with particular reference to the heart.

Part II:

Chapter IV contains Materials and Methods, Chapter V describes Results and Chapter VII the discussion. The last chapter (Chapter VII) will be dedicated to the future aims of this work that are inspired by a group of results that need to be further analyzed, but that open an interesting window on mIGF-1-induced recruitment of stem cells. We think that contributions of stem cells may be important for complete regeneration of an injured tissue and that mIGF-1 plays multiple role in regulating survival and proliferation, not only of most known components of the heart, such as cardiomyocytes and endothelial cells, but also of a possible cardiac or circulating progenitor cell pool.

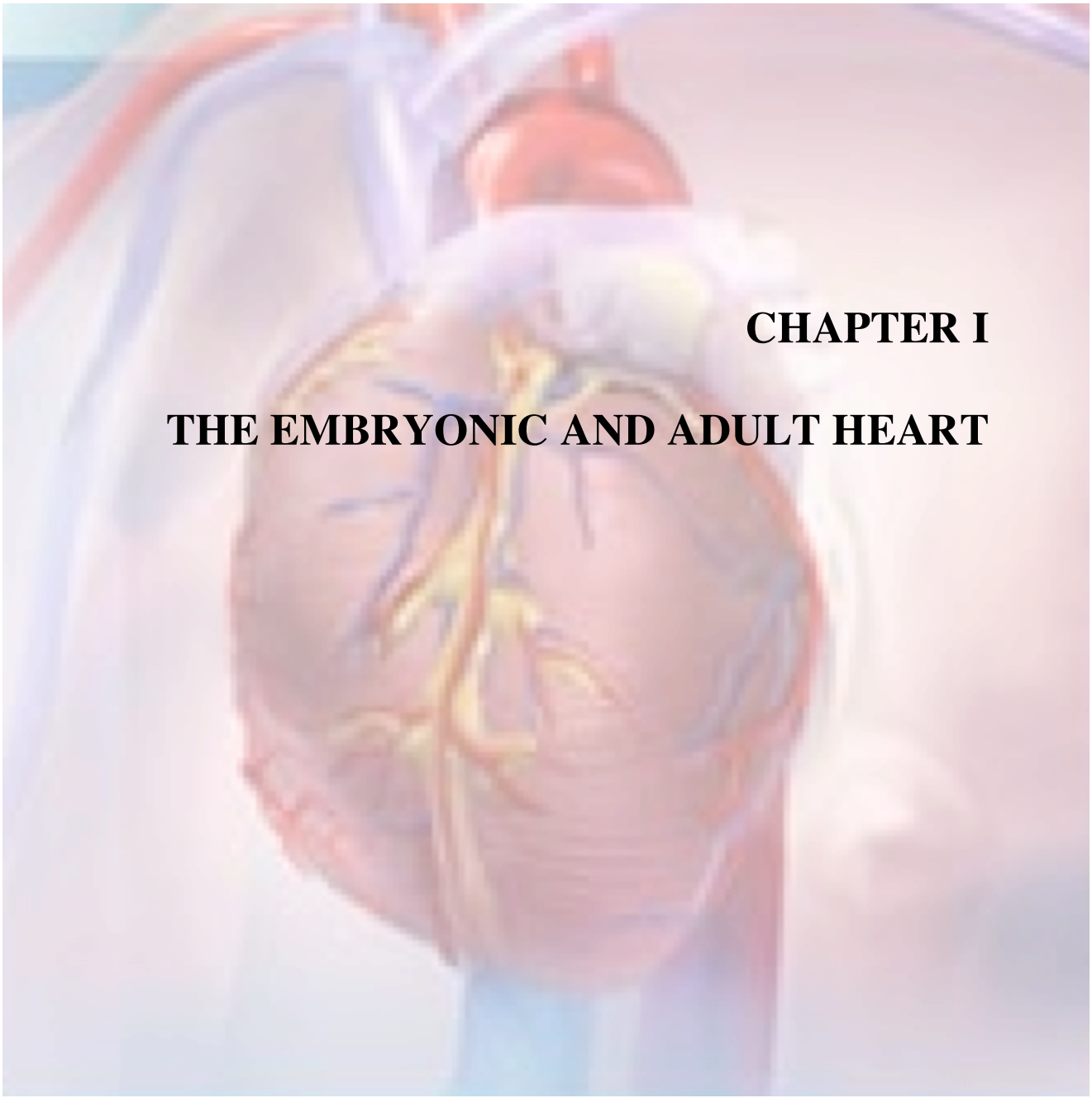

CHAPTER I

THE EMBRYONIC AND ADULT HEART

1. HEART FORMATION AND SPECIFICATION

The heart is one of the first structures to form during organogenesis (*3, 4*). It is initially established as a single tube consisting of two epithelial layers: the inner endocardium and outer myocardium (*5*). The primitive tubular heart partitions further into two chambers, atrial and ventricular, confined by atrioventricular septa. Myocardial contractions begin during this double-walled stage of heart formation. Initial pulsations are generated at the right myocardium and spread posteriorly to anteriorly over the whole myocardium. Except for the pacemaker cells, the cardiac conduction system has not yet developed at this stage. The two-chambered heart is the mature form in the primitive vertebrates such as fish. In contrast, the heart of higher vertebrates further undergoes a series of morphogenetic steps: looping, septation, which generates the four compartments characteristic of the adult heart, trabeculation and thickening of the ventricular walls, and the cranial shift of the atrial chambers that assume their adult position rostrodorsal to the ventricles (Figure 1.1). The survival of the thickened ventricular myocardium relies on the coronary vessel system.

The initiation of cardiac differentiation has been the topic of vigorous investigation (*6, 7*). The heart precursors are localized together with the cranial mesoderm in the embryonic mesoderm domain. Further lineage analysis of the embryonic cardiac precursor cells has shown that descendants of this population contribute predominantly to the myocardium and to a lesser extent to the endocardium and to the pericardium (*8*). Transplantation experiments were not sufficient to reveal whether cardiac lineages share a common progenitor. Nevertheless, it has been suggested that in zebrafish blastula, the endocardium and the myocardium may be derived from common progenitors, and that these two lineages may segregate later during development (*9, 10*). Although no single transcription factor that is responsible for the differentiation of lateral plate mesoderm into cardiac cells has been identified, the localization of the heart precursors in the mesoderm of 7.0- to 7.5-day mouse embryos coincides with the distribution of the transcripts of the endothelial-specific *GATA4* and *Flt1* genes (*11, 12*), and the *Nkx2-5* gene, which is expressed in the precursors of the myocardium (*13*). The following sections describe the remodelling of the embryo heart and the intracellular and extracellular signalling involved.

1.1. INTRACELLULAR SIGNALING

1.1.1 Cardiogenesis and cardiac differentiation

The GATA family of zinc-finger containing transcription factors appears to be potentially critical for differentiation of precardiac cells. Three GATA family genes have been identified as being expressed in the developing heart: *gata4, gata5 and gata6* (*14*). GATA factor function has been well conserved throughout evolution: in *Drosophila* the *gata4* homologue *pannier* is required for normal proliferation of cardiogenic precursors (*15*), and in *zebrafish* the *faust* mutation, which results in cardia bifida and impaired cardiac differentiation, lies in the *GATA5* gene (*16*). Gene deletion of GATA factors in the mouse has not been as informative as one would predict, due either to the role of GATAs outside the heart field in early embryogenesis, or to genetic redundancy (*17-20*). The early endodermal defect in *gata*4 knockouts and the peri-implantation lethality of *gata6* knockouts preclude the analysis of this GATA factors in further steps of myocardial differentiation. *In vitro* studies showed that in P19 embryonal carcinoma cell lines induced to differentiate in cardiac cells, *gata4* and *gata6* antisense oligonucleotides cause an arrest in cardiac differentiation and apoptotic death (*21, 22*). Moreover, the potential of *gata4*-null embryonic stem cells to undergo cardiac differentiation is reduced (*23*).

Much excitement was generated by the discovery of the *tinman* gene in *Drosophila*, which is required, although not sufficient, for the generation of cardiac cells (*24*). The *tinman* gene encodes a NK-class homeodomain-containing transcription factor, homologue to the vertebrate gene *Nkx2-5*. This gene is a predominantly cardiac gene. Generation of mice lacking *Nkx2-5* results in a poorly developed myocardium, characterized by the inability of this primitive cardiac structure to grow beyond the earliest stages of heart looping (*25-27*). In mice *Nkx2-5* is required for the establishment and maintenance of a ventricular gene expression program (*25, 26*). Other NK-class transcription factors have been identified, such as Nkx2-3 and Nkx2-6, but genetic ablation studies indicate no discernable role in cardiac development (*28, 29*).

Myocardin is a specific cardiac transcription factor important for the early differentiation of cardiac cells (*30*). Powerful *in vitro* activation of several cardiac

gene promoters via serum response factor (SRF)-binding sites has been identified as a major function of myocardin. Experiments in frog embryos using a dominant-negative myocardin molecule indicate that it may be necessary for high level expression of *Nkx2-5* (*30*). Although the importance of this molecule is undisputed, the role of myocardin *in vivo* remains to be defined.

1.1.2 Migration of cardiac precursors

GATA is involved in the movement of the paired progenitor pools that coalesce to form the linear heart tube. In this regard, it has been shown that GATA4 in the mouse and GATA5 in zebrafish are primarily controlling normal formation of the endoderm underlying the myocardial precursors (*16, 18, 19*). If the function of GAT4/5 is reduced, endodermal cells do not normally differentiate, their ventral migration is inhibited, and this prevents the concomitant movement of myocardial cells with consequent generation of cardia bifida (*16, 18, 19*).

The basic helix-loop-helix (bHLH) transcription factor MesP1 has been shown to be required for an earlier step in the migration of cardiac precursors. In the absence of MesP1, mesodermal cells, fated to become cardiac myocytes, fail to migrate normally out of the primitive streak during gastrulation, resulting in complete or partial cardia bifida (*31*). Mice lacking *MesP1* and its related gene *MesP2* have a complete block in migration of the mesoderm from the primitive streak, resulting in the lack of cardiac and other mesodermal derivatives (*32*). Interestingly, double knockouts for *MesP1*/*MesP2* reveal a specific cell autonomous role for these transcription factors in ventricular, but not atrial, formation. This analysis argues for a distinct lineage difference between atrial and ventricular precursors (*33, 34*).

1.1.3 Regulation of chamber morphogenesis and chamber-specific gene expression

Although individual cardiac chambers do not become morphologically distinguishable until after cardiac looping, their cell fates seem to be genetically programmed much earlier. The linear heart tube is segmentally patterned along the anterior posterior axis into precursors of the aortic sac, outflow tract (conotruncus), ventricles and atria (Figure 1.2). Each cardiac chamber differs in its morphological and contractile properties and its pattern of gene expression.

Few regulators of chamber-specific gene expression have been identified to date. *Iroquois homeobox gene 4* (*Irx4*) is a member of the *Iroquois* family of homeodomain-containing transcription factor genes, which have been implicated in patterning events in *Drosophila*. Expression of *Irx4* is restricted at all stages of development to the ventricular myocardium in all species examined (*25, 35, 36*) . Irx4 expression is reduced in mice lacking *Nkx2-5* or *dHand*, in which ventricular differentiation is compromised, suggesting that Nkx2-5 and dHand specifically regulate *Irx4* (*25*). Experiments in avian embryos have demonstrated that Irx4 is involved in positive and negative regulation of chamber-specific *myosin heavy chain* gene expression in the ventricular myocardium. Mice with targeted disruption of *Irx4* have only a disturbance of ventricle-specific gene expression, including decreased *eHand* expression in the embryonic heart, and *atrial natriuretic factor (ANF)* derepression in the ventricle after birth, leading to impaired cardiac function and further cardiomyopathy (*37*). The expression of additional *Irx* genes in the developing heart suggests the possibility of genetic redundancy. Interestingly, it has been found that Irx4 controls the expression of atrium-specific *slow myosin heavy chain 3* (*SmyHC3*) gene in the ventricle (*35, 38*). Irx4 does not bind directly to *SmyHC3* promoter elements required for ventricular repression, but may interact with the retinoic acid receptor/vitamin D receptor (RAR/VDR) complex of proteins (*38*). Another factor involved in the regulation of chamber specific gene expression is *Hey2*. It is a ventricle-specific transcription factor related to the Hairy family of bHLH transcription factors (*39-41*) . Mice lacking *Hey2* do not have aortic coarctation and develop a severe postnatal cardiomyopathy (*42*) .

Chamber morphogenesis is controlled in part by *dHand* and *eHand* genes, which are expressed in the right ventricle (RV) and in the left ventricle (LV) respectively. In mammals both *Hand* genes appear to be required for normal growth of the developing myocardium of the chamber in which they are restricted (*43-48*) . The role of *eHand* in the LV development is not clear, due to early embryonic lethality caused by extra-embryonic defects (*46, 47*). Interestingly, the RV and the outflow tract are initially formed in *dHand*-null embryos, but subsequently the RV precursors undergo dramatic apoptosis, impairing the expansion of this segment and resulting in the absence of the RV (*49*) .

Another factor determining the chamber morphogenesis is *Tbx5*. *Tbx5* is expressed initially throughout the cardiac mesoderm in the earliest stages, but its expression pattern is rapidly refined to a posterior-anterior gradient in the linear heart tube, until mid gestation, when it is restricted to the atria and LV. *Tbx5* levels decrease in the LV during subsequent stages of development (*50, 51*). Lack of *Tbx5* results in severely hypoplastic atria and LV, with RV and outflow tract growth remaining intact (*52*). Expression of *Irx4* and *Hey2* decreases in the Tbx5 deficient embryos, and overall ventricular differentiation is impaired. In lower verterbrates, such as frogs and fish, *Tbx5* as well as *Hand* genes are expressed throughout the single ventricle and appear to be involved in the morphogenesis of the entire heart (*53, 54*). This implies that in higher vertebrates, with the addition of the pulmonary circulation and the acquisition of the RV chamber, duplication and specialization of these two genes occurred to regulate chamber-specific morphogenesis. This was presumably accompanied by restricted expression of *Tbx5* and *Hands* to specific segments of the developing heart.

An unexpected role for MEF2C transcription factor in ventricular growth has been elucidated from the generation of mice with disrupted *Mef2c* genes, in which cardiogenesis is initiated, but in which the segments of the heart corresponding to both RV and LV are severely hypoplastic. However, ventricle-specific gene expression appears normal in *Mef2c*-/- embryos (*55*).

Considerably less is known about the genetics of atrial development. The orphan nuclear receptor COUP-TFII is expressed in atrial precursors and is required for atrial, but not ventricular, growth (*56*). A major player in establishing atrial identity is the transcription factor Pitx2. Mice lacking *Pitx2* have a single right atrium with abnormal connection of veneae cavae and pulmonary veins (*57-60*).

1.1.4 Chamber Maturation and Septation

Maturation of the heart into fully functional trabeculated chambers, and septation of the atria and the ventricles from one another and between their left and right sides, are important processes that require precise integration of growth and differentiation signals. Defects in this processes account for the majority of congenital heart

malformations in humans, including atrial and ventricular septal defects (ASDs and VSDs respectively), tetralogy of Fallot (TOF), common atrio-ventricula canal, and double-outlet right ventricle. Genetic analysis of inherited cardiac septation defects has shown that mutations, conferring sustained function or depleted function in Nkx2-5 and Tbx5, are the major factor in septal morphogenesis. One example is the Holt-Oram syndrome, which is characterized by a spectrum of cardiac defects including hypoplastic left ventricle, atrial septal and ventricular septal defects (*52*). The cardiac defects occurring in this syndrome resemble those caused by *Nkx2-5* mutations and it is thought that haploinsufficiency of *Tbx5* is the cause of the syndrome (*61-64*).

The multi-type zinc finger transcription factor FOG-2 has been implicated in cardiac septation. FOG 2 is similar to the *Drosophila* U-shaped proteins, which function as positive or negative regulators of transcription via interaction with GATA proteins (*65*). In *Drosophila* U-shaped proteins negatively regulate cardiac cell numbers, and repress a cardiac-specific promoter regulated by tinman and pannier (*65*). Surprisingly, deletion of FOG2 in mice does not lead to increased cardiac proliferation, but instead to ventricular and atrio-septal defects, accompanied by a general failure of coronary vessel formation (*66*).

The transcription enhancer factor-1, TEF-1, regulates Troponin C and alpha skeletal actin genes in cardiac myocytes (*67*). A retroviral gene trap insertion into the mouse TEF1 gene resulted in embryonic lethality, in part due to defects in trabeculation and thinned ventricular myocardium (*68*). Although it has not yet been determined which are the genes regulated by TEF-1, it is intriguing to note that mice deficient in the protoncogene transcription factor N-myc also have identical defects (*69*).

1.1.5 Downstream targets

A major gap in our knowledge is the identification of specific targets of transcription factors, as well as the physical interactions in signalling that are responsible for the formation and specification of the heart. *ANF* and *connexin 40* (*cx40*) have been identified as *bona fide* targets of Nkx2-5 and Tbx5 (*27, 52*). Tbx5 regulates in dose-dependent ANF promoter activation *in vivo* and *in vitro* (*52, 70*), as well as Cx40 promoter, by occupancy of multiple sites (*52*). A 50% decrease in Tbx5 expression

leads to complete elimination of *cx40* and *ANF* transcription in the mouse heart (*52*). Nkx2-5 plays an important role in the regulation of both promoters, but less critical than that of Tbx5. In fact, a complete lack of Nkx2-5 causes only a partial decrease in *ANF* expression *in vivo* (*27*).

The *cardiac ankryn repeat protein* (*CARP*) and *Pitx2* genes have also been identified as *bona fide* targets of Nkx2-5 (*71, 72*). GATA 4 and other GATA factors have been shown to be potentially important for the regulation of multiple cardiac genes, such as *ANF*, several contractile genes, *gata6*, *Nkx2-5* and *dHand* (*14, 73*). Embryonic cardiac expression of the *SM22α* and *α-skeletal actin* genes is regulated *in vivo* under the control of CarG boxes, which are bound by SRF and probably by myocardin (*74, 75*). It is interesting to note that SRF-binding sites, as well as MEF2-binding sites, are required for muscle-specific expression rather than cardiac specific expression; it is possible that GATA4, Nkx2-5, or myocardin must be required to specify cardiac regulation in the developing heart (*42*).

A more complicated aspect of cardiac specification has been revealed by the identification of multiple physical interactions between factors on DNA regulatory elements. Nkx2-5 physically interacts with Tbx5 and GATA4 to synergistically activate transcriptional target genes (*52, 70, 76*). GATA4 can also interact with FOG-2 to activate or repress transcription of GATA-dependent targets (*65*). Mice with GATA4 mutation, designed to abolish GATA-FOG interactions, have phenotypes similar to those found in FOG-2 deficient mice (*66, 77*). It is important to underline that the GATA4 missense mutations lead to impaired outflow tract septation, resulting in mice with double-outlet right ventricle, a phenotype not present in FOG-2 deficient mice. This suggests that other factors bind to GATA4 at this site (*66, 77*). Finally, although a direct *in vivo* interaction between Nkx2-5 and dHand was not shown, mice deficient for both proteins do not form a ventricle and have abolished *Irx4* expression (*49*).

From this survey it is clear that although the identities of crucial regulators defining cardiogenesis has been uncovered, it is still unknown which transcription factors are involved in the earliest differentiation of cardiac cells from the mesoderm. Moreover,

the downstream pathaways regulated by transcription factors responsible for key morphogenetic events are still unknown. It also remains to be addressed whether protein functions are maintained or inactivated through posttranslational modification during development.

1.1.6 The secondary heart field

Several lines of evidence have led to a surprising shift in the established paradigm regarding the origin of cardiac myocytes. It is now recognized that a second population of cardiac precursors migrates into the outflow region of the looped heart, providing mature cardiomyocytes that contribute to the right ventricle, and probably to the atria and left ventricle as well (*78-81*). Marking experiments *in ovo* suggest that the atrioventricular canal, atria and conotruncus are added secondarily to the straight heart tube during looping (*81*). The heart tube elongates during looping, concomitant with accretion of new myocardium. The atria are added progressively from the caudal primary heart fields bilaterally, while the myocardium of the conotruncus is elongated from a midline secondary heart field of splanchnic mesoderm, beneath the floor of the foregut. This population of cells is called secondary heart field or anteroior heart field. As the cells in the secondary heart field begin to move into the outflow or inflow myocardium, distinguishable later as the outflow and inflow tract of the forming heart, they express HNK-1 initially and then MF-20, a marker for myosin heavy chain. FGF-8 and BMP-2 are present in the ventral pharynx and secondary heart field/outflow myocardium respectively, and appear to effect induction of the cells in a manner that mimics induction of the primary myocardium. Neither FGF-8 nor BMP-2 is present when the inflow myocardium is added from the primary heart fields. Precursors of this heart field probably arise close to the cardiac crescent, where primary heart field cells also arise, and subsequently migrate to the anterior pharynx, contributing later to the heart. Secondary heart field myoblasts express many of the same cardiac markers as those previously analyzed in the primary heart field, including Nkx2-5 and GATA4, but they remain undifferentiated until later in development. The addition of a secondary myocardium to the primary heart tube provides a new framework for understanding several null mutations in mice that cause defective heart development.

1.2 EXTRACELLULAR SIGNALING

1.2.1 Specification of cardiac cell fate by extracellular cues

Two families of peptide growth factors have been studied most extensively for their positive and negative effects on the establishment of cardiac cell identity: Bone Morphogenetic Proteins (BMPs) and Wnt proteins. BMPs are a subset of the transforming growth factor-β (TGFβ) superfamily, shown to promote cardiogenesis in vertebrate embryos (*82*). Equivalent effects have been shown also in *Xenopus* and avian embryos explants, using soluble inhibitors of the BMP ligand-receptor interaction such as noggin (*83*), and dominant –negative BMP receptors (*84*). In mice, mutations of certain BMPs or of any BMP receptor are lethal at gastrulation, obscuring the potential role of BMPs in cardiogenic specification. Notably, epiblast-specific deletion of the type IA BMP receptor is permissive for gastrulation, but markedly impairs the inception of heart development (*85*).

Wingless in *Drosophila* and the related Wnt proteins in vertebrates are the second class of secreted signal for cardiac specification. The primary mode of Wnt signaling is through an intracellular cascade that inhibits the activity of glycogen synthase kinase-3 (GSK3). Inhibition of GSK3 leads to β-catenin stabilization and its interaction with the transcription factors of T-cell factor (TCF) family (*86*). It has been reported that Wnt signaling can either suppress either activate cardiac specification. This feature is present among different species and intra-species. Wingless in *Drosophila* is essential for cardiogenesis, as cells exposed to Dpp, an endogenous inhibitor of Wingless signaling, become visceral muscle instead (*87*). On the contrary, Wnt signaling blocks cardiogenesis in heart field explants from the chick, and in microinjected *Xenopus* embryos overexpressing Wnt3A and Wnt8 (*88-90*). (*88-90*). Intriguingly, Wnt11 stimulates cardiogenesis in avian explants, *Xenopus*, and mouse P19 cells (*91-93*). In this case, the pro-cardiogenic signal is transduced by the “non-canonical” Wnt pathway, involving PKC and JNK (*91*). It is clear that the role of Wnts in vertebrate heart formation is very complex, encompassing a game of induction or suppression of cardiac specification by expression of different Wnt isoforms.

1.2.2 Extracellular Signal for Ventricular Growth

Prior to embryonic day 9.5 in the mouse, the looped heart tube is a thin-walled structure with the atrial and molecular chamber already specified, but indistinct. Growth of the heart from this stage onwards involves proliferation of myocytes along the walls of the heart tube and within the developing interventricular septum. As the wall thickens, cardiomyocytes along the inner wall become organized into finger-like projections called trabeculae, which are thought to enhance oxygen and nutrient exchange, and to increase contractile area.

The epicardium, the thin layer of cells surronding the heart, serves as a source of mitogenic signals that are necessary and sufficient to stimulate proliferation of cardiomyocytes. Retinoic acid produced by the epicardium is one critical regulator of cardiac growth. Knockout mice lacking the retinoic acid receptor RXRα dye during embryogenesis from a failure in proliferative expansion of ventricular cardiomyocytes, resulting in a thin-walled ventricle (*94, 95*). This defect is recapitulated by epicardium specific deletion of RXRα, but not by cardiomyocytes specific deletion of the gene (*96, 97*). Consistent with the role of epicardium as a source of Retinoic Acid for myocardial growth, the epicardium express high levels of retinhaldehyde-oxidizing dehydrogenas (RALDH2), which is a Retinoic Acid synthetic enzyme. Importantly, Retinoic Acid also is involved in posterior chamber specification (*98, 99*).

Growth signals from the endocardium are also critical. The neuregulin family of peptide growth factors and their tyrosine kinase receptors, ErBs, have been shown to promote growth of embryonic cardiomyocytes *in vivo* (*100*). Knockout mice lacking ErbB2, Erb4, and neuregulin-1 die at midgestation from cardiac growth defects, characterized by the absence of trabeculae (*101, 102*). Cardiac specific deletion of ErbB2 results in dilated cardiomyopathy with ventricular wall thinning in adult animals (*103*), reminiscent of certain phenotypes observed in breast cancer patients receiving anti-ErbB2 antibody therapy.

1.3 CARDIOMYOCYTE PROLIFERATION

Cardiac development involves the robust proliferation of cardiac myocytes during embryonic life, culminating in the completion of cycling soon after birth, virtually abrogating the potential for further hyperplastic growth. Sevaral lines of evidence indicate that cardiac myocyte DNA synthesis occurs in two distinct phases (*104*). The first phase occurs during fetal life and it is maximal at embryonic day (E) 12, when karyokinesis and cytokinesis are coupled, resulting in an expansion of the cardiac myocyte population. The second phase occurs early in neonatal life and peaks 4-6 days after birth. During this phase, kariokinesis occurs in the absence of cytokinesis, resulting in binucleation of ventricular myocytes (*105*).

Cyclin D-dependent kinase activity is critical for early G1 phase progression, but dispensable in late G1 for S phase-entry in many cultured cell lines (*106*). Members of the cyclin-D family are expressed in distinct tissue-restricted patterns, suggesting specialized roles for these proteins in different tissues. All three types of cyclin D are detected in embryonic and neonatal ventricles, but are downregulated in adult heart (*104*). Similarly, Cdk4, mediating the early G1 transition, and Cdk2, active later in G1, both are expressed in the embryonic ventricle, but not in adult hearts. Transgenic mice overexpressing cyclin D1 under the control of the α-MHC promoter showed a 40% increase in heart weight, ascribed to a two fold increase in cardiac myocyte number at 14 days (*104*). Although the relative amount of proliferation increased (0.05%) compared to control (0.0003%), the absolute magnitude of this event was small, and there is no evidence that cyclin D1 can suffice for enhancing DNA synthesis and cytokinesis. In contrast to skeletal muscle, where forced expression of cyclin D1, A or E inhibited myogenic differentiation (*107*), several markers of cardiac differentiation were normal in D1 transgenic hearts, indicating a lineage-specific difference in fundamental mechanisms inducing differentiation.

Cyclins D act by hyperphosphorylation and inactivation of “pocket proteins”, for which the archetype is Rb. Rb and other pocket proteins exert their function through binding and inactivation of E2F family of transcription factors (*108*). Quiescent cells express an active hypophosphorylated form of Rb, whereas cells in S- and M-phase contain active/hyperphosphorylated Rb.

The exact expression pattern for these protein members in cardiac muscle is controversial. Some authors reported that Rb is expressed as early as E12 in developing ventricles, with Rb messanger remaining constant through development, but with protein expression subsequently downregulated (*109*). Other reports have failed to confirm the presence of Rb in fetal heart (*110*). Interestingly, the pocket protein p130 and the factor E2F are the major components of cell cycle present in the adult heart, indicating a possible differential role at this time of heart development. Pocket proteins act also as cofactors and their importance in myocyte differentiation has to be taken in consideration.

The factors that regulate embryonic cardiac myocyte proliferation are largely speculative, because loss of function, which is usually the best way to gain insight protein function *in vivo*, can be confounded by premature lethality, systemic defects, and maternal rescue of secreted factors. Fibroblast growth factor (FGF) family is an exception in this regard. FGF1 and FGF2 are expressed in the developing rat myocardium and are produced by cardiac myocytes themselves (*111*). In cultured rat myocytes, FGF1 can induce cell cyle reentry, and in avians, FGF1 and FGF2 can trigger proliferation of precardiac mesoderm (*112*). A kinase defective FGFR1 was introduced into the embryonic chick ventricle by inoculation of a recombinant retrovirus (*113*). This truncated receptor forms heterodimers with all known FGFRs, preventing their autophosphorylation and activation. Myocytes infected with the truncated receptor had a reduced clonal expansion, indicating an important role for endogenous FGF as a mitogen for proliferating ventricular muscle cells.

Recent studies have challenged the dogma that cardiac myocytes are permanently withdrawn from cell cycle, and have no capacity of regeneration. In rat cardiac myocytes after cardiac injury or with hypertrophy, mitotic myocytes have been reported, with an increasing proportion of cells in the S and G2/M phases (*114, 115*). However, other studies have failed to confirm these increases in DNA synthesis (*104*). This discordance between models suggests the possibility that cell cycle regulators are absent or inactive in the normal adult myocardium and that the basis of a postmitotic state resides in this inability. A species-specific difference was also observed, since

cyclins E, A and B, as well as Cdk2 and Cdc2, were upregulated after infarction in the surviving myocytes of the rat heart, whereas similar upregulation was not observed in murine models of cardiac hypertrophy (*116*).

The clinical outcome of human myocardial infarction is a limited capacity to restore cardiac functions due to cardiac fibrosis and hypertrophy (*117, 118*). Current therapies to prevent the extension of hypertrophy are aimed to improve cardiac workload and contractility, although increased myocardial mass caused by increase myocyte number could provide an alternate strategy to obviate the development of maladaptive growth. More detailed studies are needed in order to attempt this task.

2. POSTNATAL CARDIAC GROWTH CONTROL (HYPERTROPHY)

Growth of the heart during embryogenesis occurs primarily through proliferation of cardiac myocytes, however soon after birth cardiac myocytes withdraw irreversibly from cell cycle, and subsequent growth of the heart occurs through hypertrophy rather than myocyte hyperplasia. The hypertrophic growth of cardiomyocytes is initiated by mitogenic stimuli, canonical cardiac agonists, and passive mechanical stress or haemodinamic burden. All these stimuli induce cardiac remodelling during postnatal development to maintain a balance between physiological demands for contractile work, and the capability of muscle tissue to meet those demands (*119, 120*).

The features of hypertrophy are an increase in cardiomyocytes size, enhanced protein synthesis, and higher organization of the sarcomeres. Hypertrophic growth involves control at multiple molecular levels: transcription initiation, transcription elongation, and protein translation (Figure 1.3). As described by Molkentin and Dorn, "no single intracellular transduction cascade regulates cardiomyocyte hypertrophy in isolation, but each pathway operates as an integrated component of an orchestrated response between interdependent and cross-talking networks" (*121*). These networks culminate in the nucleus with the post-translational activation of a set of transcription factors that have a role in early heart development. When activated in the adult myocardium, these factors reactivate a "fetal cardiac" gene program. Common examples are the re-expression of atrial natriuretic peptide (ANP), α-skeletal actin, atrial myosin light chain-1, and β-myosin heavy chain (β-MHC). Although elements of this program might be important adaptation signals to stress, their prolonged expression leads to maladaptive changes in cardiac function, associated with myocyte loss through apoptosis and replacement with fibrotic tissue (*122*). These processes lead to a transition from hypertrophy to cardiac failure.

There are two forms of cardiac hypertrophy: physiological, as occurs in response to exercise, and pathological, as occurs in response to abnormal stress. Stress signals inducing hypertrophy include hypertension, pressure overload, endocrine disorders, myocardial infarction, and contractile dysfunction from inherited mutations in sarcomeric or cytoskeletal proteins. Cardiac hypertrophy eventually normalizes the increase in wall tension, thereby abrogating the initial stimulus; where this possibility

is impaired, it results in pathological hypertrophy that frequently progresses to dilated cardiomyopathy.

Numerous questions remain about the physiological border between the good and the bad of hypertrophy. Stress-induced hypertrophy may be initially adaptive and leads to cardiac demise only when prolonged. There is general agreement that cardiac hypertrophy is triggered by abnormalities in calcium homeostasis (*123*), although the mechanism remain vagues whereby calcium, which fluctuates by orders of magnitude during a cycle of contraction, can activate hypertrophic signals. The various pathways leading to cardiac hypertrophy are discussed below.

2.1 GROWTH FACTORS AND CYTOKINES

2.1.1 gp130-Mediated Factors

Recently, cytokines were recognized to play a critical role in the development and homeostasis of many organs. In particular, IL6, IL11, leukemia inhibitory factor (LIF), cardiotrophin-1, and oncostatin M, which all share the common signal transducer gp130 in their receptor, have been implicated in both normal and pathological cardiac growth (*124*). Recently, gp130 was deleted specifically in ventricular cardiac myocytes using the cre/lox technology (*125*). These mice developed normally, however, when they were subjected to hemodynamic stress caused by aortic banding, they developed marked abnormalities, including rapid development of cardiomyopathy associated with myocyte apoptosis (*125*). From this analysis results it is clear that gp130-mediated signaling is crucial for myocyte survival in the development of compensatory hypertrophy.

The physiological ligand for gp130 in the heart is unknown, but one potential candidate is cardiotrophin-1, a member of the IL6-cytokine family, known to induce cardiac hypertrophy and reduce cardiac myocyte apoptosis (*126*). Another potential candidate is IL6, which is produced by cultures of fetal cardiac myocytes, and is upregulated in the adult myocardium in response to many pathological stimuli (*127*). Transgenic mice overexpressing IL6 or IL6 receptor in the heart did not exhibit increased cardiac growth, but developed dramatic cardiac hypertrophy when the two lines were crossed (*128*).

A schematic representation of gp130-mediated signaling is presented in Figure 1.4. Induction of gp130-dependent signaling leads to activation of both MAPKs and JAK/STAT pathways (*119*). Specifically, STAT3 is translocated to the nucleus in response to gp130 activation, which results in the induction of genes involved in cardiac survival and hypertrophy (120). Overexpression of STAT3 in transgenic mice is sufficient to induce cardiomyocyte hypertrophy *in vitro* (*129*) and *in vivo* (*130*). It was shown that adenovirus-mediated gene transfer of either wild-type or dominant negative STAT3 stimulates or attenuates respectively LIF-induced cardiomyocytes hypertrophy (*129*). These results clearly establish an important role for IL6 family of ligands and gp130-STAT signalling in regulating cardiac hypertrophy and survival.

2.1.2 Fibroblast Growth Factor 2 (FGF2) and Transforming Growth Factor Beta (TGFβ)

FGF2 and TGFβ can induce a fetal-like gene program in cultured rat neonatal ventricular myocytes, consistent with induction of the hypertrophic program (*131*). Since this initial observation, a number of additional studies have demonstrated the importance of FGF and TGFβ as mediators of the hypertrophic program. Cardiomyocytes and non-myocyte cells within the heart produce both growth factors, each of which binds to a separate membrane receptor that has tyrosine (FGF2) or serine (TGFβ) kinase activity to elicit further signalling.

TGFβ can induce two different signalling pathways, one leading to activation of Smad proteins, and the other to activation of TGFβ-activated kinase (TAK1). It is not yet clear whether Smads are involved in hypertrophy, but it is known that TAK1 induces JNK and /or p38 activation, known mediators of cardiac hypertrophy, and upregulates the α-skeletal actin promoter in cultured neonatal cardiomyocytes (*132*). *In vitro* studies showed that adenovirus-mediated overexpression of TGFβ1 in cultured neonatal cardiomyocytes increased sarcomeric actin, suggesting a growth response (*119*). In addition, angiotensin II-induced neonatal myocyte hypertrophy required paracrine TGFβ1 release from non-myocytes in culture (*119*).

2.1.3 Insulin-like Growth Factor 1 (IGF-1)

Growth of the heart after birth has been shown to involve the IGF-1 signaling pathway, through the activation of the PI3K/AKT signaling (*133*). This same pathway controls cells, organs, and body size in *Drosophila* (*134*). Although the role of IGF-1 in the heart is still controversial due to usage of different isoforms in overexpression studies (*135, 136*), it is well established that skeletal muscle growth and hypertrophy are mediated by activation of the AKT/mTOR pathway, leading to upregulation of the translational machinery (*137*). Compelling evidence coming from lower organisms such as *Drosophila Melanogaster,* showed that loss or inhibition of either PI3K, mTOR or p70S6K resulted in decrease of cell size (*134*). Conversely, overexpression of the insulin receptor substrate IRS-1, or AKT, or p70S6K was sufficient to cause hypertrophy of cells in which they were expressed (*138, 139*).

Consistent with the central role of this pathway in muscle growth (*2*), it has been shown that cardiac hypertrophy, induced by increased pressure overload or various agonists, can be attenuated by rapamycin, an inhibitor of mTOR activity (*140*). This growth effect appears to be functionally conserved in mammals, as p70S6K knockout mice have reduced body size and cell growth (*141*). The analysis of IGF-1 signalling in the heart is further analyzed as part of this thesis.

2.2 SIGNAL TRANSDUCERS

2.2.1 Calcineurin and Cardiac Hypertrophy

The serine-threonine phosphatase calcineurin is expressed in multiple tissues, and consists of a catalytic subunit, termed Calcineurin A, and a regulatory subunit known as Calcineurin B. Calcineurin B is encoded by a single gene, while Calcineurin A is encoded by three genes, *calcineurin Aα*, *calcineurin Aβ* and *calcineurin Aγ*. C*alcineurin Aα* and *calcineurin Aβ*, but not the third isoform, are detected both in the adult human, rat and mouse heart (*142*). Calcineurin signaling has been well established in T cells (*143*). Activation of the T cell receptor results in elevated concentration of intracellular calcium, which binds calmodulin and Calcineurin B, resulting in activation of the catalytic subunit of Calcineurin A. Calcineurin directly dephosphorylates members of the NFAT transcription factors family in the cytoplasm, and induces their nuclear translocation and consequent activation of genes involved in

the immune response (Figure 1.5). The immunosuppressive drugs Cyclosporine A (CsA) and FK506, as well the endogenous scaffold proteins AKAP79, Cain/Cabin and DSCR/MCIP are thought to act by inhibiting calcineurin and preventing NFAT nuclear translocation (*142, 144, 145*).

A conserved role for calcineurin-NFAT signaling was also identified in the heart (*146*). Overexpression of activated calcineurin in the hearts of transgenic mice resulted in profound cardiac hypertrophy, progressing to dilated heart failure within two months (*146*). A similar, but less dramatic response was obtained by overexpression of a constitutively nuclear NFAT3 mutant, suggesting that NFAT is also a principal target of calcineurin-dependent signaling in cardiomyocytes (150). Moreover, mice deficient in Calcineurin Aβ display a 12% reduction in basal heart size, and are resistant to diverse hypertrophic stimuli, such as pressure overload and infusion of isoproterenol or angiotensin II (*147*).

However, there is still confusion surrounding the role of calcineurin signalling in the heart, specifically when the calcineurin function is explored by the usage of pharmacological inhibitor, such as CsA and FK506. CsA has been shown to prevent hypertrophy of neonatal rat cardiomyocytes in response to stimulation with angiotensin or phenylephrine (PE) *in vitro* (*119*), and *in vivo* in three different murine models of hypertrophic cardiomyopathy (*148*). These results are in conflict with other studies in which calcineurin inhibitors had no effect in blocking pressure overload hypertrophy in rodents (*149, 150*). Interpretation of these conflicting results is difficult for two important reasons:

a) Calcineurin is expressed in other tissues, not only in the heart, and a systemic delivery of calcineurin inhibitors can cause collateral effects on other organs, affecting *in primis* arterial hypertension, and consequently heart maladaptative morphology and function.
b) The immunosuppressant doses used for *in vivo* heart experiments are 10-fold higher than the doses required for immunosuppression, and are associated with systemic toxicity, as illustrated by weight loss of CsA-treated animals in some studies (*119*).

This source of variability can be resolved by *in vivo* engineering of endogenous calcineurin inhibitors. Although AKAP79 and Cabin/Cain are expressed at very low level, the inhibitory proteins of calcineurin termed DSCR/MCIPs (myocyte-enriched calcineurin –interacting proteins) are highly expressed in striate muscles and may function as endogenous modulator of calcineurin activity in the heart (*151-153*). Interestingly, in MCIP/calcineurin double transgenic mice overexpression of MCIP inhibited cardiac hypertrophy and progression to dilated cardiomyopathy, but also attenuated isoproterenol-and exercise-induced increase in cardiac mass (*154*).

A lack of consensus also pervades studies on the role of calcineurin signalling in failed human hearts. Either increased calcineurin activity, or decrease in the expression as well as in the activity, have been reported in hypertrophied and failed human hearts (*155*). A promising approach in the future to elucidate the role of calcineurin signaling during hypertrophy may involve spatial and temporally controlled inhibition or activation of calcineurin, as well as by employing tissue-specific docking molecules for the phosphatase rather than pharmacological approaches.

2.2.2 Signaling via G Protein-Coupled Receptors

G Protein-Coupled Receptors (GPCRs) play an important role in the regulation of cardiac function and adaptation to changes induced by haemodynamic burden (*156*). These receptors are coupled to heterodimeric G-proteins consisting of two subunits, Gα and Gβγ. Upon receptor activation, GDP is converted in GTP on the Gα subunit, with consequent dissociation from the Gβγ subunit, and modulation of the activity of downstream signaling effectors. The functional classes of cardiovascular receptors correspond to three major classes of G proteins (Figure 1.6):

a) Beta-adrenergic receptors (βAR) are coupled to Gαs and mediate enhancement of heart rate and myocardial contractility in response to epinephrine and norepinephrine stimulation (*157*). The immediate downstream mediator of Gαs is adenylate cyclase (AC). Overexpression of β1-receptors in hearts of transgenic mice initially increases contractile function and responsiveness to isoproterenol, but eventually results in progressive deterioration of cardiac performance, cardiomyocytes hypertrophy and fibrosis

(*158*). Similar findings were obtained with overexpression of Gαs, but surprisingly were not dependent on AC activation (*159*). Conversely, overexpression of AC type VI does not exert adverse effects on cardiac function and has been reported to attenuate cardiomyopathic changes, including cardiac hypertrophy in Gαq transgenic mice (*160*). The principal target of AC activity is PKA. Interestingly, mice overexpressing PKA showed dilated cardiomyopathy, cardiac hypertrophy and fibrosis, similar to mice overexpressing β1-receptors, indicating that β1-receptors mediate their responsiveness through PKA activity, and independently from AC (*161*). In contrast to β1-receptor signalling, overexpression of β2-receptors improve basal contractile function, and the cardiomyopathic phenotype of Gαq transgenic mice (*162*).

b) Angiotensin II, endothelin, and α-adrenergic receptors (α-AR) are coupled to Gαq/G11 and modulate cardiac hypertrophy in response to pathological stimuli. Transgenic overexpression of the above receptors, as well as Gαq, leads to cardiac hypertrophy, with consequential depressed contractility and cardiomyopathy (*163, 164*), indicating that signals downstream of Gαq/G11 are sufficient to cause maladaptative cardiac hypertrophy. Cardiac-specific ablation of Gαq/G11 resulted in complete absence of hypertrophy and cardiac fetal program reactivation in response to aortic banding (*165*), indicating the necessary requirement of Gαq/G11 for pressure-overload cardiac hypertrophy. Indirect evidence for an important role of Gαq/G11 signaling in hypertrophy also stems from clinical observations of patients with cardiomyopathy, in which Angiotensin II receptor blockers conferred beneficial effects, such as inhibition of cardiac remodeling that exceeded their antihypertensive properties (*166*).

c) Cholinergic receptors are coupled to Gαi and are activated by acetylcholine. Receptor-mediated activation of Gαi subunit results in direct attenuation of AC in the heart and consequent cardiac hypertrophy and heart failure (*119*). Gαi is upregulated in human heart failure, and patients with Gαi increased levels showed impaired responsiveness to isoprenaline (*119*). Taken together these studies indicate that upregulation of Gαi and blunting of AC signaling

may represent a primary event in cardiac hypertrophy, which can contribute to transition from compensated hypertrophy to decompensated heart failure.

2.2.3 Small GTP-binding proteins and sarcomeric signaling

The small G protein family consists of multiple members, regulating diverse cellular processes such as cell growth, division and survival, organization of the cytoskeleton, membrane trafficking, and cellular motility. G proteins have GTPase activity, which hydrolyzes GTP to GDP, thus returning the molecules to their inactive state. Five families of small G proteins have been described: Rho, Ras, ARFs, Rab, and Ran.

Ras signaling (Figure 1.7) is coupled to multiple downstream effectors, including Raf, PI3K, and MAP kinase pathways, all of which participate in the hypertrophic response. Activated ras was shown also to promote nuclear localization of NFAT3, whereas a dominant-negative ras-mutant was able to abrogate the phenylephrine-induced increase in NFAT activity (*167*), suggesting a cross-talk between ras signalling and the calcineurin pathway in cardiomyocytes. Overexpression of a constitutive active Ras induced hypertrophy (*168*), whereas dominant negative Ras prevented phenylephrine-mediated increase in cell size and protein synthesis (*169*).

The Rho family of small G proteins, consist of Rho, Rac and Cdc42. Rho A signalling stimulates the transcriptional activity of SRF via changes in actin dynamics (*170*). SRF regulates many muscle-specific genes, including ANF and α-skeletal actin. Overexpression of SRF induces massive hypertrophy (*119*). A novel muscle specific sarcomeric protein, STARS, which stimulates SRF in Rho-dependent fashion, is upregulated in calcineurin-mediated cardiac hypertrophy, leading to speculation that this molecule modulates hypertrophy through Rho/SRF (*119*). Similar effects have been observed with a constitutive active Rac *in vitro* and *in vivo* (*119*).

2.2.4 MAPK Pathways

MAPKs can be divided into three major subfamilies: extracellularly responsive kinase (ERKs), c-Jun N-terminal kinases (JNKs), and p38 MAPKs. The latter two groups are also categorized as stress-responsive MAPKs, since they cannot only be activated by anabolic stimuli and agonists of GPCRs, but also by pathological stress such as

ischemia or cytotoxic agents (*171*). Overexpression of MAPK phosphatase 1 (MKP-1), which inhibits all three branches of MAPK signaling mentioned above, blocked both agonist-induced hypertrophy *in vitro*, and pressure-overload-associated hypertrophy *in vivo*, demonstrating a significant role for these pathways in hypertrophic responses (*172*).

In vivo experiments supported the notion that ERK1/2-dependent signaling is sufficient to evoke a hypertrophic phenotype (*173*). Transgenic overexpression of MEK1, a MAPK kinase that activates ERK1/2, but not JNK and p38 MAPK, resulted in considerable cardiac hypertrophy (*173*). The hypertrophic gene program was induced as in pathological hypertrophic models, with systolic function at supernormal levels, and impaired diastolic function, resembling phenotypes typical of patients with hypertrophic obstructive cardiomyopathy (*173*). Several other studies showed that ERKs were required for sarcomeric organization induced by hypertrophic agonists (*174*). Moreover, transfection of a constitutively active MEK1 augmented ANF promoter activity in cultured cardiomyocytes, whereas a dominant negative MEK1-encoding construct attenuated ANF promoter activity (*175*). Although these data strongly implicate that ERK is implicated in hypertrophic response, it has been shown that inhibition of ERK1/2 signalling with the drug PD98059 was not sufficient to block ANF promoter activity in cultured cardiomyocytes (*176*). Furthermore, transfection of an activated MEK1-encoding expression plasmid was shown to induce c-fos, but not ANF or myosin light chain 2V promoter activity in cardiomyocytes in culture (*177*). These data indicate that ERK1/2 may synergize with other intracellular signals to complete the hypertrophic program.

Three distinct JNK genes have been identified in mammalian cells, each of them directly phosphorylated and activated by MKK4 or MKK7, which in turn are regulated by MEKK1 phosphorylation (Figure 1.8). In cardiomyocytes, mechanical stretching (*178*), or agonist stimulation by Et-1 (*179*), PE or Angiotensin II (*180, 181*) results in rapid phosphorylation of JNK. Moreover, MKK7 is sufficient to induce all features of cardiomyocytes hypertrophy when overexpressed in cultured cardiomyocytes (*182*). Conversely, adenovirus-mediated expression of a dominant negative MKK4 mutant attenuates the hypertrophic response to ET-1 *in vitro* (*179*). A

target disruption of the *Mekk1* gene results in selective attenuation of JNK activity (*183*); moreover, adenoviral delivery of dominant negative MKK4 to the hearts of aortic banded rats, resulted in reduced cardiac hypertrophy in response to pressure overload (*184*).

Similar to the other branches of MAPKs, p38 activity is induced in pressure overload, ET-1/PE stimulation, physical stress, osmolar stress, and GPRC activation (*119*). Four separate p38 MAPK have been described p38α, p38β, p38γ, and p38δ (*185*). The major activators of p38 MAPKs are MKK3 and MKK6 (Figure 1.8), which phosphorylate the dual site Thr-Gly-Thr on the p38 MAPKs. Potential activators of MKK3 and MKK6 are PAK1, TAK1 and MLK3 (*185*). Interestingly, p38 phosphorylates several transcription factors involved in hypertrophic gene expression, including MEF2 (*186*), and NFAT3 (*187*). p38α and p38β are the most important isoform expressed in the human heart, whereas p38γ and p38δ are undetectable (*188*). *In vivo*, p38 MAPK activity is elevated by pressure overload hypertrophy in aortic-banded mice (*119*), and in human hearts with failure secondary to advanced coronary artery disease (*189*). Further evidence for the role of p38 as a mediator of hypertrophy, came from the observation that overexpression of an activated MKK3 or MKK6 factor in neonatal cardiomyocytes was sufficient to induce hypertrophy, and ANF expression (*119, 190*).

Interestingly, the upstream activator of p38 signalling TAK1 is upregulated after aortic banding (*191*), and transgenic mice overexpressing a constitutively active TAK1 mutant resulted in cardiac hypertrophy and subsequent heart failure, implicating that this branch of MAPKs play also essential role in pathological growth of the myocardium (*191*). Thus, MAPK signalling is involved in both physiological and pathological hypertrophy.

2.2.5 MEF2/HDAC signaling

HDACs deacetylate nucleosomal deacetylases, promoting chromatin condensation and transcriptional repression when recruited to target genes via binding of specific transcription factors, such as MEF2. HDACs can be categorized into three classes, of which HDACs class II are preferentially expressed at high levels in striated muscle

and neurons. HDACs class II contains N-terminal extensions that interact with specific cofactors and transcription factors, including MEF2, GATA and NFAT. Moreover, phosphorylation of specific sites within the N-terminal regulates these associations.

Recently, it has been shown that hypertrophic stimuli, such as pressure overload and calcineurin activation, results in activation of a HDAC kinase, which phosphorylates HDACs class II in serine residues and regulates the association with MEF2 (*192*). Adenoviral-mediated expression of HDAC5 or HDAC9 that lack the regulatory serine residues renders cardiomyocytes resistant to serum- or PE-induced upregulation of ANF and β-MHC expression, and cardiomyocytes hypertrophy. Intriguingly, mice lacking HDAC9 show normal cardiac size and function at early age, but develop spontaneous cardiac hypertrophy at advanced age; moreover, these mice show a severe response to thoracic aortic banding and calcineurin activation, underscored by superinduction of ANP, BNP, and β-MHC (*119, 192*). Contrary to these observations, expression of signal-resistant HDAC mutants in primary cardiomyocytes is sufficient to suppress fetal gene activation in response to hypertrophic signaling (*85*). Paradoxically, HDAC inhibitors, tested in clinical trial as anticancer agents, block cardiac hypertrophy and fetal gene expression (*85*), indicating the existence of certain cardiac HDACs that control the growth inhibitory function of class II HDACs (*85*).

3. MYOCARDIAL INFARCTION: ETIOLOGY AND PATHOPHYSIOLOGY

Myocardial infarction (MI) is defined as death or necrosis of myocardial cells. It is diagnosed as the result of myocardial ischemia or acute coronary syndromes. It occurs when myocardial ischemia exceeds a critical threshold, and overwhelms myocardial cellular repair mechanisms, designed to maintain tissue homeostasis. Ischemia, at this critical level, results in irreversible myocardial cell damage or death. Ischemia occurs mainly for increased myocardial metabolic demands, caused by physical exertion, severe hypertension, severe aortic valve stenosis, and/or decreased delivery of oxygen and nutrients to the myocardium via coronary occlusion (atherosclerotic plaques).

MI is cathegorized in transmural and nontransmural. A transmural MI is characterized by ischemic necrosis of the full thickness of the affected muscle segment, extending from the endocardium, throughout the myocardium, till the epicardium. In nontransmural infarct, the area of necrosis does not extend through the full thickness of myocardium, being affected the endocardium and part of the myocardium.

Approximately 800.000 people in U.S are affected by MI, and 250.000 people die prior being hospitalized (*193*). Hospitalized patients survive with a rate of 90%-95%. MI can occur at any age, with higher incidence in older individuals. The incidence increases with the increase of risk factors, such as high blood cholesterol, hypertension, and genetic or acquired components. Different therapies aimed to restore the coronary blood flow, and restrict the extension of necrotic area in the myocardium have had limited benefits in the case of delayed recognition of MI symptoms. Models of regenerative medicine, employed by several groups, and mainly based on delivery of Bone Marrow (BM) cells to the area of infarct are still under experimental analysis, although a good index of recovery has been found in patients with BM transplantation in the infarct area (*194*). (The ongoing studies on regeneration of the infarcted myocardium will be discussed extensively in Chapter 3).

While clinical trials try to find the best way to reduce limited functionality of the infarcted heart, numerous experimental analyses have dissected the biochemical features of MI. Following MI, together with loss of necrotic cardiac myocytes, a reparative process is quickly initiated to rebuild infarcted myocardium and maintain

structural integrity of the ventricle. Initially, myocardium necrosis is associated with complement activation and free radical generation, triggering to cytokine cascades and chemokine upregulation. Interleukin 8 (IL8), IL6, and C5a are released in the ischemic myocardium, and may play a critical role in neutrophil recruitment (Figure 1.9). Monocyte chemoattractant protein 1 (MCP-1) is upregulated in the infarcted area and controls mononuclear cell recruitment. Accumulation of monocyte-derived macrophages and mast cells may increase expression of growth factors, inducing angiogenesis and fibroblast accumulation in the infarct. In addition, expression of cytokines, inhibiting the inflammatory response, such as IL10, may counteract the inflammatory response of other cytokines. New blood vessels are formed (angiogenesis), and fibroblast-like cells appear and replicate (Figure 1.9).

This initial inflammatory phase of healing, with resultant granulation tissue formation, is followed by a fibrogenic phase that terminate in scar tissue, a rebuilding of infarcted myocardium (*195*). Post-infarction healing has been considered complete 6-8 weeks after MI (*195*). Matrix metalloproteinases (MMPs), involved in proteolytic degradation of fibrillar collagen, are upregulated in these initial phases of post-infarct tissue remodeling (*196*). Tissue inhibitors of MMPs (TIMPs) neutralize this collagenolytic ativity and are upregulated at 1 week after myocardial infarction, staying at high levels in the following weeks (*196*). The activity of TIMPs promotes progressive collagen accumulation in the infarcted area. The delicate equilibrium regulating the activity of MMPs and TIMPs is fundamental in tissue remodelling after myocardial infarct. Continuous activation of MMPs could cause lack of remodelling and collagen deposition, with immediate failure of the heart.

Collagen deposition, ensured by TIMP activity, avoids an early collapse of heart structure and functionality. Interestingly, collagen deposition is continuous in the infarcted area and not a transient process (*195*). Scar tissue is predominantly composed of type I and type III collagen. Fibroblast-like cells are the main cells in the infarcted area to secrete collagen. These cells express α-smooth muscle actin (α-SMA) microfilaments, and are generally termed myofibroblasts for their pale and asynchronous capacity to contract (*195*). Myofibroblasts appear to arise from interstitial fibroblasts and/or adventitial fibroblasts (*195*). Signals that induce

fibroblasts to transdifferentiate in myofibroblats are unknown, although it has been shown *in vitro* that TGFβ1 contributes to this event (*197*). Interestingly, the continuous release of collagen and the formation of fibrotic tissue is ensured by the presence of these cells, which reside in the infarcted area for months in rats, and years in humans (*198*). It is notable that these cells are present also in the site of injury in the skin, but they disappear once healing is complete via apoptosis (*199*). Their persistence in the heart is associated with progressive fibrosis and predicts organ failure.

The signals implicated in heart remodelling after myocardial infarction reveal that Angiotensin II and TGFβ1 expression remains elevated several months after infarct (*200*). Current pharmacological interventions with ACE inhibitors or AT1 receptor antagonists can reduce scar extension and hydroxyproline concentrations, if administered soon after MI.

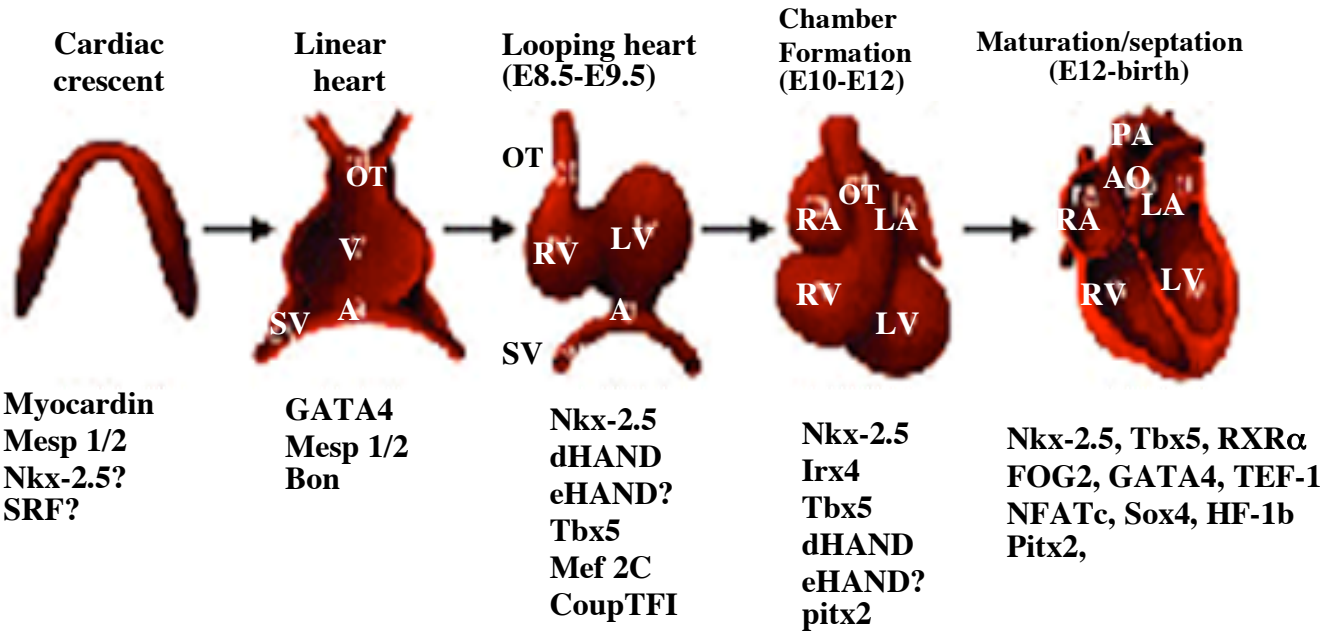

Figure 1.1: Mouse heart development. Five major stages of heart development are shown. The transcription factors involved or suspected to be involved are listed below. Abbreviations: AO, aorta; A, atrium; LA, left atrium; LV, left ventricle; RA, right atrium; RV, right ventricle; OT, outflow tract; SV, sinus venosa; PA, pulmonary artery.

Bruneau B.G. Circ. Res. 2002, 90: 509-519

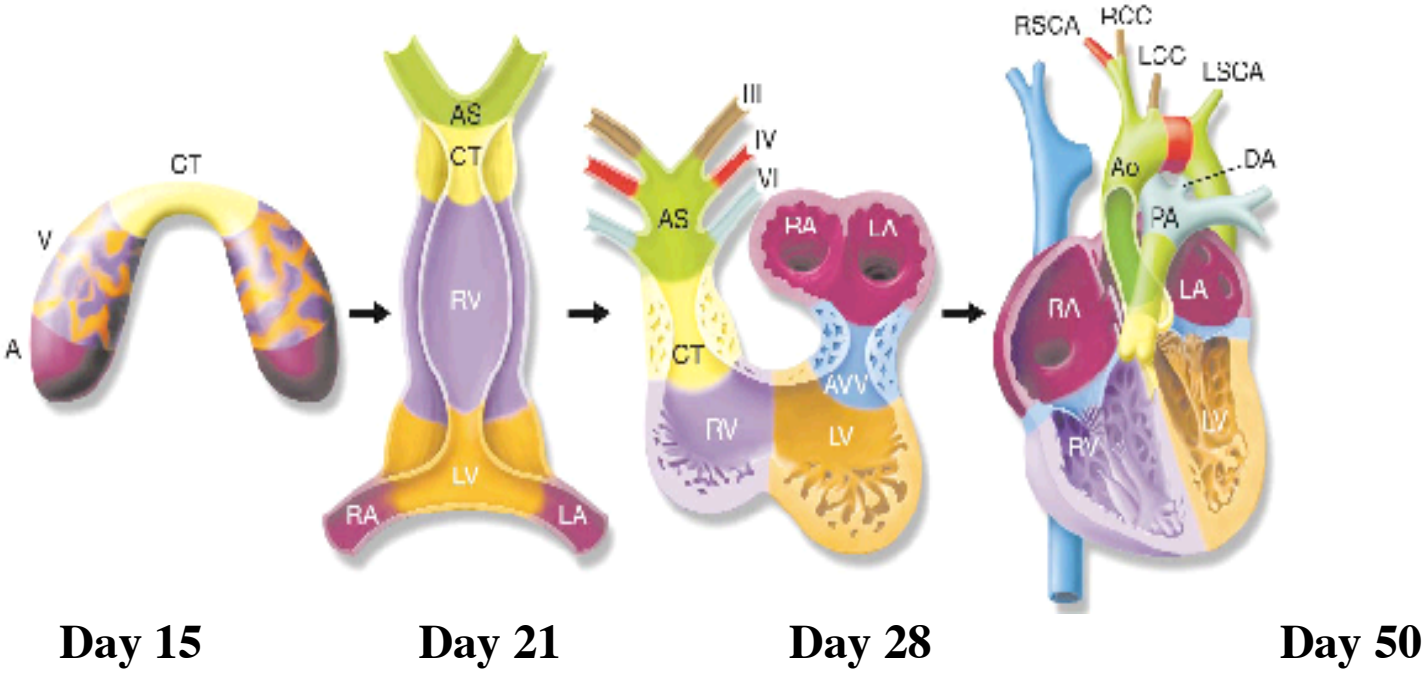

Figure 1.2: Schema of cardiac morphogenesis. The picture shows cardiac development seen from a ventral view. The heart is divided in different regions that represent specific segments of the linear tube, patterned along the anterior-posterior axis to form various specific parts and chambers of the looped and mature heart. Abbreviations: AS, aortic sac; III,IV,VI, aortic archarteries; CT, conotruncal; AVV, atrio-ventricular valve; A, atria; Ao, aorta; DA, ductus arteriosus; LCC, left common carotid; LSCA, left subclavian artery; PA, pulmonary artery; RCC, right common carotid; RSCA, right subclavian artery; RV, right ventricle; LV, left ventricle; RA, right atrium; RV, right ventricle; V, ventricle.

Srivastava D. and Olson E.N. Nature, 2000, 407: 221-226

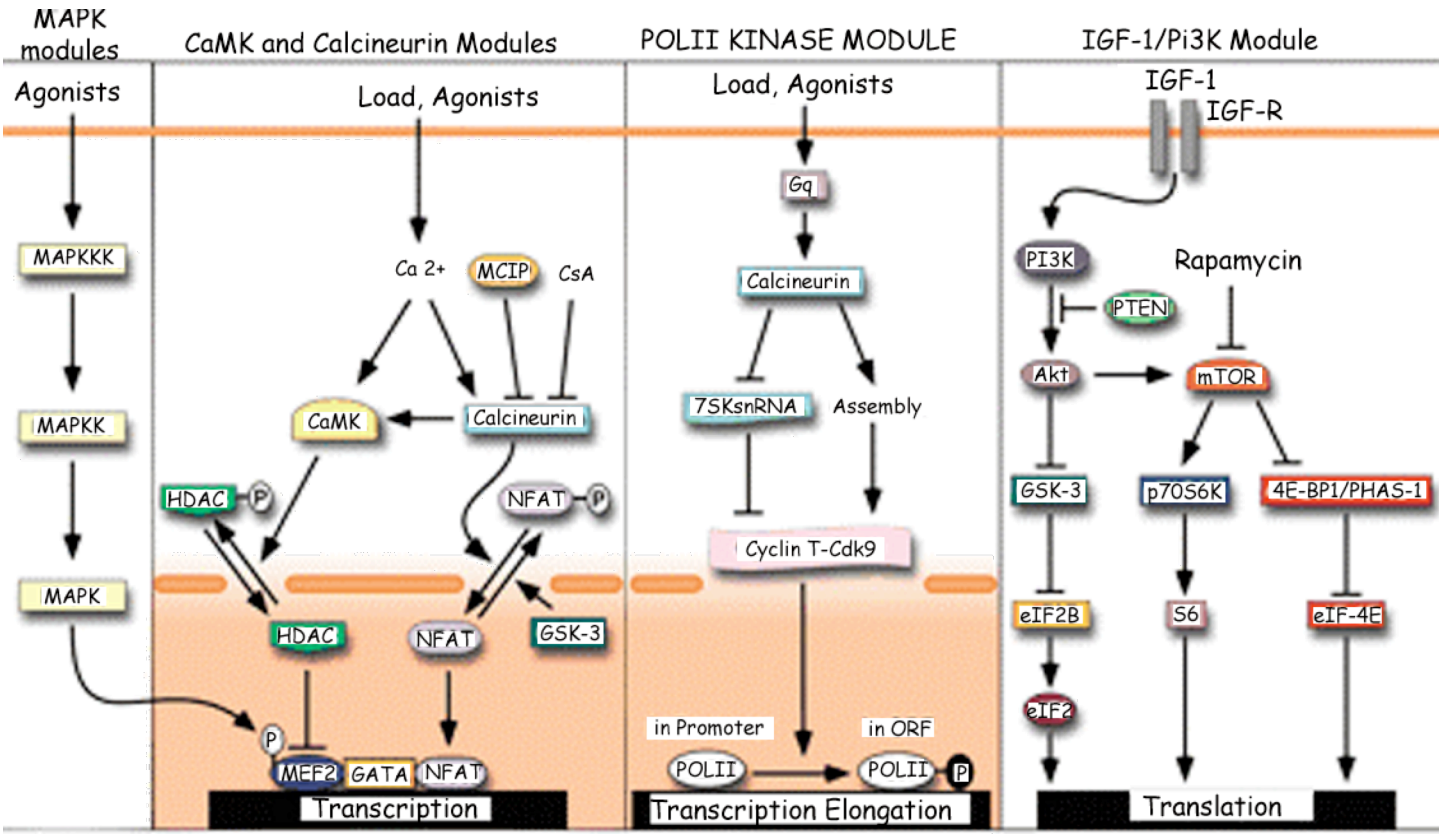

Figure 1.3: Hypertrophic signaling. Four signaling modules promote fetal gene program transcription and translation in response to diverse agonists and load control, separately or by synergistic events. These pathways are a simplification of a more complex program of signal transduction.

Olson E.N. and Schneider M.D. Genes & Development, 2003, 17: 1937-1956

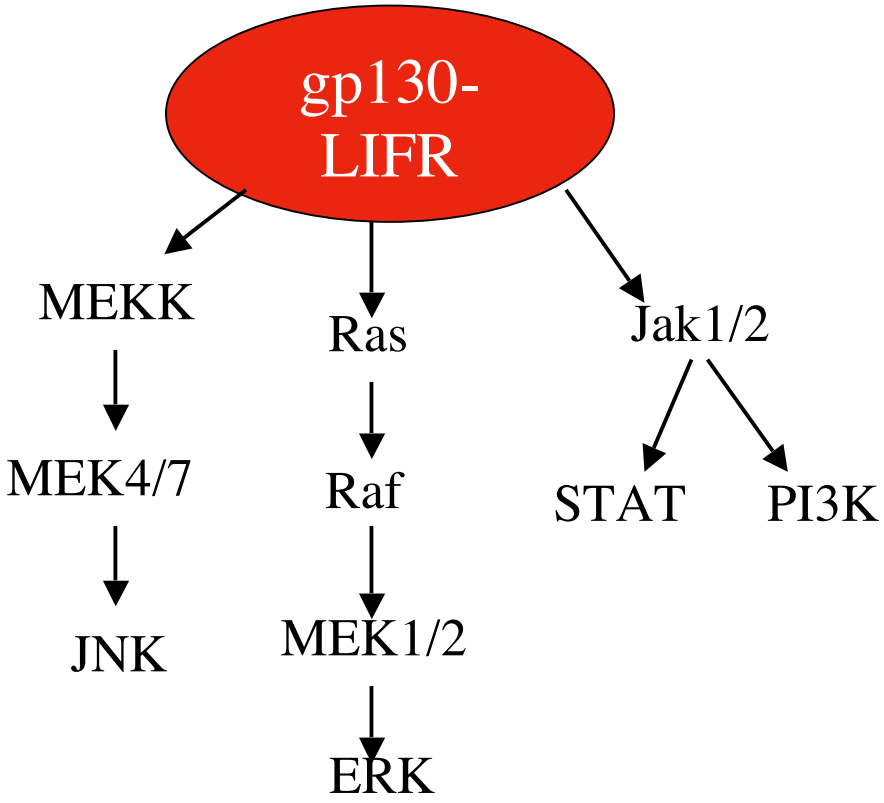

Figure 1.4: gp130 signal transducer and activator of STAT transcription signaling pathway. LIF, cardiotrophin, and other members of the IL6 cytokine family activates gp130 transmembrane receptor, which associates with the leukemia inhibitor factor receptor, LIFR, to signal at different intracellular MAPKs components, to PI3K (phosphatidylinositol 3-kinase), and to STAT transcription factors. Abbreviations: MEK, mitogen-activated protein kinase kinase; ERK, extracellular-signal regulated kinase.

Molkentin J.F. and Dorn G.W. Annu. Rev. Physiol. 2001, 63: 391-426

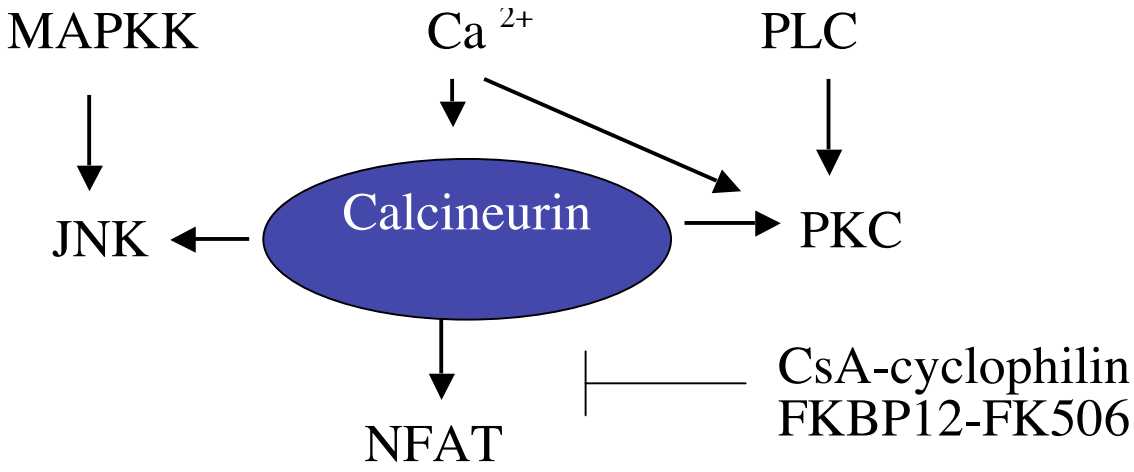

Figure 1.5: Calcineurin signaling pathway in cardiomyocytes. Calcineurin activation by calcium bound to calmodulin results in nuclear factor activated T cells, NFAT, dephosphorylation and nuclear translocation. Activated calcineurin has also been shown to promote c-jun NH2 terminal kinase (JNK) activity, as well as activation of certain protein kinase C, PKC, isoforms. Abbreviations: CsA, cyclosporine A; PLC, phospholipase C; FKBP12 FK binding protein 12; MAPKK, mitogen-activated protein kinase kinase.

Molkentin J.F. and Dorn G.W. Annu. Rev. Physiol. 2001, 63: 391-426

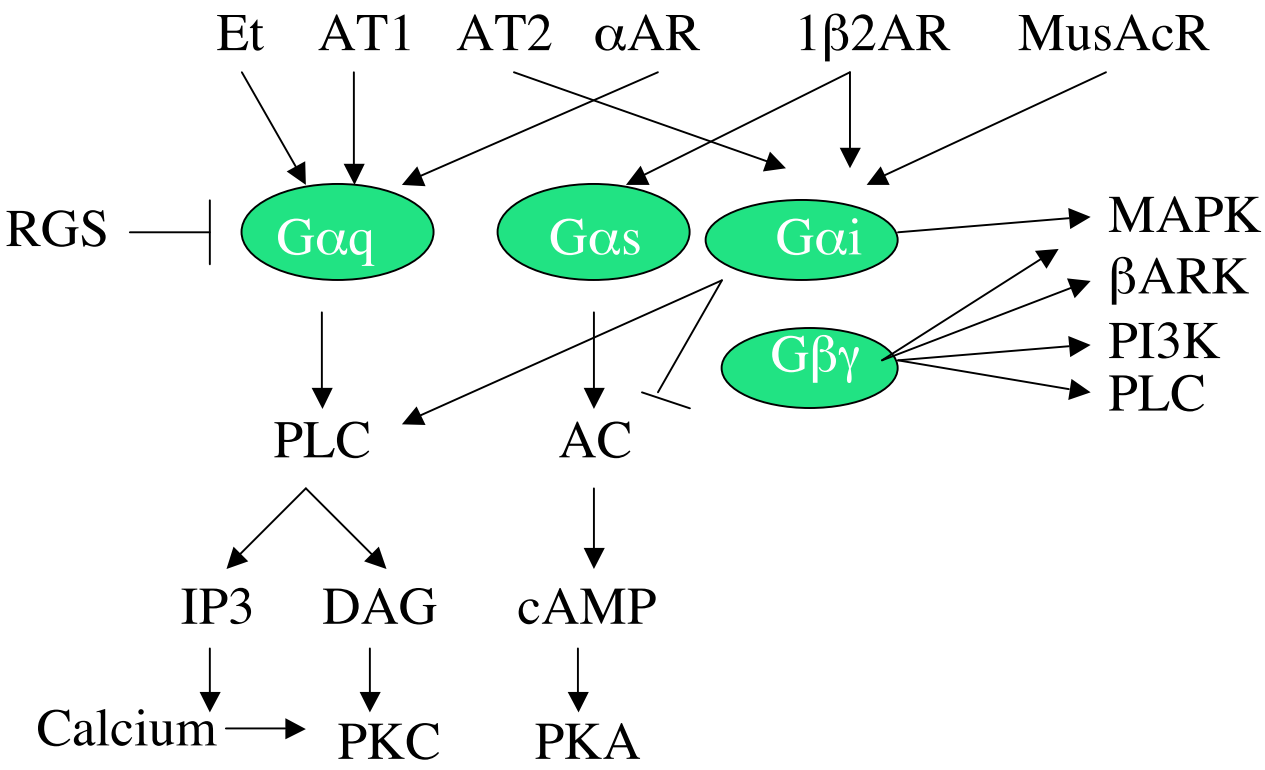

Figure 1.6: G protein-mediated signaling pathway. Multiple transmembrane spanning receptors are directly coupled to G proteins to mediate GDP-GTP exchange, dissociation of Gα and Gβγ subunits, and activation of specific signal transduction, directly involved in heart hypertrophy. Abbreviations: Et, endothelin receptor; AT1 and AT2, angiotensin receptors; AR, adrenergic receptor; MusAcR, muscarinic acetylcholine receptor; AC, adenylyl cyclase; βARK, beta adrenergic receptor kinase; IP3, inositol 3 phosphate; DAG, diacylglycerol; PLC, phospholipase C.

Molkentin J.F. and Dorn G.W. Annu. Rev. Physiol. 2001, 63: 391-426

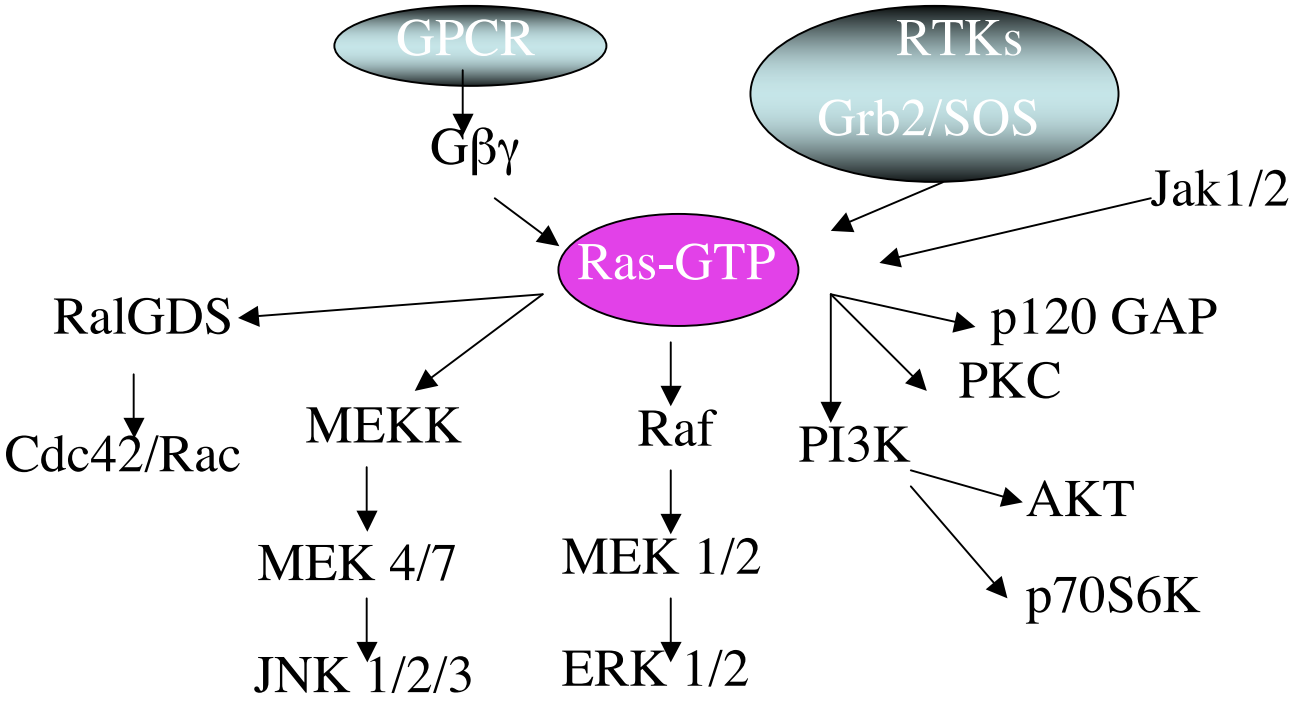

Figure 1.7: Ras signaling pathway. Ras is activated by receptor tyrosin kinases (RTKs), by G protein coupled receptors (GPCR), and Janus kinase 1 (Jak). Ras activation results in GDP GTP exchange and activation of numerous effector proteins. Abbreviations: GAP, GTPase activating protein.

Molkentin J.F. and Dorn G.W. Annu. Rev. Physiol. 2001, 63: 391-426

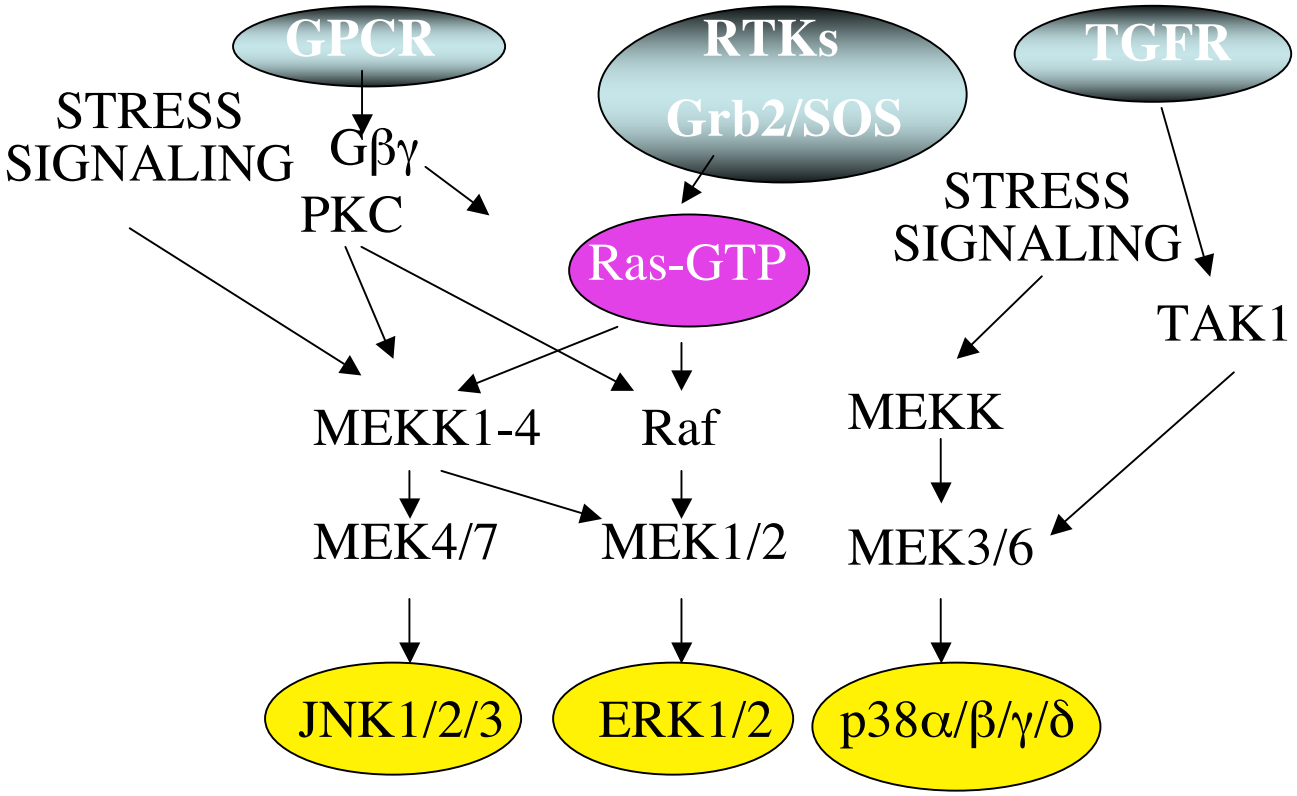

Figure 1.8: Mitogen-activated protein kinase signaling pathways. MAPK signaling is activated in cardiomyocytes by G protein-coupled receptors (GPCRs), receptor tyrosine kinases (RTKs), transforming growth factor β receptor (TGFR), protein kinase C (PKC), and stress stimuli. These upstream events result in the activation of mitogen-activated kinase kinase kinase (MEKK) signaling pathway, terminating with the activity of three canonical MAPK effectors, c-Jun NH2 terminal kinases (JNK1/2/3), extracellular-signal regulated kinases (ERK1/2) and p38. Abbreviations: TAK1, TGFβ activated kinase.

Molkentin J.F. and Dorn G.W. Annu. Rev. Physiol. 2001, 63: 391-426

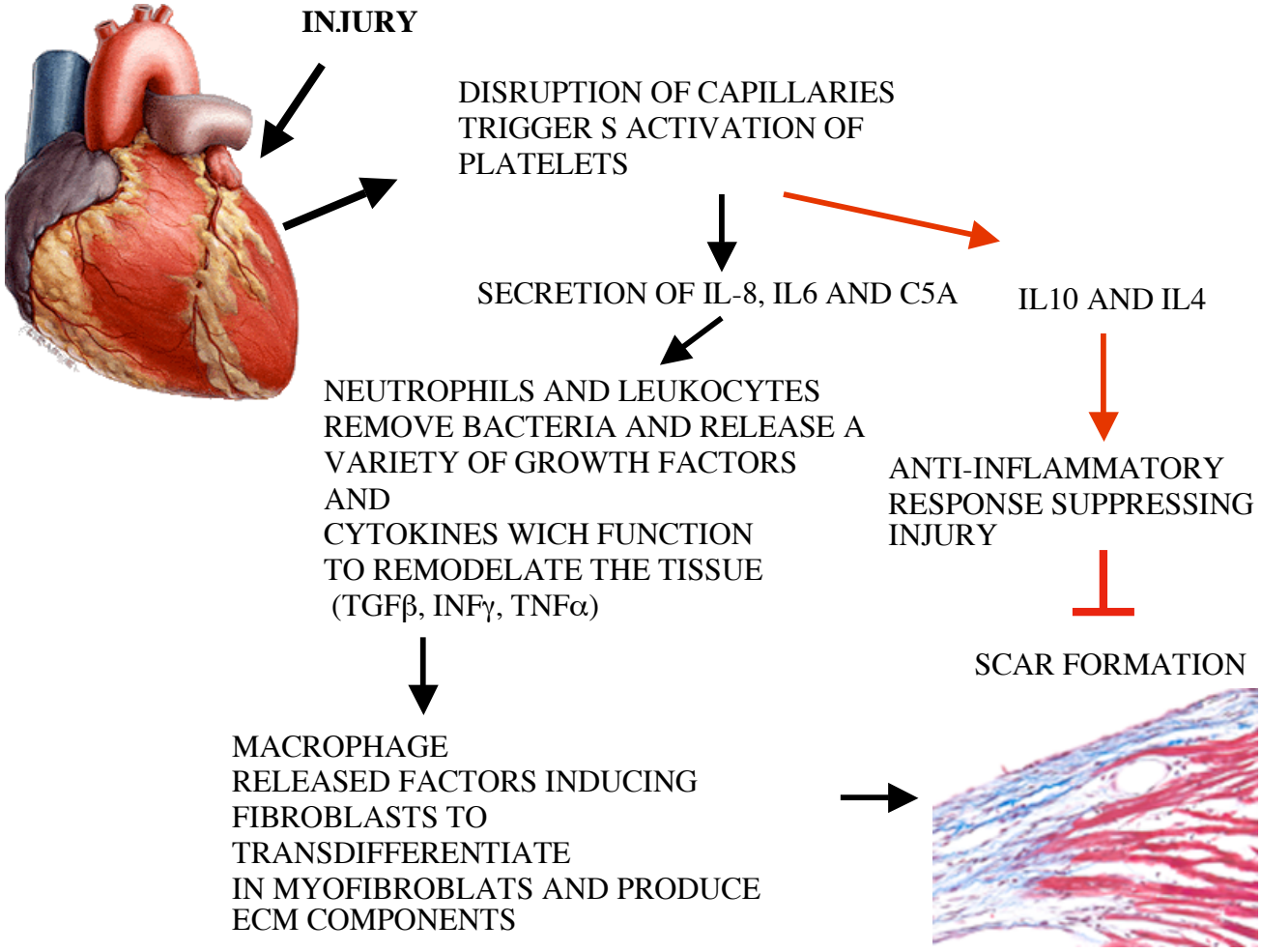

Figure 1.9: Myocardial inflammatory pathway. A general inflammatory cascade is activated in infarcted heart. The remodeling of myocardial tissue after necrosis of cells involves persistent release of collagen type I and III by myofibroblasts and formation of fibrotic tissue, which replaces the myocardium. Scar formation ultimately leads to impairment of heart functionality. Abbreviations: IL8, Interleukin 8; IL6, Interleukin 6; IL10 and 4, Interleukin 10, 4; C5A, complement 5A; TGFβ, transforming growth factor β; INFγ, interferon γ

CHAPTER II

INSULIN-LIKE GROWTH FACTOR-1 (IGF-1) STRUCTURE AND FUNCTION

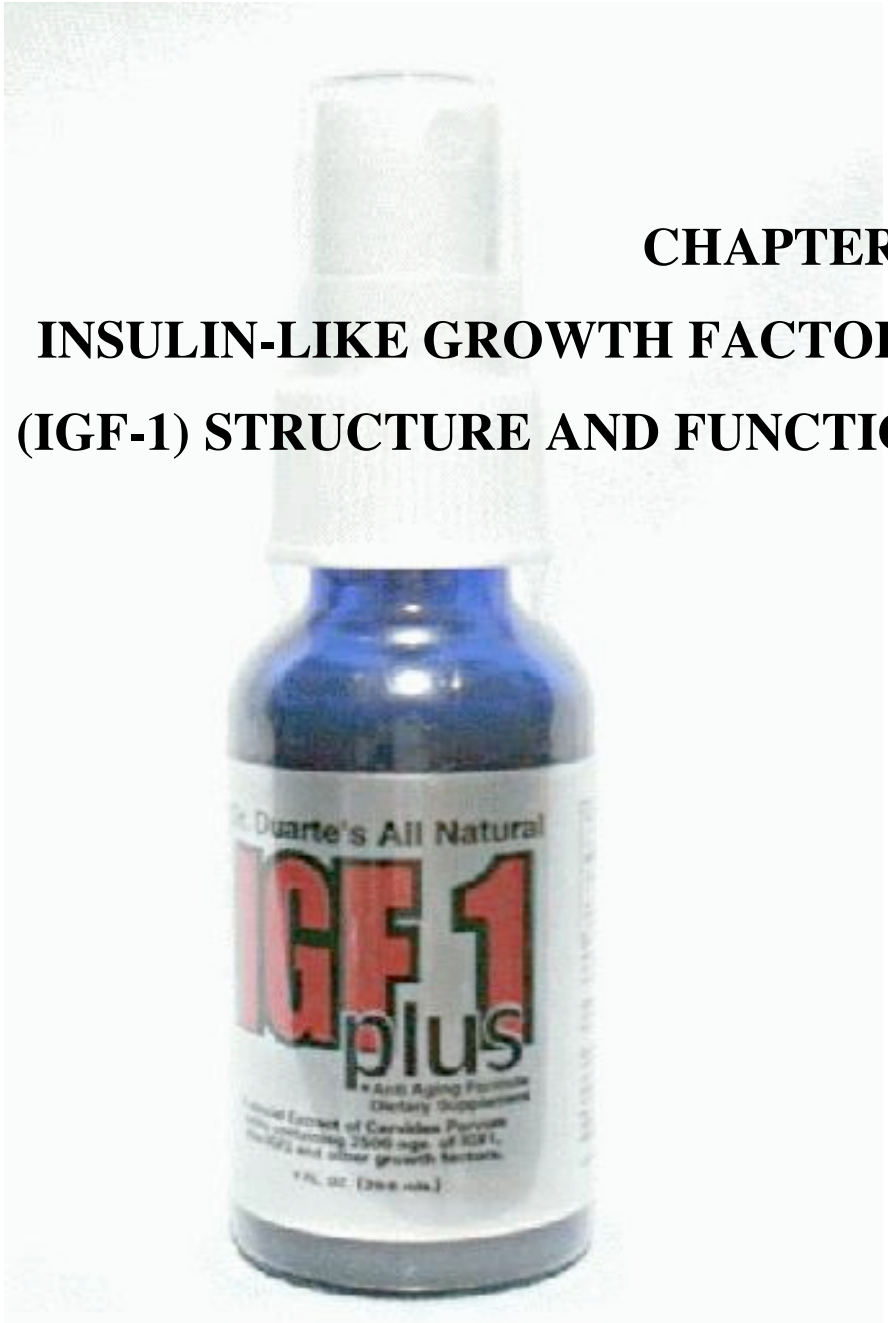

1. BYOSYNTHESIS, STRUCTURE AND ACTION OF IGF-1

The expression of various components of the insulin-like growth factor system of ligands (IGF-1 and IGF-II), receptors (IGF-1R and IGF-IIR) and soluble binding proteins (IGFBP1-6) is ubiquitous throughout intrauterine and postnatal development (*201*). The IGF family of ligands and receptors is homologous to the insulin/insulin receptor (IR) combination, suggesting a common evolutionary heritage. The IGF-1R is activated by IGF-1 and IGF-II, and like the IR has an $\alpha 2\beta 2$ heterotetrameric structure (*201*). The receptors are coupled to several common intracellular second messenger pathways, although there are increasing evidence for more specific interaction with second messenger (*202*).

Several analyses showed that IGF signaling is essential to promote growth *in* and *ex utero* (*203, 204*). Gene-targeting disruption of *Igf-II* or *Igf-IIR* revealed clearly that IGF-II acts primarily during embryonic development, stimulating fetal growth throughout its interaction with IGF-1R and IR (*205*). *Igf-1* gene disruption showed that IGF-1 is critical in both embryonic and postnatal development (*206, 207*), indicating a broad temporally regulated spectrum of action of this gene. Interestingly, IGF-1 is involved in a plethora of different biological functions, including the control of growth and metabolism, as well as survival and proliferation in several organs and tissues during embryonic and postnatal development. The pleiotropic functions of IGF-1 reflect the complicated structure and regulation of *Igf-1* gene, as well as the post-translational modifications that remodel IGF-1 structure during protein biogenesis. This intriguing peculiarity will be discussed in the following paragraphs.

1.1 STRUCTURE AND TRANSCRIPTS OF THE *Igf-1* GENE

The complete structure of the *Igf-1* gene has been elucidated in rats (*208-210*). The gene is large, spanning more than 90kb of genomic DNA, and contains six exons separated by five introns (Figure 2.1). Exon 3 and exon 4 encode for the identical sequence found in all rat IGF-1 cDNAs, including the IGF-1 coding sequence. Exon 3 encodes 27 amino acids that are part of the signal peptide, as well as part of the mature peptide. Exon 4 encodes the rest of the mature peptide, and 16 amino acids of the amino-terminal region of the E-peptide. Exon 1 and exon 2 are termed 5' leader exons and encode part of the signal peptide and for different 5' UTRs, determined by

different transcription starting sites and splicing variants with the other exons. Exons 5 and 6 encode two distinct carboxy-terminal peptides, termed Ea peptide and Eb peptide, as well as the 3'UTR. Rat IGF-1 transcripts encoding the 35 amino acid Ea domain, derive from splicing of exons 4 and 6 together, and exclusion of exon 5 (Figure 2.1). Rat IGF-1 transcripts encoding the 41-amino acid Eb domain derive from splicing of exons 4, 5, and 6 together (Figure 2.1). Exon 6 is a large exon of more than 6kb, specifies for a small amount of coding sequence, and is composed primarily of 3'UTR. This exon contains multiple polyadenylation sites (*209, 210*), which account for the size heterogeneity of IGF-1 transcripts observed on Northern blots. The large molecular weight (7.5 kb) IGF-1 transcript contains all of the exon 6 sequence and an unusually long 3'UT, whereas smaller IGF-1 transcripts use upstream polyadenylation signals and contain shorter 3'UTs (*211*). Available evidence suggests that the *Igf-1* genes of all mammals studied, including humans, are similar to the rat genes in terms of size and complexity (*211*).

1.2 EXPRESSION OF IGF-1 TRANSCRIPTS AND ENCODED PRECURSORS

The first IGF-1 cDNA to be characterised was isolated from a human liver cDNA library by Jansen (*212*). In both rats and humans, the structure of the initially characterised IGF-1 cDNAs predicted an IGF-1 precursor with 70 amino acids, representing the mature peptide (B,C,A,D domains) in the midregion, and flanked by precursor peptide sequences at both amino- and carboxy-termini (Figure 2.1). The amino-terminal part is characterised by two different 5' sequences designated class 1 and class 2 sequences (Figure 2.1). In rat, class 1 IGF-1 transcripts are expressed in liver and all non-hepatic tissues analyzed at all stages of development from fetus to adult (*213, 214*). In contrast to class 1 IGF-1 transcripts, the expression of class 2 transcripts is more restricted. Class 2 IGF-1 transcripts are expressed primarily in the liver, and within the liver significant levels of class 2 mRNAs are detected only in the postnatal period (*213, 214*). These data argue for a tissue-specific transcriptional control of class 1 and class 2 transcripts. In many genes the promoters and regulatory elements that dictate tissue and cell-specific transcription and transcriptional regulation by physiological stimuli reside in the 5' sequences, flanking the transcription start sites. There is little information about the promoters or regulatory elements in the rat *Igf-1* gene that could determine the distinct patterns of expression

of class 1 and 2 transcripts. Interestingly, non-consensus TATAA or CCAAT sequences associated with transcription initiation have been found upstream the transcription start sites in exon 1 and 2 of the rat IGF-1 gene.

Cell-free translation studies suggests that class 1 and 2 transcripts initiate translation at different AUG codons (*208*). Rat class 1 transcripts initiate translation primarily at the -48 AUG to result in an IGF-1 precursor with a 48-residue amino-terminal precursor peptide (*208*). A major level of complexity is due to the fact that in some class 1 transcripts a 186 bp region can be spliced out (*210*) (Figure 2.1). Rat class 2 transcripts initiate translation primarily at the –32 AUG to result in an IGF-1 precursor with a different 32-residue amino-terminal precursor peptide (*208*). Class 2 transcripts also contain an in frame AUG at codon –44 relative to the IGF-1 coding sequence.

Within the sequence common to class 1 and class 2 there is an in-frame AUG codon at position –22 relative to the IGF-1 coding sequence. If the –22 AUG is used for translation initiation class 1 and class 2 could encode the same amino-terminal precursor, and differ only in the 5'UT (figure 2.1). Other start sites (1-4) have been found in the early 1990s, and their usage increased the possibility of different variants of IGF-1, suggesting a complicate tissue- and development-specific IGF-1 transcription (*215*), as discussed below (Figure 2.1). The function of the different amino-terminal precursors is still a matter of speculation. The amino-terminal precursors usually function as signal peptides that lead translocation of a nascent precursor into the endoplasmic reticulum, or signal peptide cleavage and glycosylation. It is possible that the different classes of IGF-1 transcripts may influence these events determining subsequent compartmentalization, binding to IGFBPs, and biological function.

The IGF-1 carboxy-terminal encodes the E domains, Ea and Eb. The 35 amino acid domain encodes the Ea domain as shown in figure 2.1. The Ea precursor peptide is highly conserved across mammalian species (*216*). An alternate 41 amino acid Eb domain results from insertion of a 52 bp mini exon at the point of sequence divergence, shifting the translational reading frame in Eb-type transcripts.

Downstream the 52-base pair mini-exon, 3' sequences in rat Eb-type IGF-1 transcripts are identical to those found in Ea type transcripts. The rat Eb precursor peptide is highly basic, and lacks the motifs associated with N-glycosilation that are found in the Ea precursor peptide (*210*). In humans, there are also IGF-1 transcripts encoding two different Ea and Eb domains, but they result from a slightly different exon-splicing pattern. Downstream from the point of divergence, human Ea and Eb type transcripts contain entirely different 3'sequences, which specify different 3' UTRs, as well as different E domain coding sequences, due to splicing in different 3' exons (*217*). Conversely to Ea, the Eb sequence is less conserved between rodents and humans (*216*).

In rats, IGF-1 transcripts encoding the Ea-type precursors are expressed in most, if not all tissues (*213*). It is not clear whether the Ea domain is processed from the pro-IGF-1 prior to secretion or after secretion, and little is known about the mechanisms involved in the processing of IGF-1/Ea precursors to mature IGF-1. Overexpression of a human transgene IGF-1/Ea precursor in transgenic mice leads to preferential overgrowth of specific organs, including brain, spleen and pancreas (*218*).

The Eb-type precursors are expressed primarily in the liver, and at much higher levels postnatally (*213*), suggesting a liver-specific role of the IGF-1/Eb precursors. Interestingly, the liver is the major source of circulating IGF-1, and the increase of IGF-1/Eb transcripts in the liver is parallel to the increase in circulating IGF-1 (*213*). The data reported suggest that the Eb domain could play a role in targeting mature IGF-1 to the circulation, whereas the Ea precursor peptide may play an important role in the local action of IGF-1. Further analyses will elucidate the role of the variable amino-and carboxy-termini.

1.3 DIFFERENTIAL ACTION OF IGF-1 SPLICED VARIANTS

IGF-1 was originally discovered as a circulating factor, termed somatomedin C, which mediates the growth-promoting actions of pituitary-derived Growth Hormone (GH) on cartilage (*219*). Subsequent studies have established that in the period from birth to puberty, GH and IGF-1 act together in an endocrine manner to regulate the linear growth of the skeleton and coordinate the growth of other organs (*220*). Liver was

then considered the major source of IGF-1, since the rates of hepatic secretion of IGF-1 were sufficient to account for levels of IGF-1 found in plasma. Studies in the early 1980s provided some evidence for the synthesis of IGF-1 in non-hepatic tissues (*221*). The production of IGF-1 in extra-hepatic tissues supports both autocrine and paracrine functions, and a different regulation from that in liver, which supports endocrine functions (*215*). Collectively, the data presented so far led to the hypothesis that class 1 transcripts, together with the Ea peptide, might encode the local IGF-1 isoform, functioning in an autocrine/paracrine manner. On the contrary, class 2 transcripts, together with Eb peptide, are regulated by GH release, and are mostly express in liver, functioning in endocrine manner.

Interestingly, the start sites present within exon 1 and exon 2 (Figure 2.1) are differentially used, corresponding to developmental stage- and tissue-specific expression (*215*). Most extra-hepatic tissues (stomach, heart, muscle, as well as testes and lung) use the start site 3, while liver, brain, and kidney use the start site 2 and 3 equivalently. Start sites 1 and 4 are used in all tissues at very low level (*215*). Exon 2 transcripts are expressed mostly in testes, lung, stomach, kidney and liver, and transcription initiation was equivalent in all the tissues (*215*). Developmental specification was also observed, since within exon 1 start site 3 was used perinatally and postnatally, whereas start site 2 was detected only at stage of weaning. Moreover, exon 2 transcripts appear only at the postnatal period (*215*). These data highlight the difficulty in mapping a common action of the IGF-1 isoforms, because of very tight and tissue-specific regulation.

1.4 IGF-1 FUNCTIONS

In general, IGF-1 shares many anabolic functions with insulin, such as stimulation of nutrients and amino acid uptake, as well as DNA and RNA synthesis. IGF-1 differs from insulin for its metabolic functions, which include stimulation of whole-body protein metabolism by increasing protein synthesis and inhibiting protein proteolysis. In contrast to other growth factors (FGF, EGF, or PDGF), which act as potent mitogens inhibiting differentiation, IGF-1 can induce both proliferation and differentiation, as shown most unequivocally in skeletal muscles *(1, 2)*.

Studies on gene disruption of *Igf-1* or *Igf-II*, as well as the respective receptors, *Igf-1r* and *Igf-IIr*, have led to important considerations about the functions of IGF-1. Mice lacking either *Igf-1* or *Igf-II* genes exhibit intrauterine growth retardation, with weights approximately 60% that of wild-type littermates (*204*). Interestingly, while exhibiting intra-uterine growth retardation, the *Igf-II*$^{-/-}$ mice have essentially normal postnatal growth. On the contrary, *Igf-1* null mice die shortly after birth, and only a small percentage survives and reaches adulthood, with severe under-developmental growth of the entire organism (*204*). More severe is the phenotype of mice lacking a functional *Igf-1r* (*204*). These mice are born weighing only 45% of normal, and die soon after birth from respiratory failure (*204*). Skin and all skeletal muscles present a generalized hypoplasia (*204*). Delays in ossification were observed in these animals, and changes in architecture of the spinal cord and brain, due to diminished number of non-neuronal cells (*204*). *Igf-IIr* null mice exhibit a completely opposite phenotype, characterised by fetal overgrowth syndrome, which results in lethality (*222*). The 70% weight reduction in pups null for *Igf-1*/*Igf-II* genes results in a dwarf phenotype. The phenotype of the double knockout (KO) *Igf-1*/*Igf-1r* is identical to that of *Igf-1r* null mice, indicating that IGF-1 is acting predominately through the IGF-1R (*202*). Interestingly, the *Igf-II*/*Igf-1r* double KO have a growth retardation more severe than that of the *Igf-1r* single KO, indicating that IGF-II acts through another receptor different form IGF-1R, identified as the Insulin Receptor (IR) (*223*). Thus, the IGFs stimulate fetal growth through IGF-1R and IR, whereas IGF-IIR appears to inhibit the effects of IGF-II on fetal growth.

Most of the phenotypes so far described exhibit a clear growth deficit, and the severe rate of mortality has led to an underestimation the function of IGF factors in different adult organs. More sophisticated studies employing the Cre/lox technology have addressed questions regarding the function of IGF-1 in different and specialized tissues during development. The most long-standing question concerns the function of IGF-1 produced in the liver. IGF-1 transcripts are expressed in the liver at a level 10- to 100-fold greater than in the majority of other tissues. Hepatic IGF-1 increases dramatically postnatally, accompanied by increased IGF-1 levels in serum, indicating that the function of hepatic IGF-1 becomes important with age (*202*). Since hepatocytes do not express IGF-1R, production of IGF-1 has been hypothesized to

affect growth of organs. By crossing the *Igf-1/lox* mice with a transgenic line overexpressing Cre under the albumin promoter, it was possible to generate mice with specific deletion of the *Igf-1* gene in the liver (*224*). Interestingly, these mice did not present any deficit in pre and postnatal growth, despite a marked reduction (75%) in the concentration of total IGF-1 in serum (*224*). Moreover, it has been found that GH levels increase in serum (*224*). These data reveal clearly that circulating IGF-1 does not affect growth of different organs, and that one possible function of circulating IGF-1 is the control of GH levels. IGF-1 in serum could function as feedback in the somatotropic axis, reducing GH release from the pituitary gland. Importantly, the control of GH levels in the circulation could account for a non-detrimental effect on growth, and for normal levels of IGF-1 in extra-hepatic tissues *(202)*. However, it has been found that in $Ghr^{-/-}$ mice IGF-1 expression in heart, lung, testis, spleen and brain, with the only exception of liver, is not affected, indicating a GH-independent circuit of IGF-1 regulation (*225*). Notably, liver-specific *Igf-1* null mice develop insulin resistance, specifically in muscles, but not in liver, arguing that circulating IGF-1 could regulate glucose homeostasis and metabolic reactions in extrahepatic tissues (*224*).

In the next paragraphs the functions of IGF-1 will be described in details in several organs with more attention on heart.

1.4.1 Role of IGF-1 in the Nervous System

It is known that IGF-1 can be transported in brain across the blood-brain barrier, but is also produced locally in the nervous system. Several lines of evidence show that IGF-1R modulates neuronal activity, resulting in the regulation of food intake, energy metabolism, reproduction, and possibly cognitive functions. Studies in the early 1990s showed that IGF-1 stimulates proliferation of neuron progenitors, induces differentiation of oligodendrocytes, and increases the survival of neurons and oligodendrocytes *in vitro (226, 227)*. In homozygous mice, disruption of *Igf-1* or *Igf-1R* genes produces pathological abnormalities and brain growth retardation (*204*). Interestingly, brain growth retardation occurs also in transgenic mice overexpressing IGFBP1 in the brain, probably because of an inhibition of IGF-1-stimulated growth (*228*). In transgenic mice overexpressing IGF-1 in the brain, the size and the weight of

the brain increases markedly (*218*). Different studies showed that the brain of these mice contains an increased number of neurons, and of total brain myelin, as well as of regional density of myelinated axons (*229*). A transgenic model with IGF-1 overexpression in the brain mainly during postnatal development showed that IGF-1 is implicated in neurogenesis and synaptogenesis in the hippocampal dentate gyrus (*230*).

Notably, IGF-1 also has an important role in the case of nerve injury. In crash-injured and freeze-injured rat sciatic nerve, local administration of IGF-1 increases axon regeneration. An interesting study, where the left musculo-cutaneous nerve of adult rats was fully transected to induce biceps-muscle paralysis, and the distal part of this nerve was co-opted to a different nerve, showed that IGF-1 infusion promoted increased myelin thickness/axon diameter ratio (*231*). Moreover, functional recovery of the paralyzed muscle was expedited in these animals, indicating that IGF-1 may have a potential role in therapeutic trials in case of exogenously- and/or endogenously-induced damage (*231*).

1.4.2 Role of IGF-1 in Bone Formation

The skeleton is a highly organized and physiologically active organ, continuously remodeling itself to preserve skeletal integrity (*232*). The mammalian skeleton is organized in an outer surface of cortical bone that surrounds the inner trabeculae elements. Both cortical and trabeculae bones undergo to a constant remodeling, which is orchestrated by different growth factors and cytokines. IGF-1 is known to be implicated, together with TGFs, in the recruitment of osteoblasts to the bone surface, for collagen synthesis, and for matrix deposition and mineralization (*233*). Although there are several genetic analyses on IGF-1 functions in bone morphogenesis and remodeling, the effective role of this growth factor is still unclear. Some studies have reported that IGF-1 induces increased uptake of thymidine incorporation in most of the cells, but its role as a mitogen in pre-osteoblasts proliferation is limited. Moreover, its action on osteoclast differentiation is still elusive (*232*). However, Rubin and collegues have demonstrated that IGF-1 stimulates the secretion of Receptor Activator of nuclear factor kappa B ligand (RANKL), important for recruitment of osteoclasts (*234*).

Although mice lacking *Igf-II* gene do not show any phenotype related to bone growth and remodeling, genetic disruption of the *Igf-1* gene leads to short bone phenotype and low bone mineral density (*235*). A more striking phenotype was observed in mice with targeted deletion of the *Igf-1* gene in osteoblasts (*236*). These mice show a significant defect in bone formation with reduced osteoblastogenesis; overall the mice present a dramatic reduction in bone mineralization occurring by three weeks of age, indicating that IGF-1 signaling is fundamental in the process of bone mineralization (*236*).

1.4.3 IGF-1 functions in Skeletal Muscles

The role of IGF-1 in striated muscles has been studied in transgenic models overexpressing various IGF-1 isoforms. Whereas mice lacking *Igf-1* and *Igf-1R* genes exhibit marked muscle hypoplasia, mice overexpressing *Igf-1* transgenes showed enlarged myofibers and hypertrophy (*2*). Increased fiber size, protein content, and nuclei within myofibers has been found in mice overexpressing the class 1/Ea IGF-1 isoform in skeletal muscles (*2*). These features were accompanied by activation of GATA2, a novel marker of myocytes hypertrophy (*237*). Moreover, this isoform of IGF-1 confers muscle mass and strength during aging, in neuromuscular disease, and after injury (*2*). In contrast, a class 2/Eb transgene increased the numbers of dihydropyridine receptors, preventing their age-related decline (*238*), and extended the replicative life span of skeletal muscle satellite cells *in vitro*, although no beneficial effect on enhancing satellite cells proliferation ability was found *in vivo* (*239*).

In aging studies, it has been found that IGF-1R levels decrease in rat skeletal muscles by 80% between infancy and young adulthood, with a subsequent decrease of 10-60% during senescence (*240*). In conjunction with this decline, the ability of IGF-1 to stimulate protein synthesis is lost in adult and aged rats, together with the capacity to stimulate glucose uptake (*240*). Disuse or unweighting also induces muscle atrophy. In rat soleus, unweighting produces DNA cleavage typical of apoptosis. Whereas a combination of intramuscular IGF-1 administration and exercise reduces apoptosis, brief intense exercise alone, or prolonged intermittent exercise, partially restores

muscle responsiveness to IGF-1, indicating that plasticity for IGF-1 anabolic effects is retained in aging muscles (*241*). An interesting study conducted by De Luca in 1997 showed that, in aging rat muscle, conductance to chloride is reduced, with subsequent decrease in muscle contractility. Administration of IGF-1 or GH increased muscle conductance to chloride, and restore muscle contractility, suggesting a shift to the young adult chloride channel expression (*242*).

In general, a variety of conditions leading to inhibition of GH-IGF-1 axis are associated with muscle catabolism. Recently, a single patient with homozygous partial deletion of the IGF-1 gene has been reported (*243*). This patient presents short stature, sensorineural hearing loss, and mental retardation (*243*). Specific evaluation of muscle physiology was not reported, but recombinant IGF-1 therapy resulted in accelerated growth and increased lean body mass. Myopathies and dystrophies, regardless of pathogenesis, are also associated with increased muscle catabolism, and IGF-1 has been proposed as an empiric therapy for muscle loss associated with Duchenne muscular dystrophies, and with inflammatory myopathies. A rationale for IGF-1 therapy in structural dystrophies is supported by the fact that degeneration of muscle following denervation or structural injury induces upregulation of IGF-1 and IGF-1R in satellite cells localized in the area of regeneration (*244*). Muscles, damaged by inflammatory myopathies, show a similar upregulation (*244*). Despite its beneficial effects in skeletal muscle injury, systemic delivery of IGF-1 remains formidable due to cost, doses and administration. Numerous side effects have been found related to edema, athralgias, temporomandibular joint pain, and headaches (*245*). Recently, it has been shown that co-administration of IGF-1 with IGFBP-3 minimizes side effects over the course of a short trial (*246*).

In summary, IGF-1 plays a critical anabolic and trophic role throughout the life of myocytes. Proliferation of satellite cells in response to injury and/or myopathies seems to be mediated by IGF-1 signaling, which provides a clear benefit to the total architecture of the muscle, as well in muscle functionality. For these reasons, IGF-1 may offer effective myotherapy for a spectrum of metaboloic and structural myopathies.

1.4.4 IGF Family of Binding Proteins (IGFBPs)

IGFs are normally bound in serum to a family of six structurally and evolutionary related binding proteins, termed IGF-binding proteins (IGFBPs). IGFBPs act as carrier of IGFs, and function as modulator of IGFs availability and activity (*247*). IGFBPs1-5 bind the two IGFs with similar affinities, whereas IGFBP6 has a higher affinity for IGF-II. Notably, in the last few years it has been reported that IGFBPs, precisely IGFBP3 and IGFBP5, have important biological functions independent of their ability to bind IGFs (*248*), and that both binding proteins translocate from the extracellular compartment to the nucleus of rapidly dividing human lung and breast cancer cells (*249*). Although IGFs can translocate to the nucleus with IGFBP3, it is believed that the function of IGFBP3 in the nucleus is independent of IGFs (*249*). Other *in vivo* and *in vitro* data support the importance of IGFBPs for cell growth by IGF-dependent and -independent mechanisms.

All six IGFBP members share a common structure, which is characterised by an N-terminal domain and a C-terminal domain, with conserved amino acidic sequence among all IGFBPs, and the midregion, which shares similarity less than 15%. The N-terminal domain contains 80-93 amino acid residues after the signal peptide, and shares approximately 58% similarity. IGFBPs1-5 contain 12 cysteines in this domain, whereas IGFBP6 contains only 10 cysteines. The high number of these residues argue for the formation of disulfide linkages in the primary structure. Indeed, these cysteines form intra-domain bindings, which do not affect the C-terminal domain (*250*). As is the case for the N-terminal domain, the C-terminal domain is highly conserved, and shares a similarity of approximately 34%. Other 6 cysteines are found in this domain and are strictly conserved. They are involved, as described for the N-terminal domain, in intra-domain disulfide bond formation (*250*).

N- and C-terminal domains bind IGF-1 with strong affinity (k_d 10^{-10} M). Spencer and Chan (*251*) generated IGFBP3 fragments that essentially correspond to the N-terminal half (residues 1-147), and the C-terminal half (residues 151-263) of the IGFBP, and showed that each of these fragments bind IGFs, but with less affinity than intact IGFBPs. Sequential C-terminal deletion studies with recombinant bovine IGFBP2

suggested that loss of the region spanning the last four cysteines reduced IGF binding (*252*). Interestingly, the C-terminal domain, besides its capacity to bind IGFs, participates in binding the cell surface and the extracellular matrix (ECM) proteins, via its heparin-binding sites (XBBBXXB), where X is any amino acid and B is a basic residue such Arg, His, or Lys, (*253*). It is hypothesized that the IGFBPs interaction with ECM may provide a local reservoir of IGFs (*254*).

The IGFBP variable midregion segment, ranging in size from 55 amino acid residues to 95 amino acids, functions as a hinge between the N-terminal and the C-terminal domains. Intriguingly, all the posttranslational modifications occurring in the IGFBPS have been found so far in this region. Among the posttranslational modifications analyzed, the most well characterised are glycosylation, phosphorylation, and proteolysis. No evidence of glycosylation has been found for IGFBP1 and 2, but IGFBP3 and 4 are N-glycosylated, whereas IGFBP5 and 6 are O-glycosylated (*250*). The ability to bind IGFs seems not to be affected by glycosylation, although other functions may be regulated, such as resistance to proteolysis (*250*).

Three of the six IGFBPs, IGFBP1, 3, and 5 are phosphorylated (*250*). The purpose of phosphorylating secreted proteins is still unclear, but some evidence suggests that phosphorylation enhances the affinity of hIGFBP1 for IGFs by 5 fold (*250*). Interestingly, phosphorylation of IGFBP3 can be upregulated by IGFs, and this event can affect the interaction of IGFBP3 with the cell surface or with the acid-labile subunit (ALS), typically complexed with IGFBP3 (*250*).

Proteolysis is a mechanism that ensures IGFBP availability and activity. It has been shown that cleavage by endoproteases generates fragments that have greatly reduced IGF-binding affinity (*250*). Usually IGFBP-degrading proteases are considered as growth stimulators, since they increase local IGF availability. This phenomenon is well illustrated in ovarian follicular development, where IGF actions are blocked by IGFBP4 during follicle atresia, and restored by the action of a IGFBP4 proteases, induced during follicular development (*250*).

No relevant insights have come as yet from genetic deletion of the *igfbp* genes. Transgenic analysis (*255*) showed more relevant inputs regarding the function of several binding proteins during postnatal development. IGFBP1-4 transgenic mice showed impaired brain development, altered glucose homeostasis, reduced body weight gain, hypoplasia of smooth muscle cells, and impaired fecundity. More analyses supported by tissue-specific gene deletion and overexpression will hopefully provide further insights of IGFBPs function.

1.5 IGF-1 SIGNALING

As described previously, the pleiotropic functions of IGF-1 reside mainly in its complicated genetic structure, in different post-translational modifications, and in tissue- and developmental-specific transcription and transcriptional regulation. Further complexity is provided by a tight regulation of the IGFBPs that bind IGF-1, inhibiting or activating its functions.

The IGF-1 signaling pathway arose early in the evolution, possibly as regulator of cellular proliferation in relation to nutrient availability (*256*). This signaling is conserved among invertebrates and vertebrates, and probably, in the first unicellular organisms (Yeast) was to regulate the capacity to survive during states of reduced metabolism (Figure 2.2). In all organisms, homologous players characterise IGF-1 signaling (Figure 2.2).

IGF-1 signals into the cells via activation of the IGF-1R, which, upon ligand binding, autophosphorylates 8 of the 15 tyrosine residues present in the cytoplasmic domain (*257*). Like IR, IGF-1R exists as covalent dimers of two αβ monomers in the unliganded state. Ligand binding favors receptors dimerization and activation. The immediate downstream mediators of IGF-1R activation are the members of IRS family. Interestingly, IGF-1R phosphorylates and activates preferentially IRS1, whereas IR preferentially interacts with IRS2 (*258*). This phenotype is reminiscent of the phenotype of *Irs1* and *Irs2* KO, which show diabetic phenotype and growth retardation respectively (*259*). In *Drosophila* the homologs of IGF-1R (Inr) and IRS (Chico) are structurally and functionally related to their mammalian counterparts.

Partial loss of *Inr* and complete loss of *chico* function result in dramatically reduced cell, organ and body size (*260*).

IRS activation can lead either to Ras-MAPK pathway through the adaptors Grb2 and SOS to stimulate cell proliferation (*261*), or to induction of the PI3K/AKT pathway, which is implicated in metabolism, growth and cell survival. Both signaling pathways are conserved in mammals and in *Drosophila* (Figure 2.2). Interestingly, mutations of the Drk- (Grb2 homolog) binding site in Chico is not required for Chico-mediated growth effects, in contrast to mutations on the PI3K binding site (*262*). The fact that an activated version of PI3K dramatically affects heart growth and cardiomyocyte size in mice shows that the biological growth function of this downstream mediator of IGF-1 signaling has been functionally conserved during evolution (*263*).

Mediators of PI3K downstream signaling are AKT, phosphoinositide-dependent kinase 1 (PDK1), and Target of Rapamycin (TOR), (Figure 2.2). AKT, also termed protein kinase B, is fully activated by binding of PIP3 in its PH domain, and by additional serine/threonine phosphorylation events mediated by PDK1 (*264*). Mutations analysis of AKT in *Drosophila* clearly showed that at least in flies, PI3K-induced growth is mediated by AKT, since loss of AKT function generates flies with severe impairment in cellular growth and decreased body size (*265*). Conversely, overexpression of AKT can cause overgrowth in the eye and wing tissues (*265*).

TOR was first discovered in budding yeast as a regulator of growth in response to nutritional alterations (*266*). Rapamycin inhibits the function of TOR by forming a complex with FK506 binding protein–12, which then binds a conserved region immediately upstream of TOR's kinase domain (*266*). TOR is known to respond positively to the presence of amino acids, and induces upregulation of translation through activation of ribosomal S6 kinase (p70S6K or S6K) (*267*). Exciting work in *Drosophila* has shown that TOR and S6K regulate growth. Loss of function of dTOR decreases cell size and growth in part through downregulation of S6K activity (*268*).

Interestingly, the same signaling is preserved in mammalian cells. In skeletal muscle, it has been reported that growth and hypertrophy are mediated by activation of the

AKT/mTOR pathway, leading to upregulation of the translational machinery (*137*), and that IGF-1 induces skeletal myotube hypertrophy by the PI3K/AKT/mTOR pathway. Moreover, the inhibition of mTOR activity by rapamicyn blocks compensatory hypertrophy *in vivo* (*137*). However, in mammalian cells the precise pathway connecting PI3K to the activation of p70S6K and consequently of the translational machinery is a matter of some dispute (*134*). It is interesting to note that, independently from AKT, PDK1 has been found to directly phosphorylate p70S6K (*134*), indicating that AKT has a dispensable role for signaling to p70S6K. It is noteworthy that mutational inactivation of PI3K and AKT in *Drosophila* still leaves S6K and, presumably, TOR activity intact, suggesting that TOR and S6K can reside in another pathway independent from PI3K (*268*). In the worm *Caenorabditis Elegans* inactivation of TOR produces a phenotype that partially resembles amino acid starvation (*269*), but not the developmentally delayed phenotypes caused by IGF/insulin pathway mutations.

Lately, another player in IGF-1 signaling has been discovered. Studies on *Caenorabditis Elegans* showed that the serum- and glucocorticoid-inducible kinase (SGK) forms a kinase complex with AKT1 and AKT2, upon activation of DAF2 (homologous of IGF-1R in mammals) and PDK1, to phosphorylate and inactivate DAF16 (homologous of forkhead-transcription factor FKHRL1). This mechanism accounts for dauer formation, development and stress tolerance (*270*). The authors showed that whereas AKT1 and AKT2 activation are important for regulating dauer formation, SGK activation is crucial for the control of development, stress response and longevity (*270*). In mammals, recent studies revealed that SGK plays an important role in cell survival signaling (*271*) (Figure 2.3), although the mechanisms distinguishing stress resistance, survival, and growth have not yet elucidated in higher organisms as it has been done in the worm.

In mammals, other signaling pathways are regulated by IGF-1 (Figure 2.3). The expression of the class 1/Ea IGF-1 isoform, termed mIGF-1, in post-mitotic myoblasts induced transcription of calcineurin (*2*). In this study, a cross-talk between calcineurin signaling and GATA activity has been observed. The calcineurin-activated transcription factor NFATc1 interacts with GATA2 in muscle overexpressing the

class 1/Ea IGF-1 isoform, and could account for the strong hypertrophic phenotype observed in mIGF-1 transgenic mice (*2*).

Finally, the survival signaling attributed to IGF-1 is mediated by AKT-induced inhibition of the pro-apoptotic factor Bad, inactivation of caspase 9 (*272*), and of forkhead family of transcription factors, FOXO (*273*). Interstingly, IGF-1/ PI3K/AKT-mediated inhibition of FOXO1 prevents expression of muscle atrophy-induced ubiquitin ligase, indicating that the signaling through inhibition of FOXO rescues, to some extent, deterioration of muscle fibers (*274*) (Figure 2.2).

2. IGF-1 SIGNALING AND FUNCTION IN THE HEART

The functions of IGF-1 in the heart have been extensively analyzed, although several groups reported different and contradictory roles of the growth factor *in vivo* and *in vitro*. The first demonstration that IGF-1 induces cardiac hypertrophy came from Ito and coworkers (*275*), who showed that fully processed IGF-1, which does not contain class 1 or 2/E peptides, increases the transcription of muscle specific genes, induced a two fold increase of cell size in neonatal rat cardiomyocytes, and promotes protein synthesis, indicating its functional role in regulating cardiac cell hypertrophy. These effects could be inhibited by addition of IGFBP3 to cultured cardiomyocytes, indicating that this binding protein could bind and inhibit IGF-1 (*275*). The signals leading to IGF-1-induced hypetrophy involves activation of IRS1, PI3K, ERK, and p90-S6 kinase (*276*). Supporting these data, the phenotype of transgenic mice overexpressing a constitutive active form of PI3K in the heart (*263*), displays evident cardiac hypertrophy and increased cardiomyocyte size. Contrasting with this phenotype, transgenic mice overexpressing dominant-negative PI3K have smaller hearts and individual fibers compared to wild-type littermates (*263*). More insights into IGF-1-induced hypetrophy come from transgenic overexpression of intermediary molecules in IGF-1 signaling. Overexpression of AKT is sufficient to induce cardiac hypertrophy without affecting systolic function (*277*). Cardiac hypertrophy induced by AKT overexpression is attenuated by rapamicin, indicating that hypetrophic signaling occurs through mTOR (*133*). Interestingly, rapamacin blocks the increase in cardiomyocyte size, resulting from oxidative stress (*278*), treatment with PE (*279*), or Angiotensin II (*280*).

In vivo, intravenous infusion of fully processed IGF-1, lacking class 1 or 2/E peptides, induced increased protein synthesis particularly in the heart, which was not accompanied by significant changes in blood glucose (*281*). Interestingly, administration of IGF-1 alone or in combination with Growth Hormone (GH) in normal adult rats increased the left ventricular weight compared with placebo-treated rats (*282*). It is important to stress that in all these animal models, IGF-1 significantly increases systolic and diastolic left ventricular function, without affecting collagen deposition, which usually accompanies cardiac overload-induced hypertrophy (*282-284*). These effects were evident in experimental postinfarction models, in which IGF-1, given early after myocardial infarction, improved left ventricular function, enhanced cardiomyocyte hypertrophy, and reduced adaptive fibrosis in non-infarcted myocardium (*283, 284*). In contrast to these studies, mice overexpressing a truncated form of human IGF-1 (IGF-1A, which does not encode class 1 or 2 signal peptides) under the control of an α-skeletal actin promoter induced physiological and then pathological cardiac hypertrophy, associated with decreased systolic performance and increased fibrosis (*135*).

In contrast to these studies, in which IGF-1 induced hypertrophy in a mechanism dependent from PI3K/AKT/mTOR signaling, different *in vivo* analyses emphasized the role of IGF-1 in inducing proliferation of cardiomyocytes. Transgenic mice generated with the human IGF-1B cDNA expressed in the heart showed no striking differences in heart size and cell volume when compared to control mice, but the number of myocytes in the heart was 55% higher in transgenic animals, indicating that overexpression of this IGF-1 isoform is coupled with myocyte proliferation (*136*). Supporting these data that argue for a proliferative function of IGF-1, a recent report showed that *in vivo* administration of IGF-1 in sheep did not stimulate cardiomyocyte hypertrophy but, on the contrary, led to a decreased percentage of binucleated cells (*285*). In culture, IGF-1 induces increased myocyte bromodeoxyuridine (BrdU) uptake dependently from PI3K and ERK activation (*285*). In another set of studies *in vitro*, cultured neonatal cardiomyocytes treated with an antisense probe to IGF-1 receptor, showed suppressed DNA replication, mitosis and cell proliferation (*286*). Moreover, the antisense treatment did not alter the expression of ANF in myocytes or

cellular hypertrophy (*286*), suggesting that IGF-1 controls cell division rather than cell growth.

IGF-1 has been shown to protect myocardium against death in animal models of infarct and ischemia-reperfusion injury. Qiong Li and co-workers (*287*) showed that mice overexpressing the human IGF-1B under the control of the rat α-myosin heavy chain (α-MHC) promoter respond to coronary ligation with attenuated increase in diastolic wall stress, cardiac weight, ventricular dilatation, and hypertrophy, due mainly to a prevention of cardiac cell death. In a model of ischemia-reperfusion, rats treated with IGF-1 presented reduced myocardial apoptosis and injury (*288*). In other reports, IGF-1 was shown to protect against apoptosis in cultured (*289*) and primary cardiomyocytes (*182*).

The beneficial effects of IGF-1 in animal models match well the results from human clinical trials. IGF-1 has been used to improve cardiac performance in human patients suffering from cardiac failure (*290, 291*). Growth hormone (GH) deficiency in humans causes numerous defects, and the heart and the cardiovascular system are also affected. Patients with GH-deficiency show decreased left ventricular mass (*292*), and replacement treatment with both GH and IGF improved notably cardiac performance and morphology (*293*). Despite these promising indications, further studies need to be employed to verify the clinical importance of IGF-1 and to understand whether a coadjuvant therapy with IGFBPs and GH can be salutory in certain cardiac diseases.

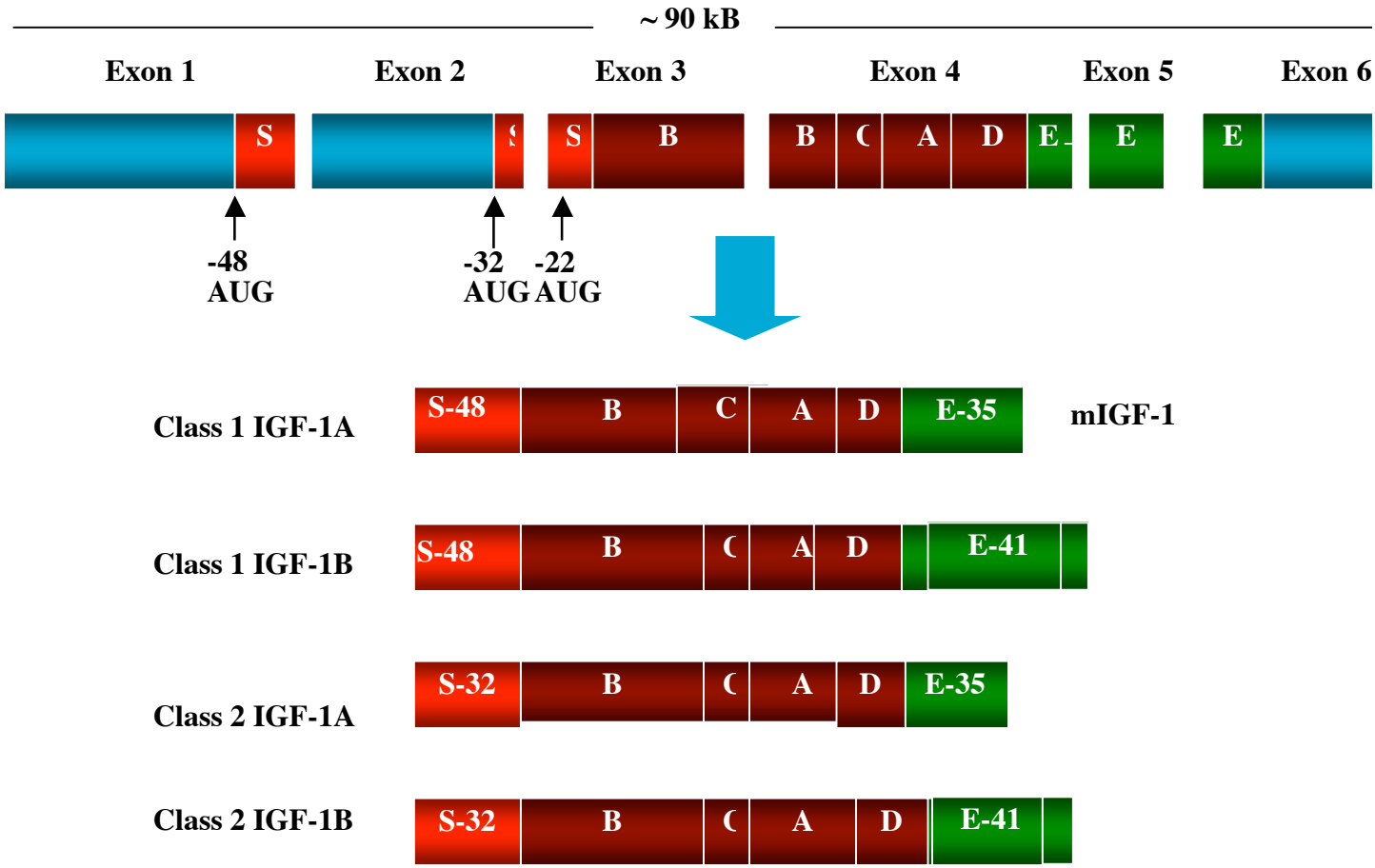

FIGURE 2.1: Schema of the rat *igf-1* gene and derived IGF-1 mRNAs. Red boxes indicate different spliced signal peptides; green boxes different spliced E peptides. The brown boxes represents the mature IGF-1 peptide. The different splicing sites generate Class 1 and Class 2 peptides. The arrows indicate different starting sites on exon 1 and 2.

Winn N *et al*; *Cold Spring Harbor symposia on Quantitative Biology*, Vol LXVII, 2002

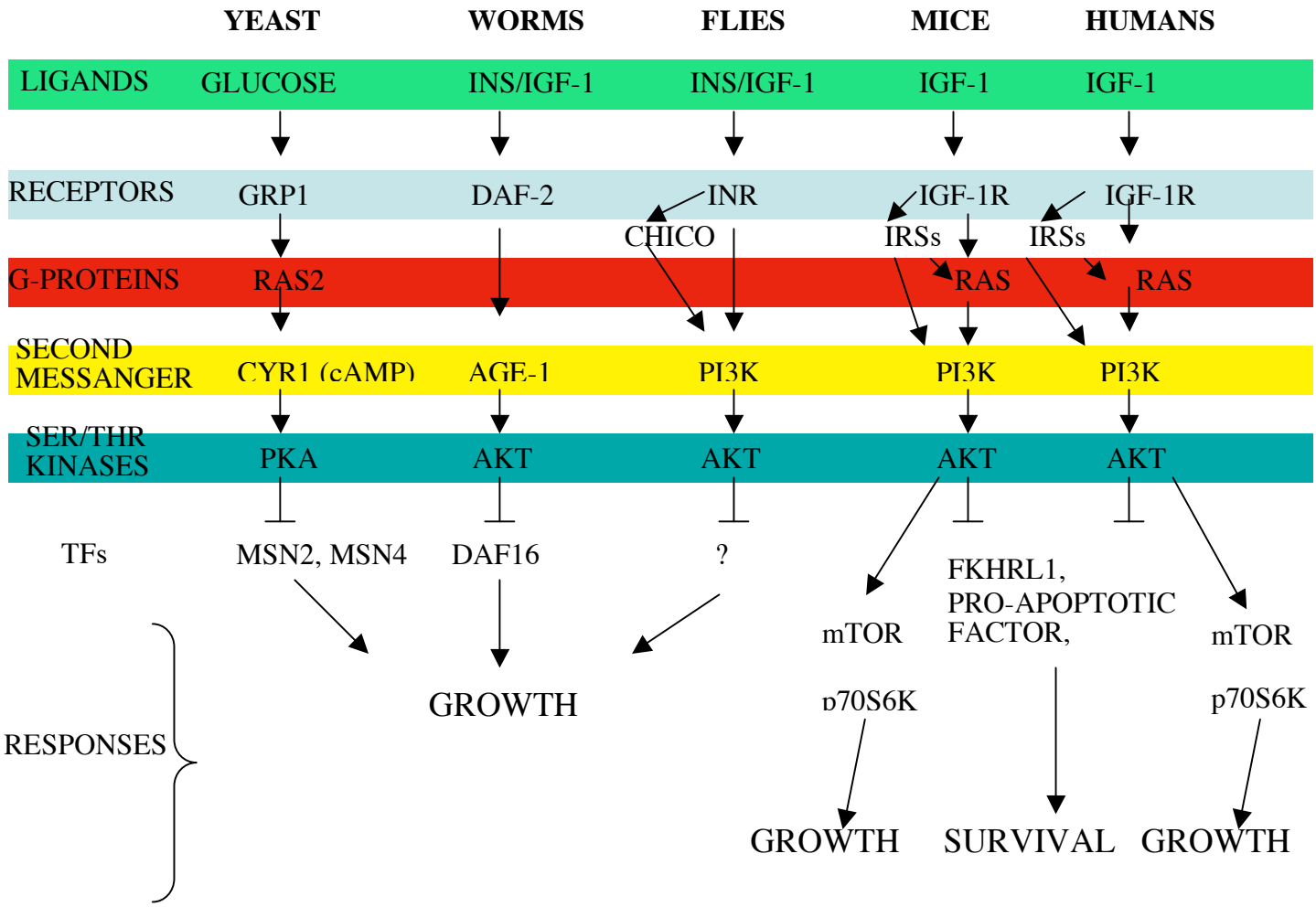

Figure 2.2: Conserved regulation of IGF-1 signaling promoting survival and growth.

Longo V.D.and Finch C.E. 2003, Science, 299: 1342-1345.

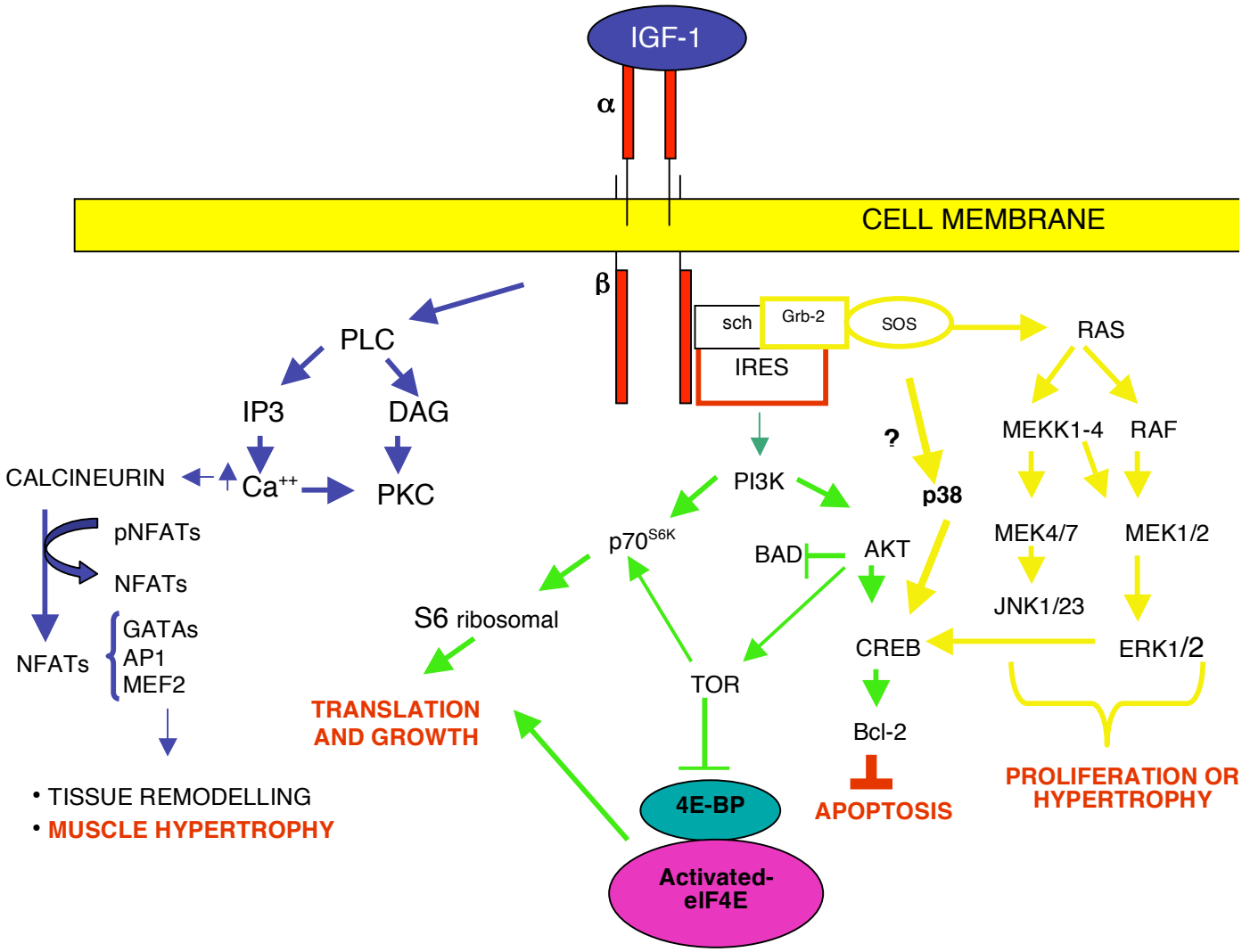
IGF-1
α
CELL MEMBRANE
β
PLC
IP3
DAG
CALCINEURIN
Ca++
PKC
pNFATs
NFATs
NFATs
GATAs
AP1
MEF2
• TISSUE REMODELLING
• MUSCLE HYPERTROPHY
sch
Grb-2
SOS
IRES
RAS
MEKK1-4
RAF
?
PI3K
p38
p70S6K
BAD
AKT
MEK4/7
MEK1/2
JNK1/23
S6 ribosomal
CREB
ERK1/2
TOR
Bcl-2
TRANSLATION AND GROWTH
APOPTOSIS
PROLIFERATION OR HYPERTROPHY
4E-BP
Activated-eIF4E

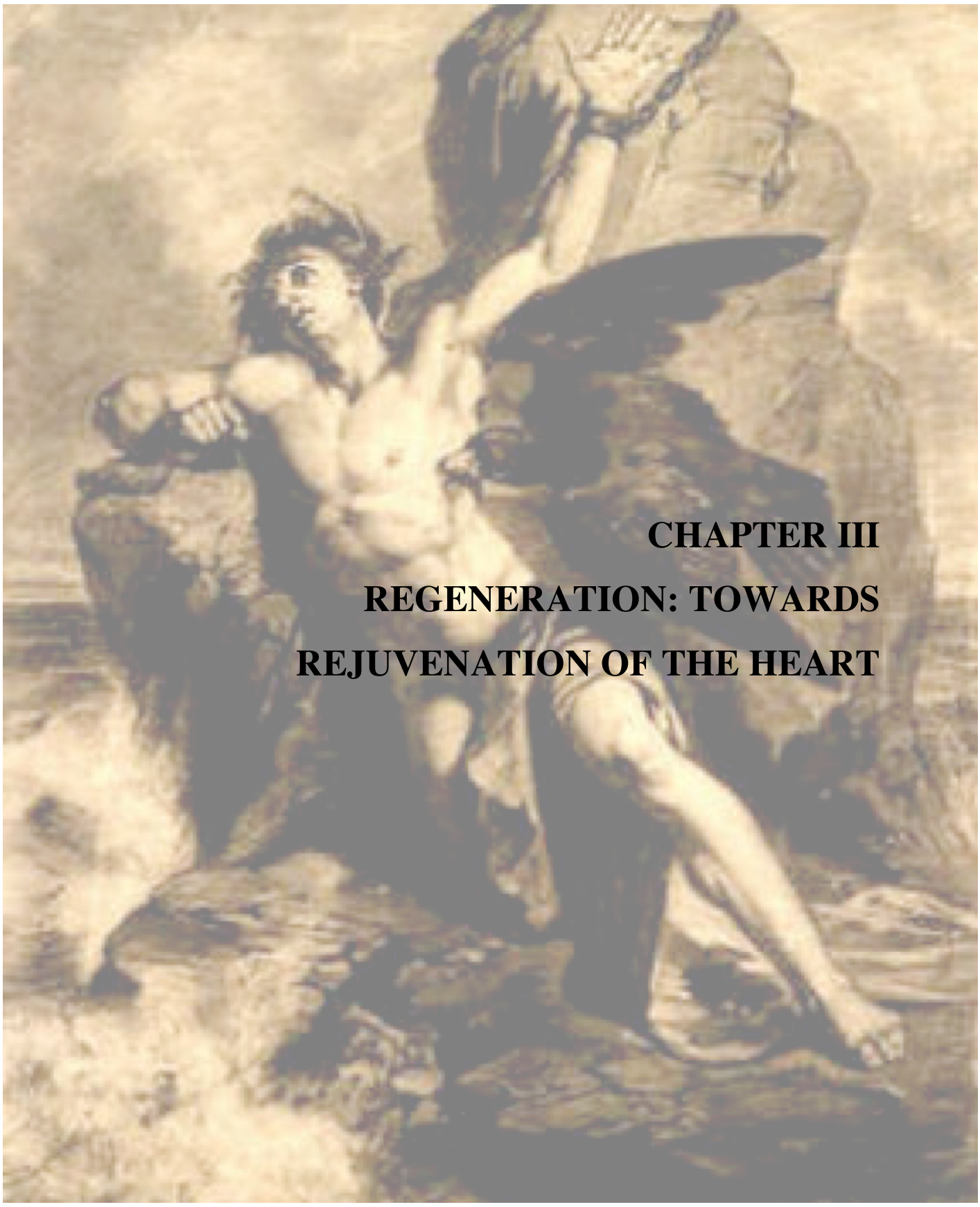

CHAPTER III

REGENERATION: TOWARDS REJUVENATION OF THE HEART

1. REGENERATION: EVOLUTIONARY MECHANISMS

Wound repair in most vertebrate organs is dominated by a fibro-proliferative response leading to scar formation. The injured organ is not restored at its original physiological state, but it is rather patched (*294*). The only adult vertebrates that have the incredible capacity to restore the complete structure, the morphogenesis and functionality of an entire organ are the urodele amphibians, newt and axolotl. The adult newt can regenerate its limbs upon distal amputation (at level of radius and ulna), or mid-proximal amputation (at level of mid-humerus) (*295*) (Figure 3.1). Interestingly, newt can regenerate jaws, lens, retina, and large sections of the heart in response to molecular events that signal tissue removal or damage (*296, 297*), (Figure 3.1).

Urodele amphibian limb regeneration proceeds through a series of cellular events that are elusive in mammalian cells. After amputation epithelial cells cover the stump area and form the wound epidermis; the mesenchymal cells underlying the wound epidermis enter to cell cycle, and the cartilage, the connective tissue and muscle cells lose their differentiated features, re-enter cell cycle, and form the blastema with the mesenchymal cells (Figure 3.1) (*296*). Transplantation experiments showed that the urodele strategy of regeneration of most structures is due to the re-specification of differentiated cells to give rise to local progenitor cells, since limb blastema cells produce an ectopic limb after relocation to the anterior chamber of the eye (*298*). De-differentiation, as it occurs in newt limb regeneration, is a very well defined process involving two main cellular tasks: loss of a differentiated phenotype to acquire a proliferative capacity. It has been found that a thrombin-activated serum factor can drive differentiated salamander myotubes back into the cell cycle, but does not cause loss of proteins normally expressed in differentiated cells, such as muscle myosin expression (*299*). This serum factor appears to be important also for trans-differentiation of retinal PECs to lens, and, although not tested, it is likely that it is also required for heart and lens regeneration (*300, 301*).

In mammals, there are few examples of regeneration *in vivo*, other than liver regeneration and deer antler seasonal regeneration (*295, 302*). Although these impressive capacities suggest that higher vertebrates can to some extent regenerate,

most organs lose this capacity, when the damages overwhelm the homeostatic ability of single tissues to restore missing structures.

Why are some animals able to regenerate complex organs and structure, after tissue removal or amputation, and others apparently not? Interestingly, regeneration is a conditions that can vary among the individuals belonging to the same species (*296*). In 24 urodele species, 4 to 6 species showed little or not regenerative capacity (*296*). It has been argued that regeneration is an evolutionary variable (*303*), lost in some species for secondary reasons, not yet understood, but representing a basic, primordial attribute of metazoans.

Interestingly, Harty and collegues (*304*) hypothesized that the regenerative capacity of lower vertebrates resides in their unspecialized immunological systems. Regenerating urodeles appear to be immunodeficient compared to anurans, which have lost the capacity to regenerate. Although urodeles possess T and B lymphocytes and a diverse repertoire of Ig and T-cell antigen receptor genes, humoral immunity is mediated only by IgM and is apparently amnestic (*304*). A correlation between the changes in regenerative capacity, immune system, and scarless wound healing in *Xenopus* development also supports this view (*304*). So far it has been concluded that the components of adaptive immunity that emerge during vertebrate development are likely to account for scar formation and missing regenerative processes after injury (*304*). Although not sufficient to explain the signaling and cellular properties acquired during regenerative processes, the importance of immunodeficiency in urodeles is a tempting hypothesis to be experimentally analyzed in higher vertebrates.

2. CARDIAC REGENERATION

The traditional concept that cardiomyocytes are terminally differentiated cells (*120, 305, 306*) has changed in the last years, and recent studies have shown that adult hearts in physiological and pathological conditions contain a certain number of mitotic figures (*307-309*). Precisely, mitotic indexes between 0.03% (zone distant from infarct) and 0.08% (zone adjacent to infarct) were measured *post mortem* in patients who died after myocardium infarction (*307*). A mitotic index of 0.9% was reported in cardiomyocytes of female hearts transplanted into male recipients (*309*). However, the observed mitotic indices indicate that the process would need to be manipulated and enhanced to achieve clinical relevance in cases of post-infarct repair. So far clinical investigation accompanies and sometimes precedes the biological studies, in order to find the relevant cells that can heal a damaged heart.

Stem cell research has opened a new propelling field of analysis. Stem cells are defined by their ability to self-renew and to form one or more differentiated cell types (*310*). A clear division of the stem cell family can be drawn between those isolated from the embryo, and termed embryonic stem cells, and those in adult somatic tissues, known as adult stem cells. Embryonic stem (ES) cells have the greatest potential for organ regeneration, because of the diversity and number of cell types that they can produce. The versatility of ES cells is counterbalanced by their side-effects, and by ethical problematics that limit the studies and the applications of these cells.

Adult stem cells retain far more plasticity than was originally thought. Bone marrow derived progenitor cells were able to repair the heart of animals that underwent myocardial injury (*311, 312*). Improved cardiac function was observed when bone marrow progenitor cells expressing the receptor for stem cell factor (*c-kit*) but not differentiation markers (*lin-*) were injected directly into the infarcted hearts of mice, (*311*). Interestingly, recent studies showed that while bone marrow derived progenitor cells trans-differentiated into nearly all the haemopoietic and endothelial lineages, very few were fated to cardiomyocytes, suggesting that new blood vessel formation and increase in blood supply could account for the observed cardiac improvement (*313*).

Skeletal muscles maintain a resident population of stem cells, termed satellite cells, which are normally quiescent, but can be activated by conditions where muscle repair or hypertrophy are required (*314*). These cells were transplanted successfully in the infarcted heart, but in several studies no trans-differentiation into cardiomyocytes was observed, and even in cases of rare trans-differentiation, the cells were not electromechanically coupled with the recipient myocardium (*315*).

The existence of putative cardiac stem cells in the myocardium itself has generated much excitement. Cells expressing a progenitor phenotype ($Lin^{-}ckit^{+}$ and $Sca1^{+}$ markers) were isolated from animal heart tissue. These cells were considered a cardiac stem cell pool, or a cardiac stem cell-like pool, because they expressed cardiac markers like GATA4 or myosin, and lack of markers of haematopoietic or endothelial lineage, and for their capacity to self-renew, for their clonogenicity and multipotentiality. When transplanted into the infarcted area they seemed to improve cardiac function (*316, 317*).

Whatever the nature of the stem cells, three basic steps of clinical importance have to be considered: mobilization, homing and differentiation. Several factors seem to regulate mobilization and homing, such as stem cell factor (SCF) and stromal cell derived factor (SDF-1) respectively (*318*). Differentiation is so far precluded by the usage of non-committed cells that are potentially unable to differentiate in functional cardiomyocytes. A number of clinical trials are currently testing the efficacy and safety of using autologous bone marrow-derived or circulating stem cells to promote myocardial repair. Transplantation of skeletal myoblasts has resulted in ventricular arrhythmias, while stem cells trials have not indicated heart beat dysfunctions (*319*). Preliminary results of some trials injecting bone marrow or circulating stem cells directly into the heart have suggested beneficial therapeutic effects (end-systolic volume, stroke volume, regional contractility), without apparent adverse side-effects (*320*). Although it is difficult to draw landmark conclusions, these improvements encourage further research. However it must be emphasized that preliminary results have been generated from short-term, non-randomised trials, with low patient numbers. Moreover, the question of whether the applied stem cells act by improving tissue perfusion, or regenerate cardiac myocytes remain unresolved.

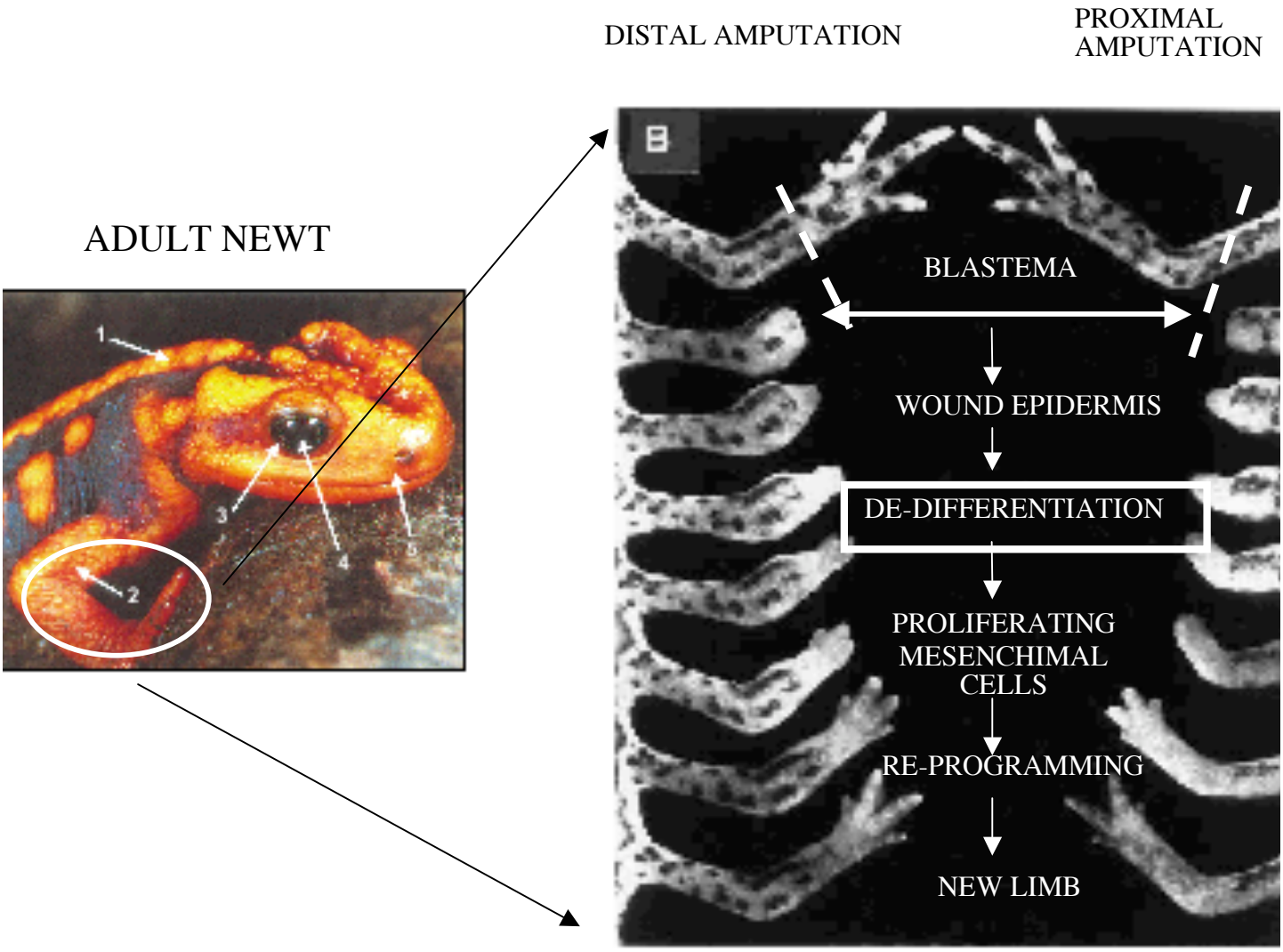

Figure 3.1: Newt limb regeneration. The newt is the only adult vertebrate that can regenerate. Regeneration occurs with the formation of a blastema enriched of proliferating mesenchimal cells and de-differentiated cartilage, muscle and bone cells. The last step includes re-programming of the proliferating cells in all the components of the limb. 1 Dorsal crest; 2 limb; 3 retina; 4 lens; 5 jaws

PART II

CHAPTER IV

MATERIALS AND METHODS

1. GENERATION OF α-MHC/mIGF-1 TRANSGENIC MICE

We generated transgenic mice (FVB) with a rat mIGF-1 cDNA driven by the mouse α-MHC promoter (*321*). *mIgf-1* insert was excised and purified to avoid introduction of vector sequences into the transgene. Transgenic mice were generated by standard methods. Transgenic mice were selected by PCR using tail digests. The animals were housed in a temperature-controlled (22°C) room with a 12:12 hour light-dark cycle. All the analyses were performed on male mice.

2. RNA PREPARATION AND NORTHERN BLOT ANALYISIS

We obtained total RNA from wild-type and αMHC/mIGF-1 transgenic hearts by RNA-TRIZOL extraction (Gibco-BRL). Total RNA (10μg) was analyzed on 1.3% agarose gels and hybridized as described (*322*).

3. HISTOLOGICAL ANALYSIS

Mice at different ages were anesthetized before cervical dislocation, and hearts were perfused with 4% paraformaldehyde (PFA) as previously described (*311*), then excised and embedded in paraffin. Paraffin sections (10μm) were stained with hematoxylin and eosin to analyze morphological features of the hearts. Connective tissue was visualized by using Masson's Tricrome stain as described by Manufacture (Sigma). Cell size was analyzed by measuring the apparent size of single nuclear cells in a 40X magnification. 10 sections (10μm) from wild-type and transgenic hearts were used for cell measurement. Cells were measured in the left ventricle. Statistic analysis was performed as described below.

4. CARDIAC INJURY

3-4 months old wild-type and transgenic mice were anesthetized by Avertin injection (0.1ml/10g of a 2.5% solution). The tongue was retracted and a tracheal cannula (1.3 x 1 mm, OD x ID, Harvard Apparatus) was inserted into the trachea. The cannula was attached to the mouse ventilator (Model 687, Harvard Apparatus) via the Y-shaped connector. Ventilation was performed with a tidal volume of 200 μl and a respiratory rate of 120/min. The chest cavity was opened in the left fourth intercostal space. The heart was exposed and 25 μl of 10μM cardiotoxin (Latoxan) were injected in the heart

wall of the left ventricle. The chest cavity, the muscle, and the skin were then closed by a 6-0 silk suture.

5. ECHOCARDIOGRAPHY

Eight 13 week-old males from both strains were weighed and slightly anaesthetized with pentobarbital (30mg/kg i.p.) to allow an analysis for cardiac anatomy and function on a Sonos 5500 (Hewlett Packard) with a 15MHz linear transducer (15L6) (Philips Ultrasound, USA). The images were stored in a digital format on a magnetic optical disk for review and analysis. The left hemithorax was shaved and an ultrasound transmission gel was applied to the precordium. The heart was first imaged in the two-dimensional mode (2D) in the parasternal long-axis view to obtain the aortic root dimensions. The aortic flow velocity and the heart rate (HR) were measured with pulsed-wave Doppler on the same section. The sample volume cursor was placed in the aortic root and the transducer angled slightly, which allowed aortic flow parallel to the interrogation beam so that maximum aortic flow velocity was obtained easily. The cardiac output (CO) was calculated from the following equation: $CO=0.785xD^2xVTIxHR$ where D is the internal diameter of the aortic root and VTI is the velocity-time integral of the Doppler aortic spectrum. Then the pulsed Doppler window was placed between the tip of the mitral valve leaflets to record the mitral inflow velocities. The maximal speed of the early (E) and late (A) mitral filling were measured as well as the mean deceleration time of the E wave (DT) and the duration of the A wave (Adur). By placing the Doppler between aortic flow and mitral valve, the isovolumetric relaxation (IVRT) time was measured. Left ventricular cross sectional internal diameters in end-diastole (LVEDD) and in end-systole (LVESD) were obtained by an M-mode analysis of a 2D-short axis view at the papillary muscle level. The ejection and shortening fractions were calculated. From this view, the diastolic septum (S) and posterior wall (PW) thicknesses were measured. The left ventricular mass (LVM) was calculated with the following formula: $LVM=1.055x[(S+PW+LVEDD)^3-(LVEDD)^3]$. All the measurements were performed on, at least three beats, according to the guidelines of the American Society of Echocardiography.

6. NON INVASIVE BLOOD PRESSURE AND HEART RATE

All measurements were performed in eight 16 week-old conscious male animals of both strains on a BP-2000 blood pressure analysis system (Visitech Systems, USA) during 5 consecutive days.

7. ELECTROCARDIOGRAM

Eight 17 week-old male mice of both strains were anaesthetized with tribromoethanol (2.5% solution, 13μL/g body wt SC) and were recorded with the 4 arms of the ECG leads attached at the origin of each paw by unipolar and bipolar lead derivations. The signal was recorded by an electrocardiograph (EKG-Burdick, Siemens) connected to a data acquisition system (MP100 and Acknowledge Software, Biopac Systems Inc).

8. IMMUNOHISTOCHEMISTRY AND BrdU ANALYSIS

BrdU (Sigma) was administered *ad libitum* at 0.1% in the drinking water or injected intraperitoneally once a day at 100μg/g. Hearts were perfused with 4% PFA and embedded in paraffin. Sections were stained with anti-BrdU (BD-Pharmingen) as prescribed by the manufacture. The amount of positive nuclei was measured by counting all nuclei and BrdU positive nuclei in 10 sections (10μm) of wild-type and transgenic hearts, bordering and covering the cardiotoxin injured side. We used a 40X magnification as field of analysis. An average of 200 nuclei was found in each field assayed in both wild type and transgenic hearts. The percentage of BrdU positive nuclei was calculated based on total nuclei amount. Statistical analysis was performed as described below.

Immunofluorescent analysis was performed on paraformaldehyde (4%) fixed-frozen sections (10 μm) with BrdU antibody purchased from Amersham. Myosin antibody (Sigma) was used at 1:250 to stain cardiac myocytes, and nuclei were visualized with Hoechst at a concentrtion of 1:1000.

9. WESTERN BLOT

Hearts from wild-type and transgenic mice were excised and the excess of blood was removed by washes in PBS 1X. Hearts were lysated in buffer containing 20mM Tris-HCl (pH 8.0), 150 mM NaCl, 5mM $MgCl_2$, 10% glycerol, 1% Triton, 0.5% NP40, supplemented with 1mM proteases and phosphatases inhibitor cocktail. 50 μg of

proteins were loaded onto SDS-PAGE gel and blotted on PVDF membrane. Phospho-AKT (Pharmingen), Phospho-S6 (Cell Signaling), phospho-JNK (Santa Cruz), and phospho-ERK (Santa Cruz) were used at a concentration of 1:500 in 5% BSA. The blots were normalized for AKT (Transduction Laboratories), S6 ribosomal protein (Cell Signaling), JNK (cell Signaling) and ERK (Cell Signaling). MEF2C, GATA4 and Nkx2-5 were purchased form Santa Cruz and used at 1:250. Phospho-histone H3 and histone H3 (Cell Signaling) were used at 1:500 in 5% BSA.

10. REAL TIME PCR AND REVERSE TRANSCRIPTASE PCR

1μg of RNA was used to set up the reaction of reverse transcription as prescribed by Manufacture (Promega). Real time PCR was performed using 10 μl of the Syber Green DynamoTM Master Mix (Finnzymes, Espoo, Finland), along with 1μl of cDNA and 0.75 μM of each primer in a total reaction volume of 20 μl. Duplicated samples were incubated at 95º for 3 min, followed by 45 cycles of amplification (95º, 10 sec; 56º, 20 sec; 72º, 30 sec). Results for each cytokine were normalized to ubiquitin ligase expression.

11. PRIMERS

IL1β, forward 5'-acatcaacaagagcttgacccaggc-3' reverse 5'-agctcatatggtccgacagcacga-3'; IL6, forward 5'-aggataccactcccaacagacgtg-3' reverse 5'-gtagctatggtactccagaagacc-3'; IL10 forward 5'-ccaagccttatcggaaatg-3' reverse 5'-tggccttgtagacacc-3'; IL4 forward 5'-catcggcattttgaa-3' reverse 5'-cgtttggcacatccatctcc-3'; GAPDH forward 5'-tgggtgtgaaccacgaa-3' reverse 5'-acagctttccagaggg-3'; ANP forward 5'-atgggctccttctccatcaccctg-3' reverse 5'-tcggtaccggaagctgttgcagcc-3'; BNP forward 5'-atggatctcctgaaggtgctgtcc-3' reverse 5'-gcgttacagcccaaacgactgacg-3'; β-myosin heavy chain forward 5'-ctgagcagaagcgcaatgcagagtcgg-3' reverse 5'-ctcctcattcaggcccttggcaccaatg-3'; α-skeletal actin 5'- atgtgcgacgaagacgagaccacc-3' reverse 5'-gccacatacatggcaggcacgttg-3'; Glucose transporter 1 (Glut1) forward 5'-gatcccagcagcaagaaggtgacg-3' reverse 5'-tggagaagcccataagcacagcag-3'; β-actin forward 5'-taaaacgcagctcagtaacagtccg-3' reverse 5'-tggaatcctgtggcatccatgaaac-3'.

12. PHOSPHOPROTEIN SCREEN

Hearts were excised and washed in PBS 1X to remove the excess of blood. Each one gram of chopped tissue was lysated in 4 ml of lysis buffer as described by Manufacture (Kinexus, www.kinexus.ca/pdf/informationpackage.pdf). 500µg of total protein amount was used to perform the KPSS-4.1 phopshoprotein screen. The Kinetworks analysis involves resolution of a single lysate sample by SDS-PAGE and subsequent immunoblotting with panels of up to three primary antibodies per channel in a 20-lane Immunetics multiblotter. The antibody mixtures were carefully selected to avoid overlapping cross-reactivity with target proteins. The comparison report compared the trace quantity of the known protein from each screen type against all relevant samples. The Corrected data were obtained by trace quantity standardization for all samples.

13. ECHOCARDIOGRAPHY IN REGENERATING HEARTS

Eight 13 week-old males from both strains were analyzed for echocardiography one month after CTX injection in the left ventricle wall. The mice were weighed and slightly anaesthetized by Avertin injection (0.1ml/10g of a 2.5% solution). Cardiac anatomy and function were measured with a Vevo 660 (VisualSonic) Ultrasound, and by the use of a 630 RMV (real-time-micro-visualization) scanhead (Visualsonic). The analysis performed resulted very sensitive due to the high-resolution images that the VisualSonic Ultrasound can acquire. The left hemithorax was shaved and an ultrasound transmission gel (Parkers Laboratories Inc.) was applied to the precordium. The heart was imaged in the two-dimensional mode (2D) in the parasternal short-axis view to obtain left ventricular cross sectional internal diameters in end-diastole (LVEDD) and in end-systole (LVESD) dimension by an M-mode analysis. The ejection and shortening fractions were calculated. From this view, the diastolic and systolic posterior wall (PW) thicknesses was also measured.

14. STATISTICS

All comparisons between wild-type and transgenic mice were performed by means of paired Student's t tests. A significant difference was considered when $p<0.05$.

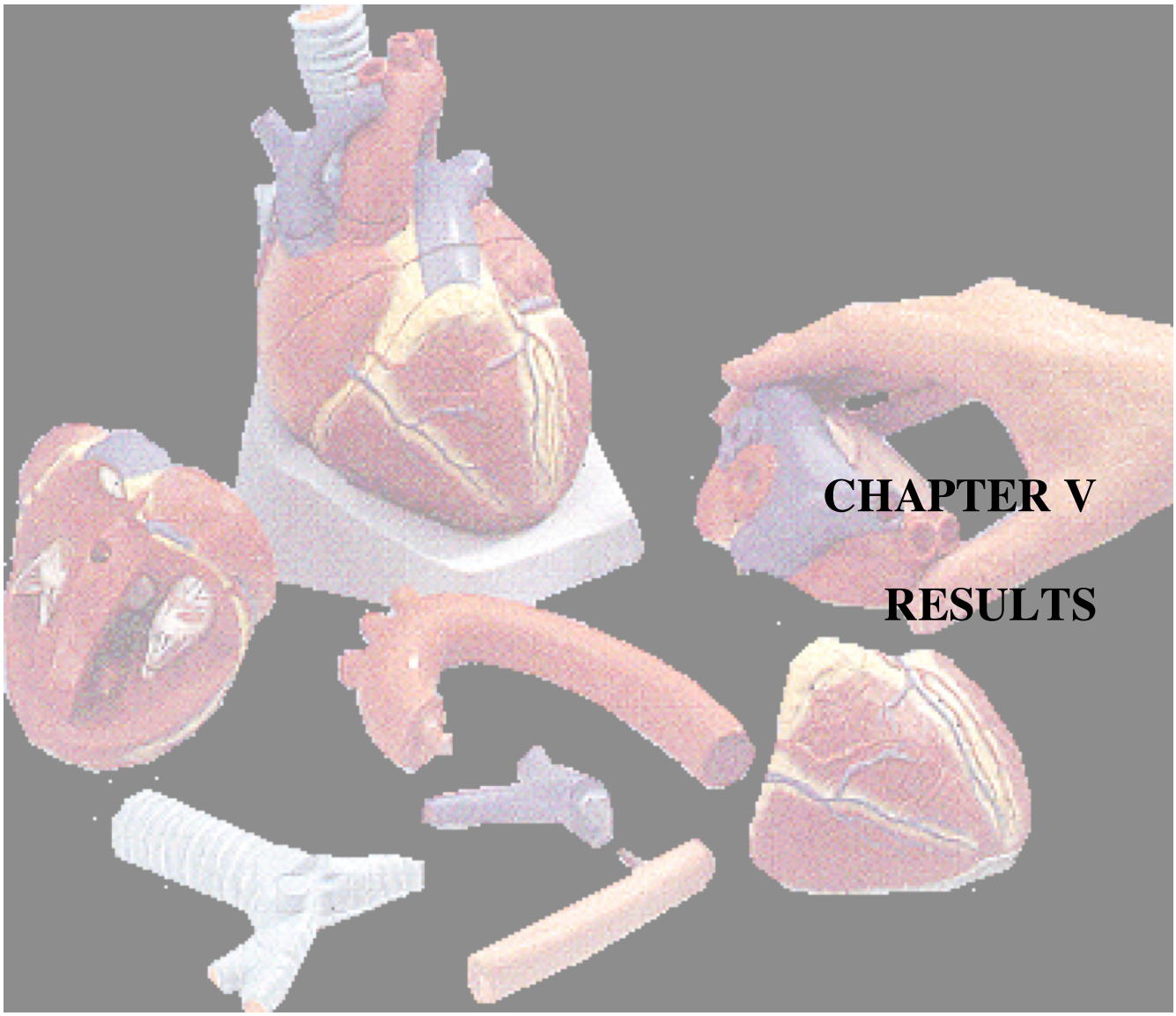

CHAPTER V

RESULTS

1. Cardiac-restricted expression of mIGF-1 transgene

We generated transgenic mice with a rat mIGF-1 cDNA driven by the mouse α-MHC promoter (Figure 5.1A) (*321*). Transgenic mice developed normally with no perturbation in reproduction and breading. Initial characterisation of three α-MHC/mIGF-1 transgenic lines with variable transgene expression levels revealed similar cardiac phenotypes. Cardiac-restricted mIGF-1 transcript expression levels increased with age in all founders tested and reached a steady-level at two months (Figure 5.1B). Expression of the transgene in adult mice was restricted to the heart (Figure 5.1C), and endogenous levels of IGF-1 were undetectable in other tissues using the rat probe. A single transgenic line was selected for further analysis (F018).

2. mIGF-1 overexpression is associated with increased ventricular mass and heart size

Postnatal transgenic mIGF-1 hearts displayed accelerated cardiomyocyte hypertrophy, precociously attaining wild-type adult heart size (Figure 5.2A). The morphological effects of mIGF-1 overexpression were analyzed in hearts from wild-type and transgenic mice at different time points of development (from E18 up to six months). Whereas wild-type and transgenic hearts were comparable in morphology and size at E18 and two days after birth (data not shown), the mIGF-1 transgenic hearts showed an increase in size at an age of one week (Figure 5.2A), that persisted at one and two months. In contrast to other transgenic models of cardiac IGF-1 over-expression, the transgenic hearts showed a comparative size with wild-type hearts at six months (Figure 5.2A). The ratio heart weight/body weight significantly ($p>0.05$) increased in mIGF-1 overexpressing hearts at 1W, 1M and 2M, but it was comparable at six months, indicating that mIGF-1 overexpression induces accelerated growth in the heart, with unknown compensatory mechanisms at adult age (Figure 5.2A). A comparison of cellular components showed a clear increase of cell size in transgenic hearts compared to wild-type hearts (20%+/-1.8%; p-value 0.0002), (Figure 5.2B).

3. mIGF-1-induced hypertrophic response is associated with a moderate diastolic and systolic dysfunction

Comparable to the histological analysis previously described, echocardiography performed on eight wild-type and transgenic mice showed that mIGF-1 mice exhibit a 20% concentric left ventricular hypertrophy ($p<0.05$ *vs* controls), all walls being involved in the same extent (Table 2). This increase in the cardiac mass is associated with a prolongation of the rate of ventricular repolarization, as attested by augmentation of the QT interval on the electrocardiogram (Table 2). In transgenic male mice, echocardiography identified a small but significant decrease of cardiac contractility, demonstrated by the 13% decrease of the ejection fraction and fractional shortening ($p<0.05$). Nevertheless, this level of contractility preserved the resting cardiac output ($p>0.05$ *vs* controls) and arterial blood pressure ($p>0.05$ *vs* controls), despite the trouble of the diastolic function. This dysfunction was identified by the 21% decrease of the E/A ratio ($p<0.05$), and the prolongation of the A wave duration (+14%). These two abnormalities were not linked to any prolongation either of the isovolumetric relaxation time, or of the mean deceleration time of the E wave ($p>0.05$). In most of the transgenic mice, an increase in the P wave amplitude was observed on electrocardiograms (Table 2) attesting to an atrial dilatation.

4. mIGF-1 signals through time-dependent regulation of MAPKs and sustained activation of S6 ribosomal protein

To better dissect the signaling activated in response to mIGF-1 overexpression, specific markers of heart hypertrophy were analyzed by reverse transcriptase PCR. Cardiac hypertrophy was related to higher expression levels of ANP at 1 and 2 months, without any further significant change (Figure 5.2C). Other markers underlining cardiac hypertrophy, such as BNP, α-skeletal actin, β-myosin heavy chain, and glutamate transporter 1 were not affected (Figure 5.2C). These results suggest that IGF-1 induces a time-dependent increase of specific hypertrophic markers when locally overexpressed.

It has been shown that heart remodeling and hypertrophy are correlated with MAPK activation in cardiac and skeletal muscle (*173*), and that cell growth mediated by IGF-1 overexpression in skeletal muscle cell lines induces S6 ribosomal protein

phosphorylation in a mechanism dependent upon activation of mTOR (*323*). To elucidate the signaling regulated by local mIGF-1 overexpression in the heart, total tissue protein extracts were analyzed by Western blot to detect the phosphorylation levels of the MAPKs, ERK1/2 and JNK. We detected a strong increase in ERK1/2 and JNK phosphorylation at one week in the mIGF-1 transgenic hearts. At the same age, JNK activation mirrored the increased phosphorylation of c-Jun, a downstream target of activated JNK. Both kinases returned to activation levels comparable to wild-type hearts at two weeks (Figure 5.3A). By one month, kinase activation was undetectable in both wild-type and mIGF-1 transgenic hearts (Figure 5.3A). Interestingly, the phosphorylation level of the proliferation marker histone H3, showed a marked decrease at one week of age in transgenic hearts (Figure 5.3A), indicating that mitotic activity is downregulated earlier during postnatal development of mIGF-1 transgenic hearts compared to wild-type hearts.

Cardiac-specific genes are regulated early during the first phases of heart development by the activation of specific transcription factors, such as MEF2C, GATA4 and Nkx2-5 (*7, 42*). We analyzed the expression levels of these transcription factors to trace a possible involvement of mIGF-1 in their regulation. None of these specific proteins were observed to be differentially expressed between wild-type and transgenic hearts, beside a slight increase of MEF2C levels in transgenic hearts at two days after birth (Figure 5.3B). By contrast, mIGF-1 transgenic hearts maintained sustained S6 ribosomal protein phosphorylation during all ages analyzed, whereas the activity of the protein in wild-type hearts displayed a more modulated regulation, with a strong activation at two months and decreased phosphorylation at four and six months (Figure 5.3D). Phosphorylation levels of AKT remained unchanged in mIGF-1 transgenic hearts (Figure 5.3C), indicating that mIGF-1-mediated regulation of the translational machinery is independent of AKT activity in cardiac tissue.

To analyze in detail the signaling regulated by mIGF-1 overexpression in the heart, a phosphoprotein screen has been performed on wild-type and mIGF-1 transgenic heart lysates by Kinetworks analysis (Kinexus Bioinformatic Corp.). The analysis showed that AKT pathway leading to S6 phosphorylation is not affected (Table 1). mTOR and p70S6 kinase phosphorylation levels were also not changed (33 CPM for control

wild-type *vs* 26 CPM for transgenic hearts) or detected respectively in mIGF-1 transgenic mice compared to wild-type littermates (Table 1). It is interesting to note that, independently from AKT, PDK1, an alternate downstream mediator of PI3K, has been found to directly phosphorylate p70S6K (*324*), indicating that AKT has a dispensable role for signaling to p70S6K. Interestingly, our data showed a strong activation of PDK1 (241CPM in wild-type hearts *vs* 507 in mIGF-1 transgenic hearts; Table 1). Our studies uncover new physiological activated targets of the mIGF-1 signaling, which are still under investigation.

Taken together these results showed that remodeling of the hearts overexpressing the local IGF-1 isoform was related to the activation of MAPKs signaling in an early precise time-window of postnatal heart development, and to a sustained regulation of the translational machinery. Both mechanisms were independent of AKT activation, but dependent on PDK1 activation, pointing out an unexpected role for a different kinase downstream the IGF-1 signaling.

5. mIGF-1 overexpression induces heart regeneration upon cardiotoxin (CTX) injury

We previously reported that mIGF-1 increases regeneration of skeletal muscles in response to pathological stimuli (*2*). To elucidate its role in heart regeneration, heart injury was induced by injection of CTX venom in the wall of the left ventricle. This snake venom acts on skeletal and cardiac muscle cells, blocking their contractile capacity and inducing cell death. Infarction by CTX injection presented several advantages compared to the more widely used technique LAD ligation – mediated infarction. First damage caused by injection of this venom is localized and controlled better among the different animals tested. Second, the mortality percentage is lower with respect the LAD ligation, allowing the analysis of a higher number of animals in each independent experiment.

The effects of CTX were analyzed at different time-points (48 hours, 1 week, and 1 month) after injection of wild-type and mIGF-1 transgenic hearts. At 48 hours and one week after injury, both wild-type and mIGF-1 transgenic hearts presented a localized and defined area of cell death and massive inflammation in both ventricles

(Figure 5.4A). Notably, mIGF-1 transgenic mice sustained a higher dosage of CTX injection, performed by a double injection of 10 μM of venom, compared to a higher mortality in wild-type animals undergoing the same regimen (data not shown). One month after injury the mIGF-1 transgenic hearts showed a well defined repair of the injured tissue compared to wild-type hearts, where massive scar formation was observed (Figure 5.4B and 5.4C).

6. mIGF-1 induces heart regeneration by lowering the inflammatory response

Myocardial infarction is associated with an inflammatory response, ultimately leading to scar formation (Figure 1.9) (*325*). To dissect the possible mechanisms leading to scarless transgenic heart healing, we performed real time PCR and reverse transcriptase PCR in wild-type and mIGF-1 transgenic hearts after 24 hours and one week from injury, using primers specific for cytokines involved in pro-inflammatory (IL6 and IL1β) and anti-inflammatory response (IL10 and IL4). The pro-inflammatory IL6 was down-regulated after 24 hours from CTX injection in mIGF-1 transgenic hearts, whereas wild-type hearts showed increasing mRNA levels of IL6 (Figure 5.5A). IL1β was not affected by CTX injection in wild-type and mIGF-1 transgenic injured hearts (Figure 5.5A), indicating that certain pro-inflammatory cytokines have a specific role in the heart in response to CTX injury.

The analysis of the anti-inflammatory cytokine IL10 by real time PCR showed a significant (p-value 0.0073) increase in mIGF-1 transgenic hearts after 24 hours from injury (36% compared to wild-type), and to a greater extent at one week (45% compared to wild-type), whereas the level of the cytokine is lower in wild-type injured heart compared to uninjured tissue (Figure 5.5B). IL4 was also significantly (p-value 0.03) upregulated in mIGF-1 transgenic hearts 1 week after injury, but to a lower extent than IL10 (20% compared to wild-type) (Figure 5.5B).

Taken together these results showed that mIGF-1 overexpression induces repair of the damaged heart without scar formation, and by lowering specific molecules involved in the inflammatory response occurring normally after injury.

7. mIGF-1 promotes increased cell proliferation one month after CTX injection

Although compelling evidence of cardiac renewal occurring throughout life in the myocardium has been extensively proved as part of cardiac homeostasis (chapter III) (*326, 327*), the complete regenerative program in cases of extended injury is precluded in mammalian heart by fibrotic tissue formation and consequent cardiac function impairment.

Our analysis suggested that the process of regenerative growth and the formation of new myocardial tissue involve modulation of the inflammatory response and changes in cytokines signaling. The myocardial tissue restoration observed in mIGF-1 overexpressing hearts could result from cardiac cell proliferation. To assess cardiac hyperplasia we assayed cell cycle by measuring the nuclear incorporation of bromodeoxyuridine (BrdU), a marker of DNA synthesis, 48 hours, 1 week, and 1 month after CTX injection. No differences in the proliferative state were found in injured heart 48 hours (13%+/-4% transgenic *vs* 16%+/-5% wild-type) and 1 week (27%+/-5% transgenic vs 32%+/-11% wild-type) after CTX injection (Fig 5.6C). The mIGF-1 transgene induced 14%+/-0.8% of total cells to enter cell cycle one month after infarct induction (Figure 5.6B and Figure 5.6C) compared to wild-type hearts (Figure 5.6A and Figure 5.6C). This increase is significant (p-value 0.0003), and explains the regeneration and myocardial reconstitution induced by mIGF-1 overexpression in response to tissue damage. We found cardiac cells that had re-entered to cell cycle (Figure 5.7A, B), although cells of diverse lineage were found in the myocardium and in the vessels (Figure 5.7A, B). The nature of these cells is still under investigation.

8. mIGF-1 induces restoration of cardiac function after CTX injection

To test whether mIGF-1-induced regeneration was accompanied also by a recovery of cardiac function, the left ventricle of 8 wild-type and mIGF-1 transgenic hearts was injected with CTX and analyzed with a high-resolution ultrasound system after one month. Transgenic hearts showed integrity of the posterior wall and normal echocardiography profiles (Figure 5.8B) compared to wild-type hearts (Figure 5.8A). Measurement of posterior wall thickness showed a significant decrease in the wild-type hearts in both diastolic and systolic parameters compared to mIGF-1 transgenic

hearts (diastole-WT 1.13 +/- 0.12 mm, diastole-TG 1.48 +/- 0.10 mm; systole-WT 1.42 +/- 0.17 mm, systole-TG 1.95 +/- 0.09 mm) (Figure 5.8D). We used two parameters to measure cardiac function. Mean values of ejection fraction (EF) and fractional shortening (FS) were significantly impaired in wild-type hearts when compared to mIGF-1 transgenic hearts (EF 61.5%+/- 6.55% compared to 78.27%+/- 2.88%; FS 33.9%+/-3.7% compared to 46.66 +/-3.48%) (Figure 5.8C), suggesting that mIGF-1 induced morphological and functional regeneration. Taken together these data suggest that the regeneration program, following the early-induced repair program, is activated as a later step in mIGF-1 overexpressing hearts (Figure 5.9).

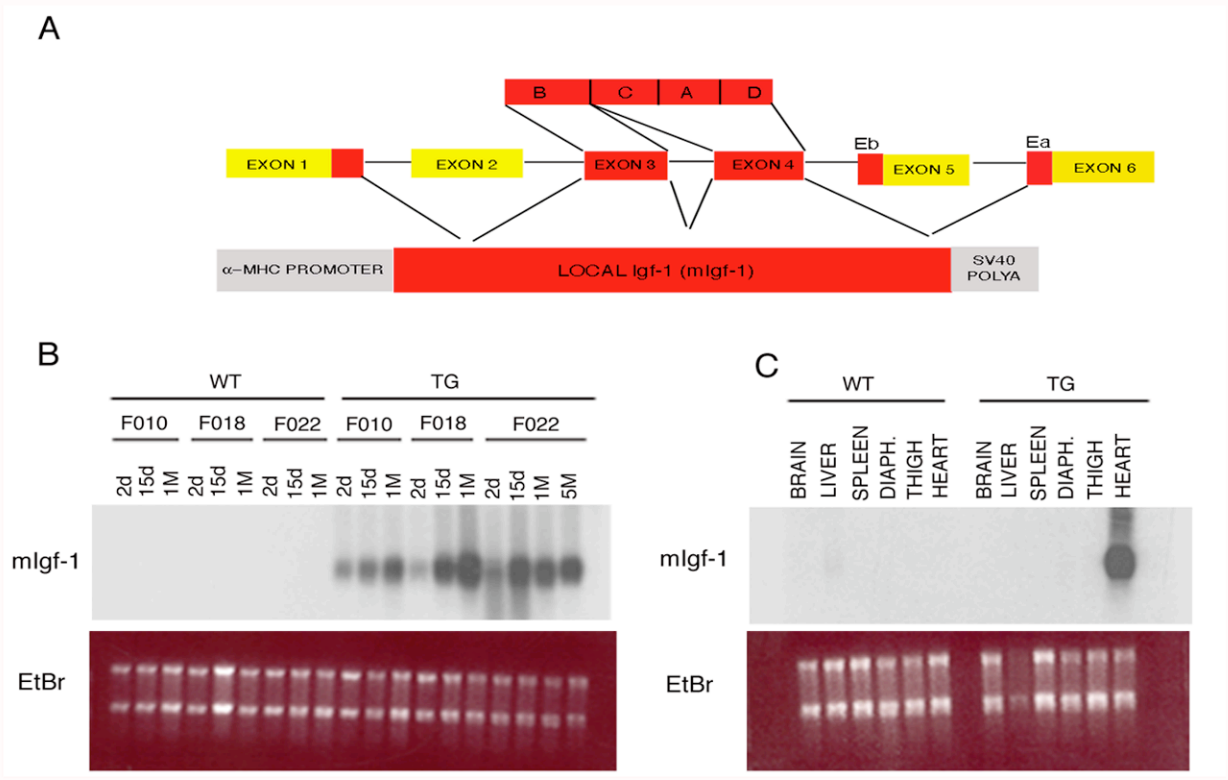

Figure 5.1: Characterization of MHC/mIGF-1 transgenic mice. (A) Schematic representation of the rodent *Igf1* gene. (B, C) Northern blot analysis of total RNA (10 µg) from different aged wild type and transgenic hearts, using the rat *Igf-1* 32P-labeled probe. Ethidium Bromide was used to verify equal RNA loading amount and RNA integrity

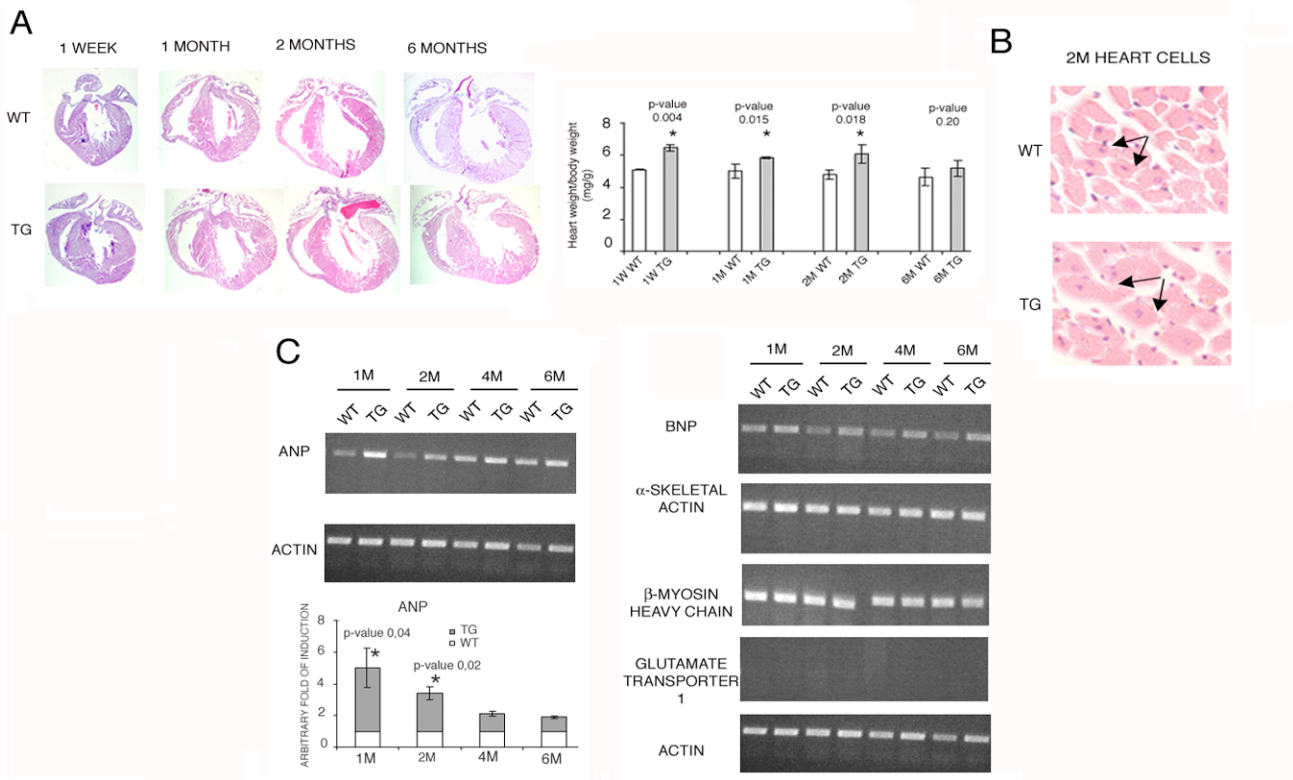

Figure 5.2: Physiological analysis of mIGF-1 transgenic hearts. (A) Histological analysis of wild-type and transgenic hearts by Hematoxylin and Eosin staining. Values are the average of six independent analyses. (B) Cell size differences in wild-type (upper picture) and transgenic (lower picture) hearts. Hearts of 2 months old mice were stained with Hematoxylin and Eosin. Cells with single nuclei were considered in the analysis to avoid false positive size from cells containing more the one nucleus. Values are the average of three independent experiments. (C) RT-PCR of the hypertrophic markers. 0.5 µg of total RNA was used for each single PCR. PCR values were normalized for β-actin content. Densitometric analysis was performed on three independent experiments. The stars indicate significative values increasing in transgenic hearts compared to wild-type (p-value<0.05).

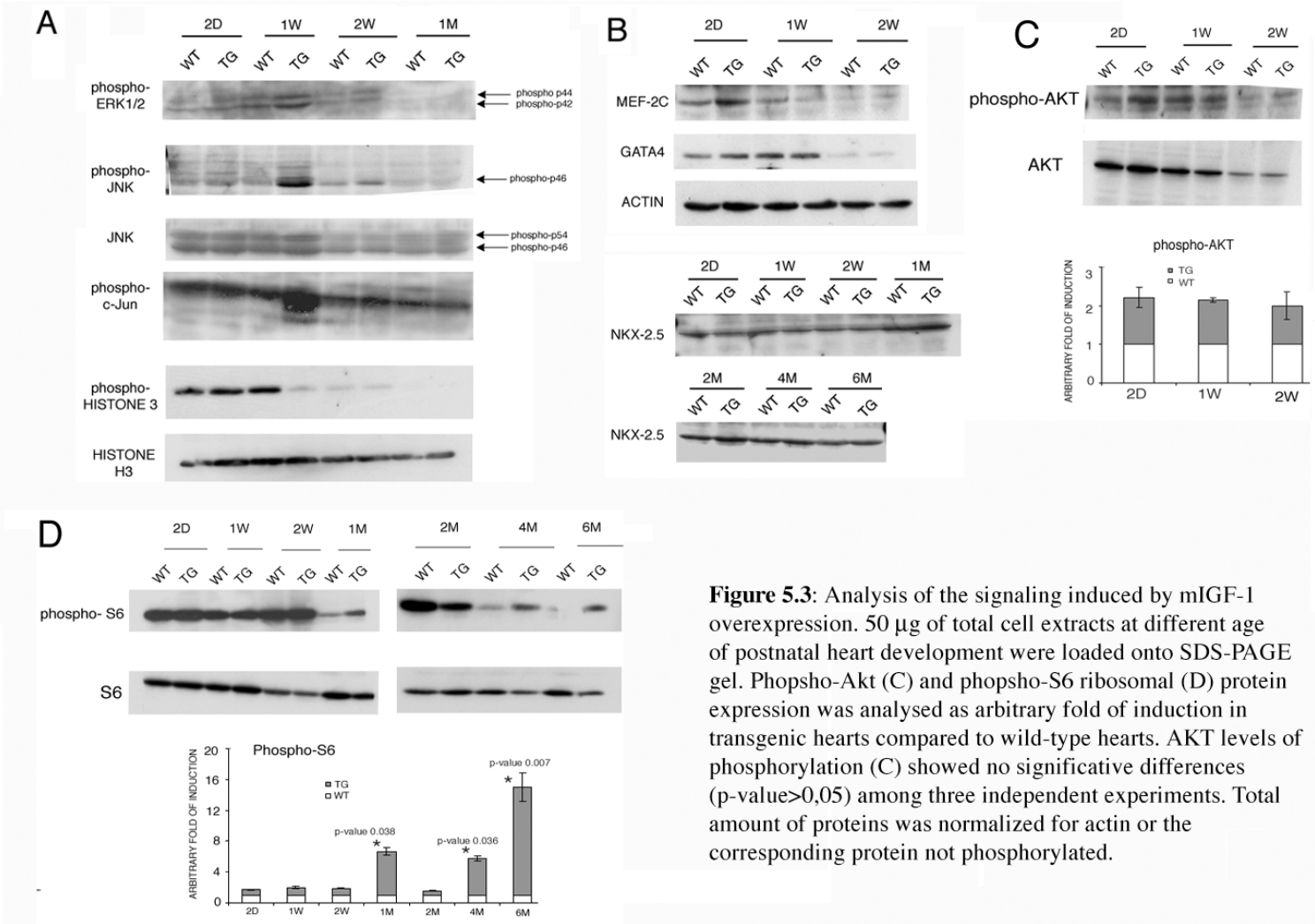

Figure 5.3: Analysis of the signaling induced by mIGF-1 overexpression. 50 µg of total cell extracts at different age of postnatal heart development were loaded onto SDS-PAGE gel. Phopsho-Akt (C) and phopsho-S6 ribosomal (D) protein expression was analysed as arbitrary fold of induction in transgenic hearts compared to wild-type hearts. AKT levels of phosphorylation (C) showed no significative differences (p-value>0,05) among three independent experiments. Total amount of proteins was normalized for actin or the corresponding protein not phosphorylated.

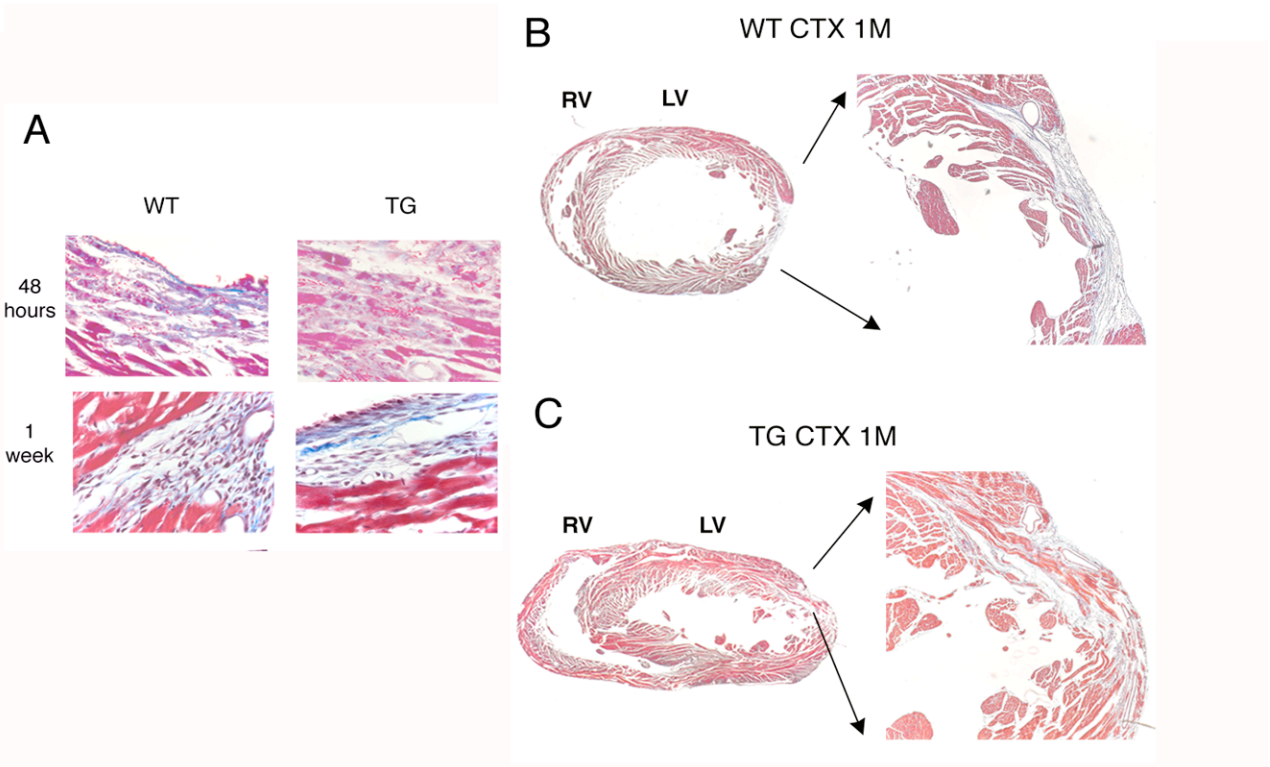

Figure 5.4: Full cardiac regeneration in mIGF-1 transgenic mice. (A, B and C) Thricrome staining of 4 months old wild-type and transgenic hearts at 48 hours, 1 week, and 1 month after CTX injection in left ventricle wall. Comparable results were obtained with similar analyses on six different groups of animals.

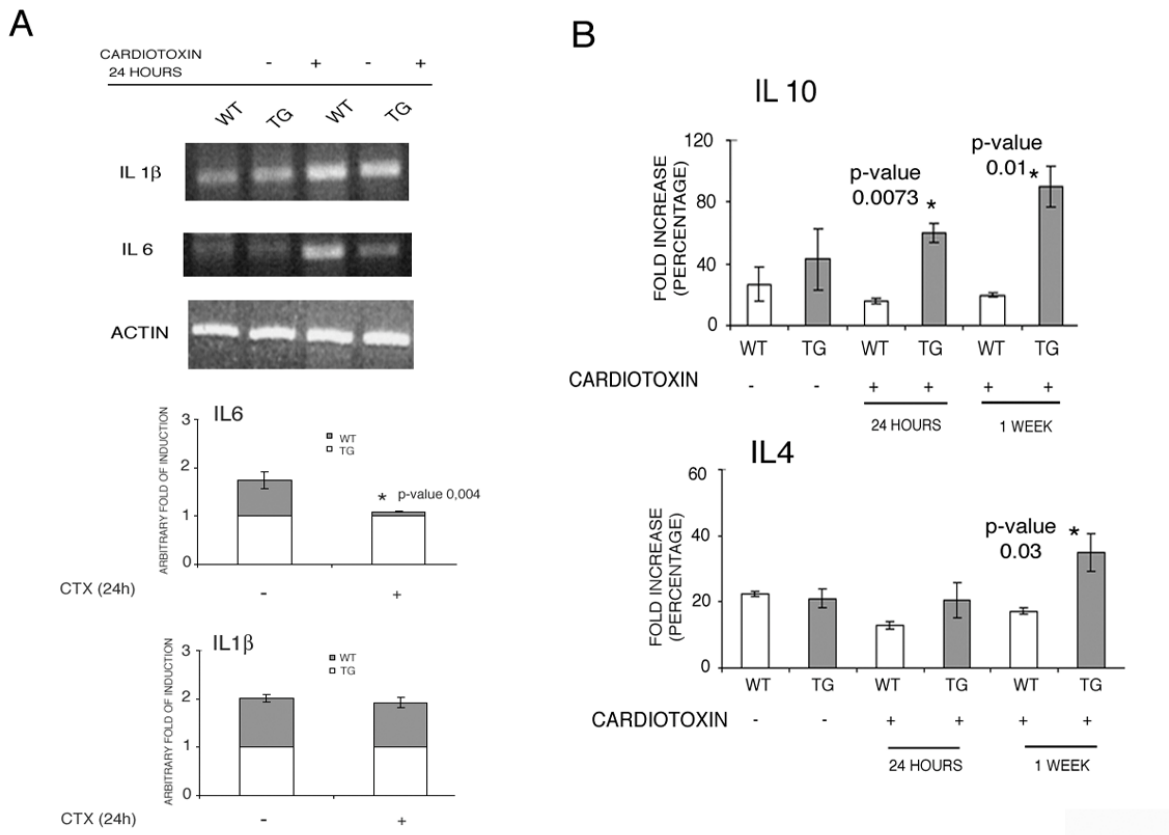

Figure 5.5: Early events characterizing mIGF-1 induced regeneration. (A) RT-PCR of inflammatory interleukins IL6 and IL1β 24 hours after CTX injection in wild-type and transgenic hearts. PCR was normalized by β-actin content in each sample. Arbitrary fold of induction was calculated in three independent experiments. Transgenic IL6 and IL1β expression were analysed respect to wild-type expression. (B) Real time PCR of the anti-inflammatory cytokines IL10 and IL4 in transgenic and wild-type hearts 24 hours and 1 week after CTX injection. The stars indicate significative values increasing in transgenic hearts compared to wild-type (p-value<0.05).The results are the average of three independent experiments.

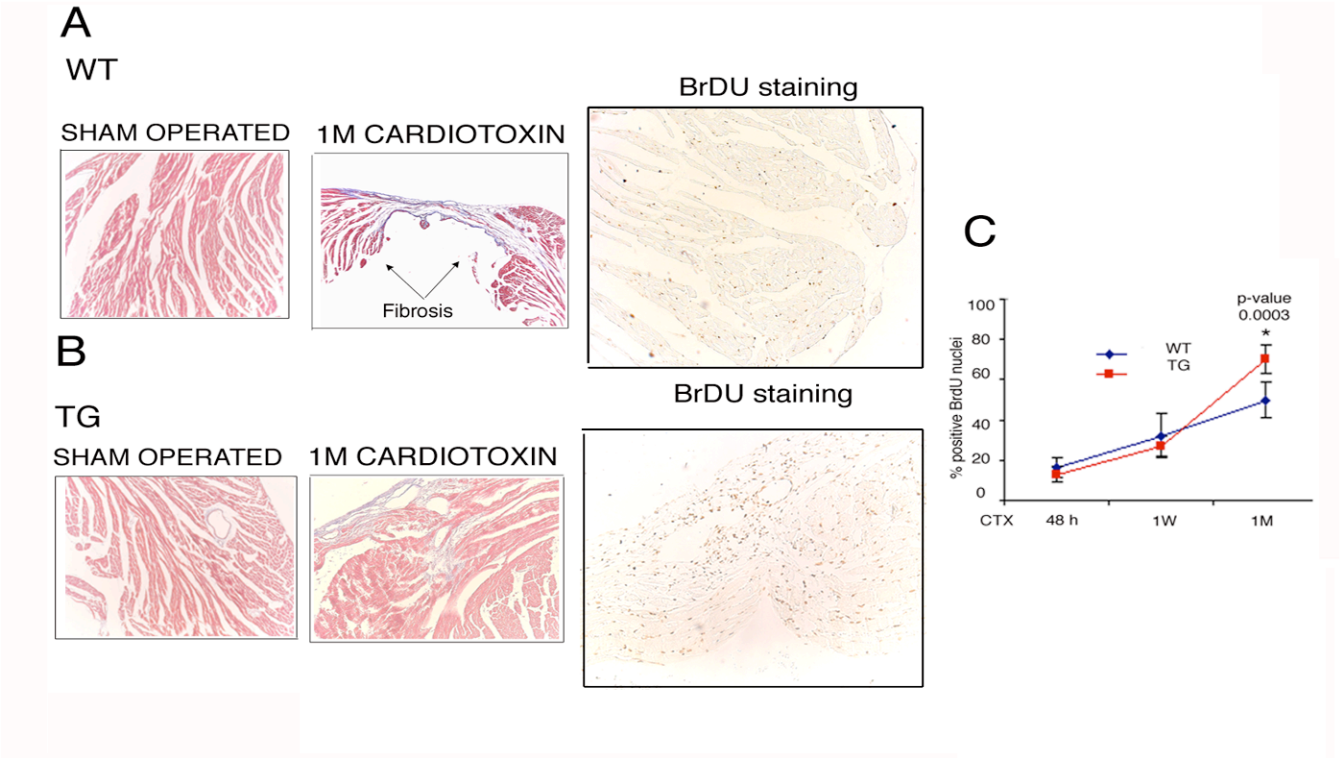

Figure 5.6: Cell proliferation accompanies mIGF-1 induced heart regeneration. BrdU was provided ad libidum for 1 month after CTX injection at 0.1% or injected intraperitoneally at 100µg/g once a day for 2 days or 1 week. Paraffin sections (10 µm) were stained with a biotynalated mouse monoclonal antibody to visualized nuclei that incorporated BrdU in wild type (A) and transgenic (B) hearts. 10 sections bordering the injured site were analysed. (C) Statistical analysis of BrdU positive cells counted at different time points after CTX injection. The values reported are the average of three independent experiments. 10 sections for each analysis were analysed and the percentage of positive nuclei was calculated based on the amount of total nuclei present in the frames observed. The star indicates significative values increasing in transgenic hearts compared to wild-type (p-value<0.05).

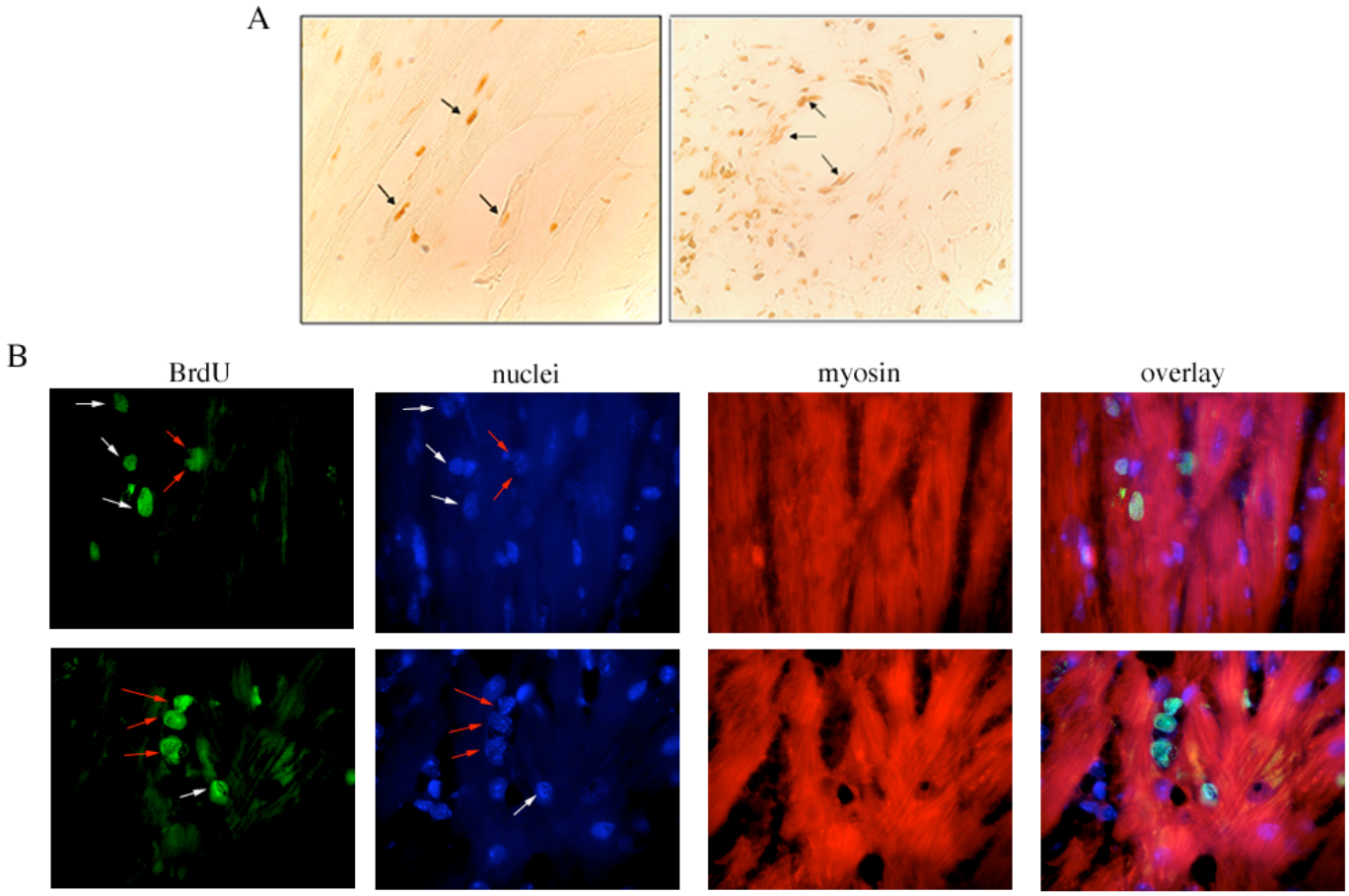

Figure 5.7: Typization of proliferating cells. (A) Paraffin sections (10µm) were stained with anti-biotinylated-BrdU antibody and magnified at 60X. Arrows show cardiac cells in the first picture and cells of different lineage around a vessel in the second picture. (B) Immunofluorescnt analysis of BrdU positive cells. Cardiomyocytes were visualized by an anti-myosin antobody. Most of cells positive for BrdU were not cardiomyocytes as shown by red arrows. White arrows show possible cardiac myocytes. The sections were magnified with a 100X objective.

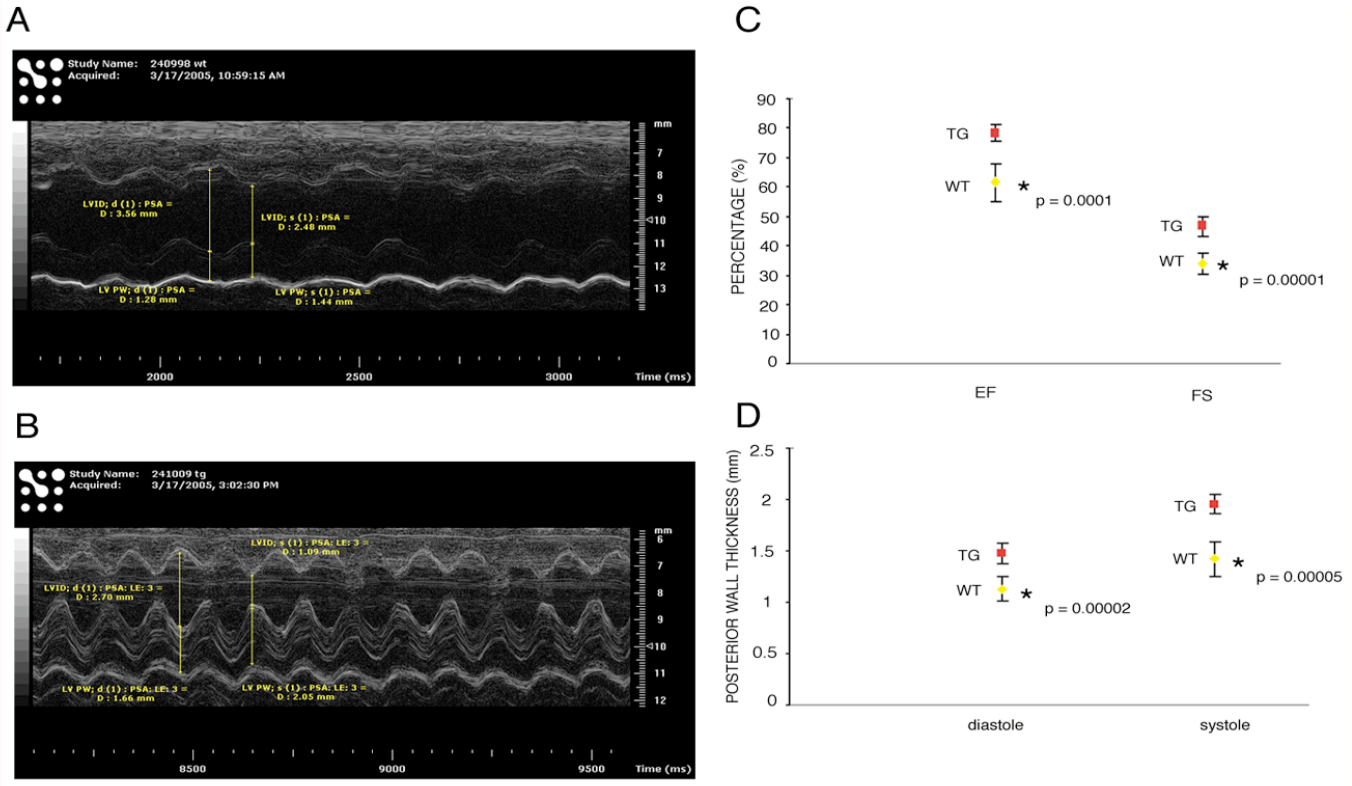

Figure 5.8: Echocardiography of CTX-injured hearts. Wild-type (A) and transgenic hearts (B) were analyzed one month after CTX injection with the Vevo 660 Ultrasound to record heart functionality. Pictures show measurement in systole and diastole of the left ventricle dimension (LVID), and the left ventricle posterior wall (LVPW). The measurements were recorded with a 630 RMV scanhead in parasternal short axis (PSA). (C, D) Eight wild-type and transgenic mice were used to average percentages of ejection fraction (EF) and fractional shortening (FS), and thickness of the posterior wall. Each mouse was analyzed with three different measurements, and the values are representative of averages between intra- and inter-measurements. The stars indicate significative differences calculated with the student's T-test, assuming $p<0.05$.

		WT Heart Normalization (CPM)	TG Heart Normalization (CPM)	WT Heart (%)	TG Heart (%)
90 kDa Ribosomal S6 Kinases (S380)	RSK1/2 Lane 7				
90 kDa Ribosomal S6 Kinases (T573)	RSK1/2 Lane 5				
AMP-activated protein kinase alpha (T172)	AMPKa Lane 9				
Bone marrow X (Eph-like) kinase (Y40)	BMX (Etk) Lane 5				
Bruton's tyrosine kinase (Y223)	Btk Lane 15				
Calcium/calmodulin-dependent kinase II (T286)	CaMK2 Lane 15				
Cyclin-dependent kinase 1 (T161)	CDK1 Lane 19				
Cyclin-dependent kinase 1 (Y15)	CDK1 Lane 16				
elF4E binding protein (S65) (16)	4E-BP1 (16) Lane 6				
elF4E binding protein (S65) (17)	4E-BP1 (17) Lane 6				
elF4E binding protein (S65) (18)	4E-BP1 (18) Lane 6				
Extracellular signal-regulated kinase 1 (T202/Y204)	ERK1 Lane 14	99	123	Control	24%
Extracellular signal-regulated kinase 2 (T185/Y187)	ERK2 Lane 14	53	62	Control	17%
Glycogen synthase kinase-3 alpha (S21)	GSK3a Lane 2				
Glycogen synthase kinase-3 beta (S9)	GSK3b Lane 2				
I-kappa-B kinase alpha (S180)	IKKa Lane 9				
I-kappa-B kinase beta (S181)	IKKb Lane 9	49	43	Control	-12%
Lyn (Y507) (44)	Lyn (44) Lane 20	214	184	Control	-14%
Lyn (Y507) (46)	Lyn (46) Lane 20	108	50	Control	-54%
MAP kinase activated protein kinase 2 (T334)	MAPKAPK2 Lane 17				
MAP kinase interacting kinase 1 (T197/202)	Mnk1 Lane 4				
MAPK/Erk kinase 1/2 (S217/221)	MEK1/2 Lane 12	74	25	Control	-66%
MKK3/6(1) (S189/S207)	MKK3/6 Lane 10				
MKK6(2) (S207)	MKK6 Lane 10	69	85	Control	23%
p38 MAPK (T180/Y182)	p38a MAPK Lane 4				
p70 S6 kinase (T389)	S6Ka p70 Lane 19				
p70 S6 kinase (T421/T424)	S6Ka p70 Lane 17				
p85 S6 kinase 2 (T412)	S6K2 p85 Lane 19				
p85 S6 kinase 2 (T444/S447)	S6K2 p85 Lane 17				
Phosphoinositide-dependent protein kinase 1 (S241)	PDK1 Lane 13	241	507	Control	110%
PKC-related kinase 1 (T778)	PRK1 Lane 13	488	555	Control	14%
PKC-related kinase 2 (T816)	PRK2 Lane 13	54	93	Control	72%
Protein kinase B (T308)	PKBa (Akt1) Lane 11				
Protein kinase C alpha/beta (T638)	PKCa/b Lane 6	115	104	Control	-10%
Protein kinase C delta (T505)	PKCd Lane 14	113	129	Control	14%
Protein kinase C zeta (T410)/lambda (T403)	PKCz/l Lane 3				
Protein kinase D (Protein kinase mu) (S916)	PKCm/PKD Lane 3	60	17	Control	-72%
Protein kinase theta (T538)	PKCt Lane 10				
Raf (S259) (60)	Raf1 (60) Lane 8	127	124	Control	-2%
Raf (S259) (70)	Raf1 (70) Lane 8	114	98	Control	-14%
Retinoblastoma Protein (S780)	Rb Lane 18	271	209	Control	-23%
Retinoblastoma Protein (S807/S811)	Rb Lane 7				
The mammalian target of Rapamycin (S2448)	mTOR Lane 13	33	21	Control	-36%
Type1 protein phosphatase alpha (T320)	PP1a Lane 8				
Zap70 (Y319)/Syk (Y352)	Zap70/Syk Lane 20				

Table 2: Phosphorylation profiling in wild-type and transgenic mIGF-1 heart tissue. Phosphoprotein screen of 31 phopshoproteins in wild-type and transgenic heart tissues was performed by Kinetworks analysis (Kinexus Bioinformatic Corp.). The trace quantity of each band is defined as CPM and is measured under its intensity profile

curve. Each value is normalized by the amount of protein in each sample. Each lane corresponds to a specific protein and the phosphorylated Tyrosine or Serine position is indicated. Transgenic increase or decrease of band intensity compared to wild-type (control) is expressed in percentage.

Echocardiography	13 week-old		23 week-old	
	NTG (n=8)	TG (n=8)	NTG (n=8)	TG (n=8)
LVM (mg)	98±5	119±6*	101±3	118±4*
LWM/BW (mg/g)	3.1±0.1	3.8±0.2*	2.9±0.1	3.3±0.2
S (mm)	0.73±0.01	0.82±0.03*	0.74±0.02	0.84±0.02*
PW (mm)	0.59±0.02	0.70±0.02*	0.64±0.02	0.70±0.01*
LVEDD (mm)	4.17±0.11	4.19±0.08	4,10±0.06	4,13±0.13
LVESD (mm)	2.76±0.10	3.03±0.07*	2,64±0.06	2.82±0.15
FS (%)	34±1	27±1*	35±1	32±2
EF (%)	69±2	60±2*	71±2	66±3
CO (ml/min)	26±1	28±2	38±3	31±3
E/A	1.61±0.08	1.27±0.11*	1,49±0.08	1.21±0.07*
Adur (ms)	35±1	40±1*	37±1	41±2*
DT (ms)	41±1.7	43±0.8	42±2.1	46±1.1*
IVRT (ms)	21±1	24±1	25±2	26±2
RV/LV	nd	nd	0.25±0.02	0.3±0.01*

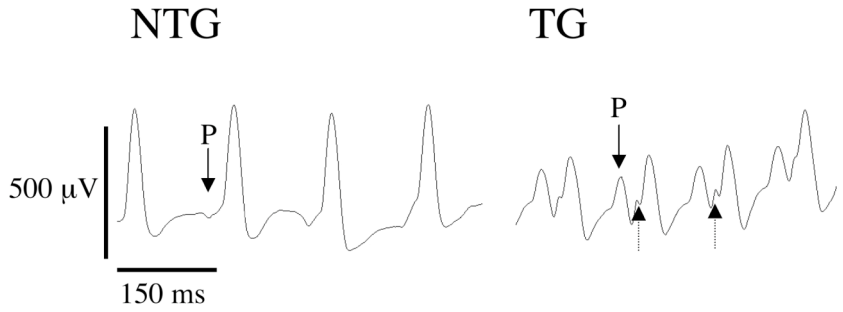

Table 2: NTG: non transgenic, TG: transgenic, SAP: systolic arterial pressure, HR: heart rate, PR: PR interval, QT: QT interval, LVM: left ventricular mass, BW: body weight, S: septal thickness, PW: posterior wall thickness, LVEDD: left ventricular end-diastolic diameter, LVESD: left ventricular end-systolic diameter, FS: fractional shortening, EF: ejection fraction, CO: cardiac output, E/A: maximal speed of early on late mitral filling ratio, Adur: duration of the mitral A wave, DT: mean deceleration time of the E wave, IVRT: isovolumetric relaxation time and RV/LV: right to left ventricular diameters ratio. Nd: not determined.

All results are expressed as means±sem. *: $P<0.05$ (paired Student's t tests for comparisons). Representative electrocardiograms obtained in non-transgenic (NTG) and IGF-1 transgenic (TG) mice in the D2 derivation. The plain arrows indicate the P waves that are amplified in the transgenic mice. The dotted arrows indicate a prolongation and non-homogenous depolarization of the ventricles in the TG mouse.

CHAPTER VI

DISCUSSION

The present study has revealed an intriguing function of local IGF-1 expression in the heart. We characterise for the first time the *in vivo* role at morphological and molecular level of the local IGF-1 isoform, mIGF-1, describing the physiological and pathological function of this isoform in remodeling cardiac muscle. We showed that germline mIGF-1 overexpression induces increased size of the entire heart during the first 4 months of postnatal life. Intriguingly, at six months the heart size of the mIGF-1 transgenic mice is comparable to wild-type mice, indicating an acceleration of the remodeling program occurring normally in the heart during adult development. The morphological phenotype was related to an increased expression of specific markers associated with cardiac hypertrophy, such as ANP, and to a time-dependent activation of MAPKs. The continuous remodeling of the mIGF-1 heart during work-load activity is sustained by activation of the translational machinery during all phases of heart development.

The mIGF-1 transgenic action also induces heart healing after myocardial infarction. We observed that heart remodeling under this pathological condition is triggered by an early step, characterised by lowering of the pro-inflammatory response and an increase of the signaling leading to anti-inflammatory pathways, and of a late step, occurring 1 month after infarct induction, where a massive increase of proliferating cells has been found around the infarct area.

1. Local IGF-1 overexpression leads to physiological hypertrophy and to activation of MAPKs in a well-defined time-window

Cardiac remodeling occurs during post-natal development to maintain a balance between physiological demands for contractile work and the capability of muscle tissue to meet those demands (*119, 120*). In pathological conditions, remodeling responses impair contractile performance, leading to dilated cardiomyopathy and myocardium infarction (*119, 120*). To elucidate whether the hypertrophic phenotype in mIGF-1 transgenic hearts could lead to pathological conditions, we performed echocardiography analysis. Measurement of cardiac function by echocardiography and electrocardiography (Table 2) showed that mIGF-1 induces a 20% concentric left ventricular hypertrophy, confirming the histological analysis (Table 2 and Figure 5.1A, B). Although systolic and diastolic components of the cardiac function were affected, the hearts were not dilated and cardiac output and blood pressure were

maintained normal and not reduced during development (Table 2). Affymetrix analysis performed in our laboratory (data not shown), revealed an upregulation in the transgenic hearts of genes implicated in contractile machinery, such as Troponin C, myosin heavy chain 2X, and myosin heavy chain IIX. We hypothesize that regulation of myosin expression could account for the hypertrophic response observed in hearts overexpressing mIGF-1. At the age of six months EKG analysis showed a comparable ratio heart weight/body weight, although the posterior wall and the septum remained larger compared to wild-type hearts (Table 2).

MAPK signaling provides an important link between the external stimuli and the nucleus via phosphorylation and regulation of multiple transcription factors. Mechanical stretch, growth factors, and G-protein coupled receptor (GPCR) agonists activate MAPK signaling (*328*), using MAPK pathways as a nodal point in regulating cell growth and hypertrophy during heart development. Despite the critical importance of MAPK function in inducing cardiac hypertrophy *in vitro* and *in vivo* (*329, 330*) (Chapter 1), different reports linked MAPKs activation to maladaptive hypertrophy. A recent publication reported that transgenic mice overexpressing MEK1, which is a direct activator of ERK1/2, showed a hypertrophic phenotype associated with impaired diastolic function (*173*). Moreover, vascular MAPK activities in hypertensive rats *in vivo* (*331*) is accompanied by increased activity of aortic ERKs and JNKs, suggesting the involvement of hypertension in the activation of MAPKs.

Our analysis showed that mIGF-1 induces activation of ERK1/2 and JNK at one week of age. In parallel to induction of JNK activity, we observed an increasing phosphorylation level of c-jun, which is one of the downstream target of the JNK pathway. The MAPK activation is related to a specific time-window of transgenic hearts development, since it was not observed in hearts of two weeks and one months of age (Figure 5.3A). The transient activation of this signaling could thus account for the physiological hypertrophy observed by histological and ecocardiographic analysis.

2. mIGF-1 overexpression is related to activation of phospho-S6 ribosomal protein

Our data show that mIGF-1 induces sustained phosphorylation levels of S6 ribosomal protein during postnatal heart development (Figure 5.3C). S6 ribosomal protein is a downstream target of the p70S6 kinase, which is activated in response to nutrients and/or to activation of the insulin receptor through a well-defined signaling cascade (*266, 332, 333*). Upon activation of the S6 ribosomal protein, the translational machinery of the cell synthesizes *ex novo* proteins, as well as ribosomal proteins that cover the needs of an upregulated translational capacity. Both hypertrophic growth and cell proliferation are characterised by increased proteins synthesis.

In skeletal muscle, as described in Chapter II, muscle growth and hypertrophy are mediated by activation of the AKT/mTOR pathway, leading to upregulation of the translational machinery (*137*). Previous studies indicate that IGF-1 induces skeletal myotube hypertrophy by the PI3K/AKT/mTOR pathway. Compelling evidence coming from lower organisms such as *Drosophila Melanogaster,* showed that loss or inhibition of either PI3K, mTOR or p70S6K resulted in decrease of cell size (*134*). Conversely, overexpression of the insulin receptor substrate IRS-1 or AKTor p70S6K was sufficient to cause hypertrophy of cells in which they were expressed (*138, 139*). This growth effect appears to be functionally conserved in mammals, as p70S6K knockout mice have reduced body size and cell growth (*141*).

The sustained activation of the translational machinery observed in mIGF-1 overexpressing hearts suggested that a continuous need of *ex novo* protein synthesis is required to maintain the rapid growth and remodeling of the mIGF-1 transgenic heart. However, as previously emphasized, the precise pathway in mammalian cells connecting PI3K to the activation of p70S6K and the translational machinery is a matter of some dispute (*134*). It is interesting to note that, independently from AKT, PDK1 has been found to directly phosphorylate p70S6K (*324*), indicating that AKT has a dispensable role for signaling to p70S6K. Interestingly, our data showed that the phosphorylation state of AKT is not affected (Figure 5.3C and Table 1), and it is not regulated in parallel to activation of S6 ribosomal protein. On the contrary, the mIGF-1 transgene induced increased activity of PDK1 (Table 1).

Together with the data mentioned above, the phosphoprotein profile (Table 1) opened an interesting field of analysis, since several phoshpoproteins are regulated by mIGF-1. Among them, PKC-related kinase 2 was strongly activated in transgenic hearts (Table 1), whereas the phosphorylation level of Lyn and Protein Kinase D are lower in mIGF-1 transgenic hearts compared to wild-type. Whether these different signals play a role in hypertrophy and/or regeneration after myocardial infarct has to be analyzed in detail. Nevertheless, the possibilities arising from our studies uncover a new physiologically activated targets of mIGF-1 signaling.

3. mIGF-1 induces cardiac regeneration after CTX injury by lowering the pro-inflammatory response and inducing cell proliferation

Although hypertrophy can increase cell mass in response to stress, it is inadequate to restore cardiac function following myocyte loss during myocardial infarction and ischemia-reperfusion. In contrast to skeletal muscle, which can regenerate following injury, the mammalian heart has limited restorative capacity.

The regenerative potential of myocardium is of particular interest, as myocardial infarction is one of the main diseases in humans. The incredible capacity of the MRL mice to prevent scar formation and to heal injured tissues, opens the possibility to use this animal model as a potential font of genetic studies to understand the molecular mechanisms of regeneration in mammalian tissues. Interestingly, genetic analyses of MRL mice suggested that the process of regenerative growth and patterning for the formation of new structures involves modulation of the inflammatory response and changes in the cytokines signaling (*304*).

To study the regenerative function of mIGF-1, wild-type and transgenic hearts were injected with a sublethal dose of CTX venom. The cobra toxin from *Naja mossambica mossambica* is known to cause muscle necrosis (*334*). The cardiotoxin model was chosen over other models of myocardial lesion because it produces a well-delineated transmural lesion, and reduces the risk of ventricular fibrillation (*335*). Intriguingly, our analysis revealed that one month after CTX injection the transgenic hearts completely regenerated the injured tissue, while wild-type hearts showed evident scar formation (Figure 5.4B, and C). From these data, we can argue that the recovery of

the mIGF-1 transgenic hearts could be due in part to the limited extension of CTX-induced injury.

Modulation of specific anti-apoptotic proteins as a protective mechanism could account for mIGF-1-induced cell survival. Interestingly, our analysis showed no differences in the apoptotic profile (data not shown) measured by the presence of apoptotic nuclei in TUNEL staining, and by the expression of specific pro- and anti-apoptotic markers, such as caspase 3, Bcl-2, Bax and Bcl-XL (data not shown). On the other hand, it has been reported that myocardial necrosis triggers Complement activation, free radical generation, chemokine upregulation, and cytokine cascades (*325*). Our data showed that the mRNA levels of the anti-inflammatory cytokines IL10 and IL4 are upregulated at 24 hours and one week after CTX injection, whereas wild-type hearts did not show changing in the anti-inflammatory interleukins, beside a slight decrease of IL10 in response to injury (Figure 5.5B). Interestingly, the pro-inflammatory IL6 was downregulated in the mIGF-1transgenic hearts compared to wild-type hearts at 24 hours after CTX injection, as analyzed by reverse transcriptase PCR (Figure 5.5B). No change was observed for IL1β, or other markers of inflammation, such as IL12, TGF-β, and INF-γ (data not shown), indicating a specific response of the heart to infarction.

The regenerative process implicates a clear restoration of tissue integrity without scar formation. Several possibilities could explain the complete restructuring of myocardial tissue by mIGF-1. One mechanism could involve activation of MMPs that reduce fibrotic tissue forming around the injured area. Collagen release is a continuous process that has been observed to be present in the infarcted area for months in rats, and years in humans (*198*), becoming deleterious for heart functionality when overactivated. Our analysis showed that neither MMP2 nor MMP9 were activated by mIGF-1 during the early and late steps of tissue regeneration (data not shown), indicating that these specific MMPs are not involved in mIGF-1 signaling, but not excluding the possibility that other MMPs may play an important role.

Another mechanism may involve proliferation of cells that constitute the structure of the heart, such as cardiomyocytes and endothelial cells, able to re-populate the infarcted area with newly forming cells. Our data showed clearly the mIGF-1 induced increased cell proliferation around the infarcted area compared to wild-type hearts, but only after one month after CTX injection (Figure 5.6A, B, C). Cardiomyocytes and endothelial cells incorporated BrdU at the border of the injured tissue (Figure 5.7A), although further analyses are necessary to quantify and better characterise the proliferative capacity of these cells.

A fascinating hypothesis comes from our analysis on stem cells present in wild-type and transgenic hearts, as described in Chapter VII. We found that mIGF-1 hearts and wild-type hearts contain an enriched $CD34^+$ side population (SP), and that mIGF-1 overexpression recruits an increasing number of these cells into the heart. The $CD34^+$ cells have the ability to form colonies composed of myeloid and erythroid cells,when plated in a media enriched for factors stimulating differentiation of all components of blood. It will be interesting in the future to analyse whether these cells contribute to tissue replacement upon CTX injection, and whether mIGF-1 could induce their proliferative and differentiation response to injury. Whatever the underlying mechanism, our data showed that mIGF-1 overexpression induces specific signaling implicated in heart remodeling, which is not associated with maladaptive processes, and highlights an intriguing function of mIGF-1 in pathological conditions as a regenerative factor.

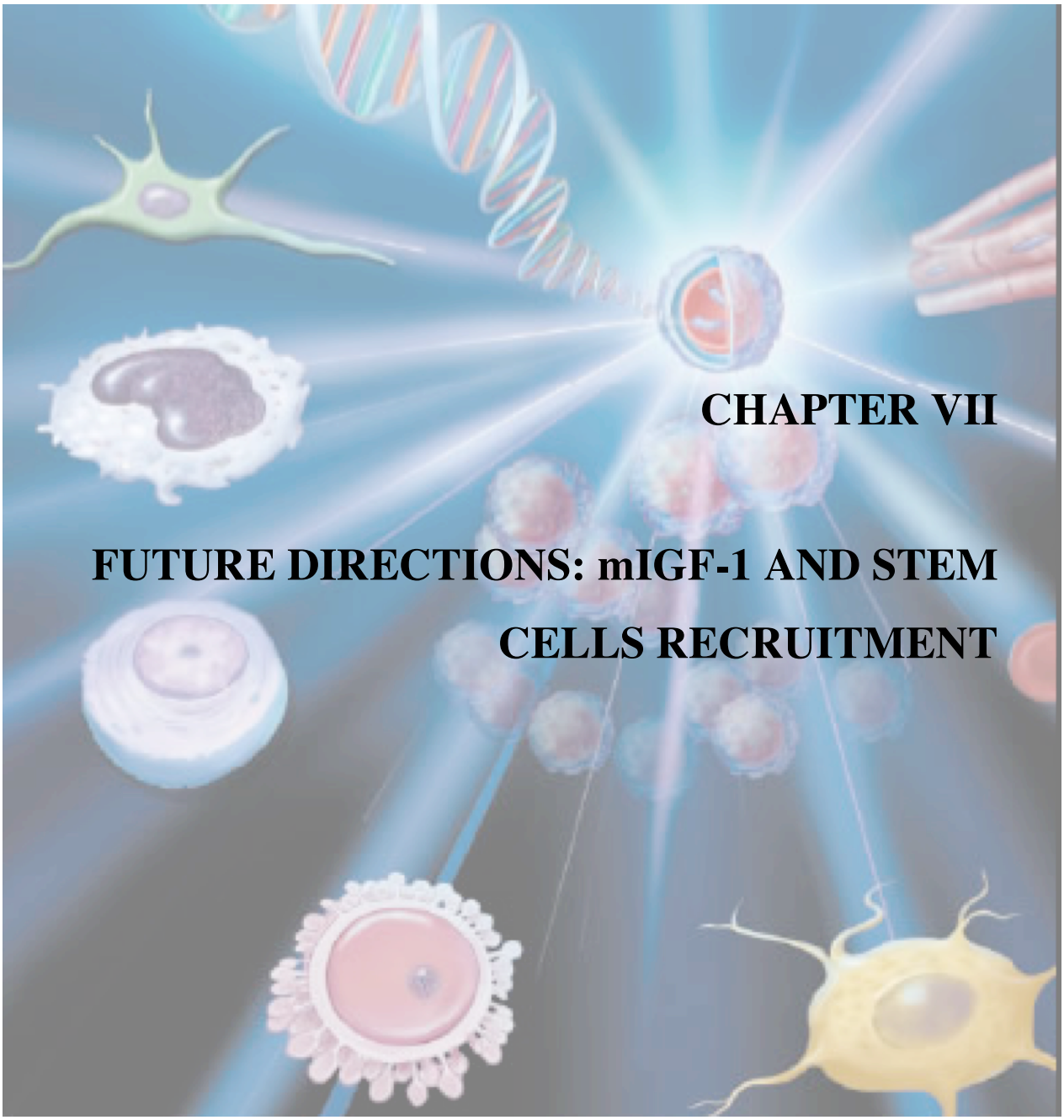

CHAPTER VII

FUTURE DIRECTIONS: mIGF-1 AND STEM CELLS RECRUITMENT

1. STEM CELLS: A HOPE FOR AMBITIOUS SCIENTISTS

mIGF-1 is a potent regenerative agent, mediating the recruitment of bone marrow cells to sites of tissue damage, and augmenting local repair mechanisms (*1*). The concept that enhanced myocardial repair induced by overexpression of mIGF-1 in the heart could depend in part on the recruitment of stem cells at the injured site, was verified by these studies.

Several practical difficulties were encountered in this analysis. One problem was represented by the impossibility to study a FACS dot plot profile in adult hearts, where extraction of total heart cells, although possible, is not optimized and compatible with the requirement of the FACS machine. Another impediment was that whereas adult hearts were successful in the analysis, CTX injection in one month old mice induced high mortality, with consequent impairment of statistical significance in each experiment. Thus, our analysis was performed on 2 days postnatal hearts in physiological conditions.

Briefly, hearts were excised and deeply washed with PBS to remove the excess of blood. The hearts were then digested at 37°C with a mixture of collagenase type II and pancreatin at 95 U/ml and 0.6 mg/ml respectively. All cells were stained by Hoechst (10μg/ml each 10^6 cells) at 37°C for 90 minutes. Whether necessary, cells where treated with Verapamil at 50μM to block the MDR-mediated efflux of Hoechst dye, or with antibodies specific for different lineages at 1:50. Sca1-FITC, c-Kit-PE, CD34-FITC, CD71-PE, FLK1-PE and CD45-CY-Chrome were all purchased from Pharmingen. FITC-, PE-, and CY-Chrome-Rat IgG2b (Pharmingen) were used as control antibodies. The analysis was performed with MoFlo triple-laser flow cytometer and SUMMIT software (Cytomation, Fort Collins, CO), at the Santa Lucia Research Center in Rome, thanks to the generous assistance of Dr. Giovanna Borsellino. To test their ability to differentiate in hematopoietic cell colonies, side population (SP) cells were sorted and plated in Methocult (Stem cell technology, Inc),

Our results showed that heart, like bone marrow, contains a side population (SP), which is considered to be the "stem-like" cell population (Figure 7.1A). Interestingly, we found that mIGF-1 transgenic hearts contain a mean percentage of cells in the SP

double compared to wild-type hearts (3.1%+/-1.1%) (Figure 7.1A). All the cells of the heart express CD45, c-kit, Sca1, CD71, CD34 and FLK1 (Figure7.1B, 7.2A), but the heart SP is only positive for MDR1, as tested by sensitivity to verapamil (Figure 7.1A), and CD34 (Figure 7.1C, 7.2B), indicating that the supposed stem cell markers are widely expressed in other cell types (*336*), and that the SP of the heart is specifically marked by an endothelial and/or hematopoietic lineage. On the basis of recent publications, Sca-1^+ cells and c-Kit^+ cells have confined clonogenicity and transdifferentiative potentiality (*316, 317*) among the stem cells isolated and/or studied in the heart. Whether $CD34^+$ cells retain multipotentiality is still unclear, although a preliminary result showed clearly hematopoietic trans-differentiation capacity (Figure 7.1D), without distinction between wild-type and transgenic cells. Interestingly, in addition to these data, we found that mIGF-1 induced overexpression of MCP-2, a known chemoattractant of myeloid cells, in all stages of heart development (Figure 7.3A), and that in adult heart mIGF-1 overexpression correlates with increasing amount of CD11b positive cells (Figure 7.3B).

We can argue from these preliminary data, that mIGF-1 expression recruits to the developing heart CD34+ cells and cells positive for myeloid markers. Whether the two cells represent the same population or whether these two populations separately contribute to the regenerative potentiality of the transgene is under investigation. To date, the usage of bone marrow cells is under intense investigation, and clinical approaches already claim the potentiality of autologous bone marrow stem cells to repair an infarcted heart. Moreover, intense research is now focusing on the usage of cardiac stem cells and/or engineered skeletal muscle cells that can graft easily in the heart and become functional units of this organ. It is notable that populations of bone marrow stem cells, as well as of possible cardiac stem cells, are both composed of heterogeneous cells that are usually represented by several different cell membrane markers or intracellular differentiation lineage markers. The potentiality of single cell types is difficult to trace, although several studies provided convincing results on this matter (*337*). Therefore, whether the pluripotency of one cell or of a heterogeneous group of cells markedly improve tissue functionality is still unclear.

From our analysis, we would like to propose an alternative strategy to heal a damaged tissue, which employs the usage of genetic modified myeloid cells, bearing mIGF-1 transgene under the control of a cardiac-specific promoter. The innate ability of these cells to home into damaged muscles constitutes a natural vehicle to deliver genes in target tissues. Once incorporated into the damaged muscle bed, activation of cardiac-specific m*Igf-1* gene in the fused or transdifferentiated myeloid nuclei will enhance subsequent recruitment and incorporation of additional circulating cells or resident cells, mediating heart regeneration.

A hope to mend a broken heart…

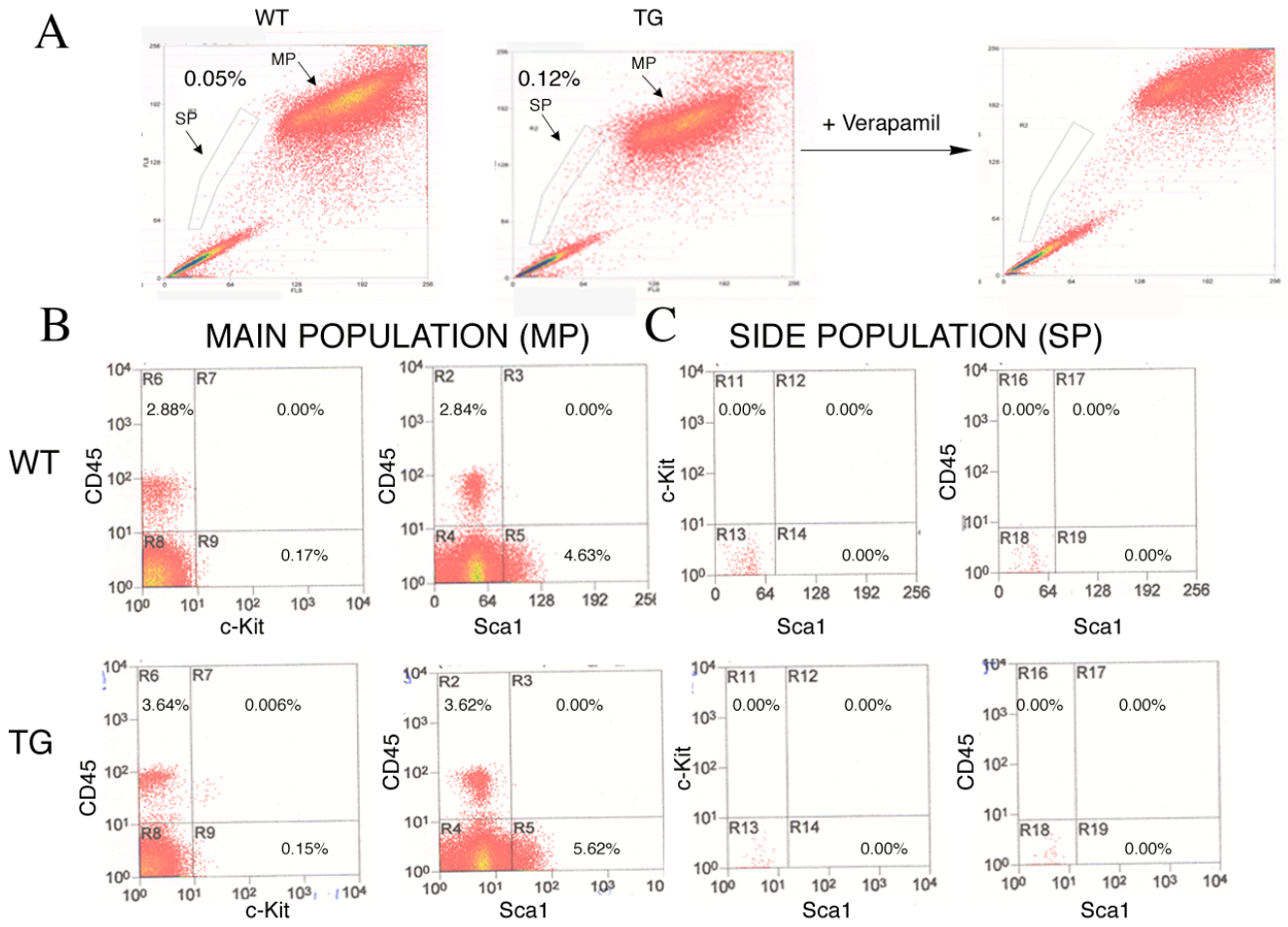

Figure 7.1: FACS analysis of heart stem cell population. (A) Amount of Side Population (SP) compared to Main Population (MP); (B) percentage of c-Kit, Sca1 and CD45 positive cells in the MP and (C) SP

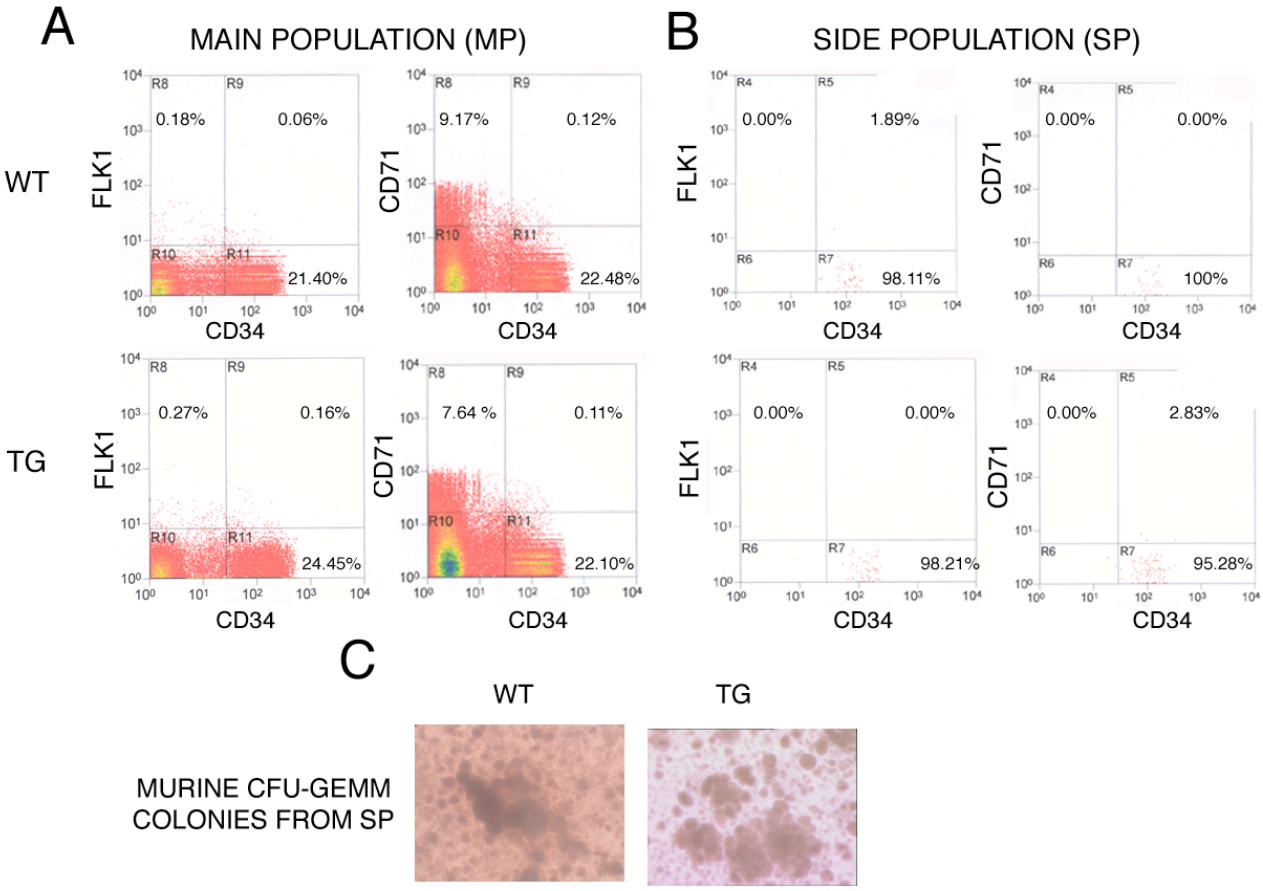

Figure 7.2: FACS analysis of heart stem cell population. Percentage of CD34, CD71 and FLK1 positive cells in the Main Population (MP) (A), and Side Population (SP) (B). (C) SP cells were sorted and plated in a murine CFU-GEMM. The pictures show forming myeloid and erythroid colonies after 15 days of plating.

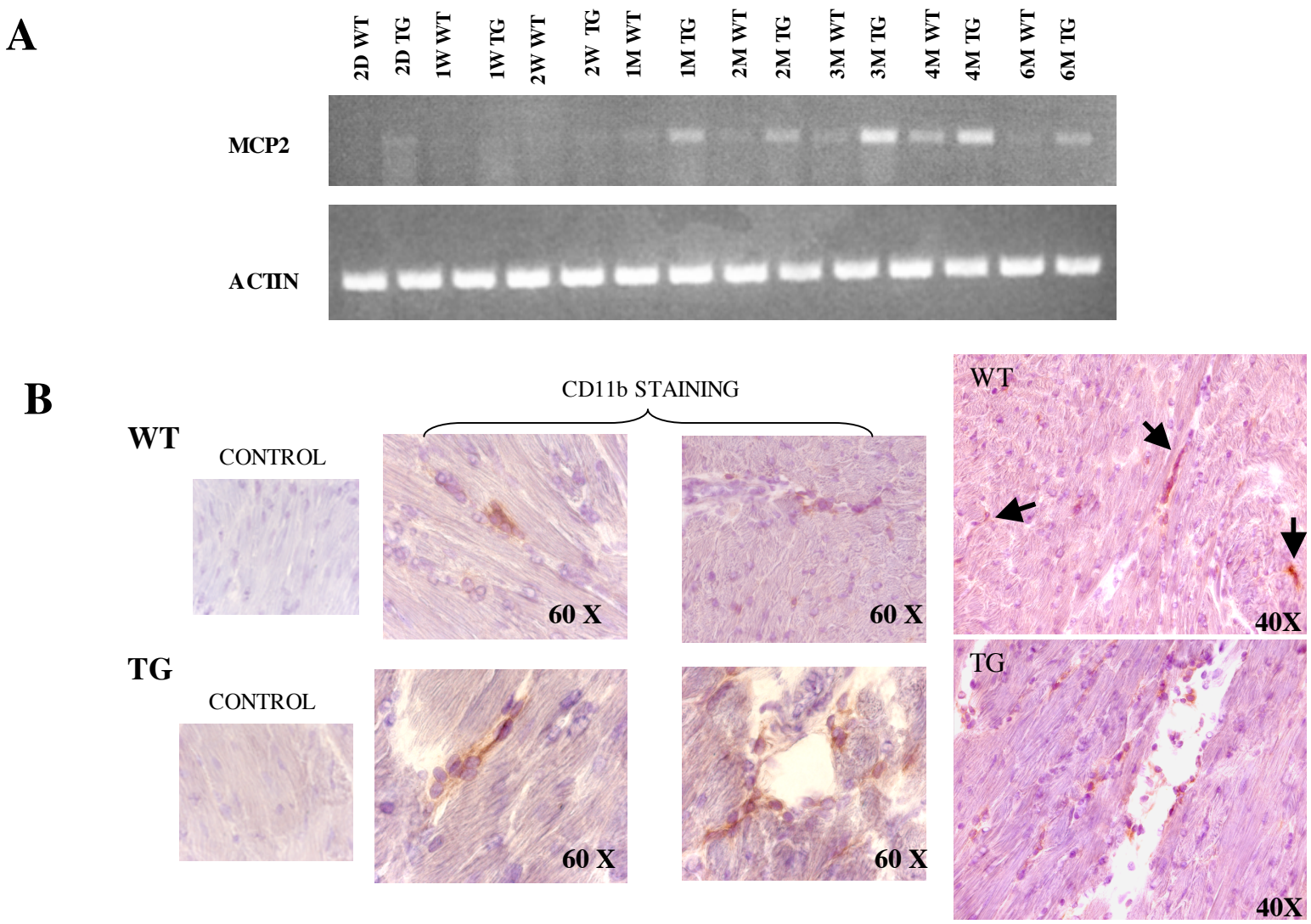

Figure 7.3: mIGF-1-mediated recruitment of CD11b^{+} cells. A) RT-PCR of monocyte chemoattractant protein 2 (MCP2) during postnatal development; B) Immunostaining of 4 months old hearts with CD11b antibody, recognizing monocytes, NK cells, and leukocytes.

REFERENCES

1. A. Musaro *et al.*, *Proc Natl Acad Sci U S A* **101**, 1206 (Feb 3, 2004).
2. A. Musaro *et al.*, *Nat Genet* **27**, 195 (Feb, 2001).
3. M. C. DeRuiter, R. E. Poelmann, I. VanderPlas-de Vries, M. M. Mentink, A. C. Gittenberger-de Groot, *Anat Embryol (Berl)* **185**, 461 (1992).
4. J. M. Icardo, *J Exp Zool* **275**, 144 (Jun 1-15, 1996).
5. F. J. Manasek, *J Morphol* **125**, 329 (Jul, 1968).
6. M. C. Fishman, K. R. Chien, *Development* **124**, 2099 (Jun, 1997).
7. D. Srivastava, E. N. Olson, *Nature* **407**, 221 (Sep 14, 2000).
8. P. P. Tam, M. Parameswaran, S. J. Kinder, R. P. Weinberger, *Development* **124**, 1631 (May, 1997).
9. D. Y. Stainier, R. K. Lee, M. C. Fishman, *Development* **119**, 31 (Sep, 1993).
10. R. K. Lee, D. Y. Stainier, B. M. Weinstein, M. C. Fishman, *Development* **120**, 3361 (Dec, 1994).
11. M. Heikinheimo, J. M. Scandrett, D. B. Wilson, *Dev Biol* **164**, 361 (Aug, 1994).
12. T. P. Yamaguchi, D. J. Dumont, R. A. Conlon, M. L. Breitman, J. Rossant, *Development* **118**, 489 (Jun, 1993).
13. T. J. Lints, L. M. Parsons, L. Hartley, I. Lyons, R. P. Harvey, *Development* **119**, 419 (Oct, 1993).
14. F. Charron, M. Nemer, *Semin Cell Dev Biol* **10**, 85 (Feb, 1999).
15. K. Gajewski, N. Fossett, J. D. Molkentin, R. A. Schulz, *Development* **126**, 5679 (Dec, 1999).
16. J. F. Reiter *et al.*, *Genes Dev* **13**, 2983 (Nov 15, 1999).
17. M. Koutsourakis, A. Langeveld, R. Patient, R. Beddington, F. Grosveld, *Development* **126**, 723 (May, 1999).
18. J. D. Molkentin, Q. Lin, S. A. Duncan, E. N. Olson, *Genes Dev* **11**, 1061 (Apr 15, 1997).
19. C. T. Kuo *et al.*, *Genes Dev* **11**, 1048 (Apr 15, 1997).
20. J. D. Molkentin, K. M. Tymitz, J. A. Richardson, E. N. Olson, *Mol Cell Biol* **20**, 5256 (Jul, 2000).
21. F. Charron, P. Paradis, O. Bronchain, G. Nemer, M. Nemer, *Mol Cell Biol* **19**, 4355 (Jun, 1999).

22. C. Grepin, L. Robitaille, T. Antakly, M. Nemer, *Mol Cell Biol* **15**, 4095 (Aug, 1995).
23. N. Narita, M. Bielinska, D. B. Wilson, *Dev Biol* **189**, 270 (Sep 15, 1997).
24. R. P. Harvey, *Dev Biol* **178**, 203 (Sep 15, 1996).
25. B. G. Bruneau *et al.*, *Dev Biol* **217**, 266 (Jan 15, 2000).
26. I. Lyons *et al.*, *Genes Dev* **9**, 1654 (Jul 1, 1995).
27. M. Tanaka, Z. Chen, S. Bartunkova, N. Yamasaki, S. Izumo, *Development* **126**, 1269 (Mar, 1999).
28. C. C. Wang *et al.*, *Dev Biol* **224**, 152 (Aug 15, 2000).
29. M. Tanaka, N. Yamasaki, S. Izumo, *Mol Cell Biol* **20**, 2874 (Apr, 2000).
30. D. Wang *et al.*, *Cell* **105**, 851 (Jun 29, 2001).
31. Y. Saga *et al.*, *Development* **126**, 3437 (Aug, 1999).
32. S. Kitajima, A. Takagi, T. Inoue, Y. Saga, *Development* **127**, 3215 (Aug, 2000).
33. A. Redkar, M. Montgomery, J. Litvin, *Development* **128**, 2269 (Jun, 2001).
34. M. V. de la Cruz *et al.*, *Cardiol Young* **11**, 588 (Nov, 2001).
35. Z. Z. Bao, B. G. Bruneau, J. G. Seidman, C. E. Seidman, C. L. Cepko, *Science* **283**, 1161 (Feb 19, 1999).
36. R. J. Garriock, S. A. Vokes, E. M. Small, R. Larson, P. A. Krieg, *Dev Genes Evol* **211**, 257 (May, 2001).
37. B. G. Bruneau *et al.*, *Mol Cell Biol* **21**, 1730 (Mar, 2001).
38. G. F. Wang, W. Nikovits, Jr., Z. Z. Bao, F. E. Stockdale, *J Biol Chem* **276**, 28835 (Aug 3, 2001).
39. H. Kokubo, Y. Lun, R. L. Johnson, *Biochem Biophys Res Commun* **260**, 459 (Jul 5, 1999).
40. O. Nakagawa, M. Nakagawa, J. A. Richardson, E. N. Olson, D. Srivastava, *Dev Biol* **216**, 72 (Dec 1, 1999).
41. C. Leimeister, A. Externbrink, B. Klamt, M. Gessler, *Mech Dev* **85**, 173 (Jul, 1999).
42. B. G. Bruneau, *Circ Res* **90**, 509 (Mar 22, 2002).
43. C. Biben, R. P. Harvey, *Genes Dev* **11**, 1357 (Jun 1, 1997).
44. D. Srivastava *et al.*, *Nat Genet* **16**, 154 (Jun, 1997).

45. T. Thomas, H. Yamagishi, P. A. Overbeek, E. N. Olson, D. Srivastava, *Dev Biol* **196**, 228 (Apr 15, 1998).
46. A. B. Firulli, D. G. McFadden, Q. Lin, D. Srivastava, E. N. Olson, *Nat Genet* **18**, 266 (Mar, 1998).
47. P. Riley, L. Anson-Cartwright, J. C. Cross, *Nat Genet* **18**, 271 (Mar, 1998).
48. P. R. Riley, M. Gertsenstein, K. Dawson, J. C. Cross, *Dev Biol* **227**, 156 (Nov 1, 2000).
49. H. Yamagishi *et al.*, *Dev Biol* **239**, 190 (Nov 15, 2001).
50. B. G. Bruneau *et al.*, *Dev Biol* **211**, 100 (Jul 1, 1999).
51. C. M. Liberatore, R. D. Searcy-Schrick, K. E. Yutzey, *Dev Biol* **223**, 169 (Jul 1, 2000).
52. B. G. Bruneau *et al.*, *Cell* **106**, 709 (Sep 21, 2001).
53. S. Angelo *et al.*, *Mech Dev* **95**, 231 (Jul, 2000).
54. D. Yelon *et al.*, *Development* **127**, 2573 (Jun, 2000).
55. Q. Lin, J. Schwarz, C. Bucana, E. N. Olson, *Science* **276**, 1404 (May 30, 1997).
56. Y. Qiu *et al.*, *Genes Dev* **11**, 1925 (Aug 1, 1997).
57. P. J. Gage, H. Suh, S. A. Camper, *Development* **126**, 4643 (Oct, 1999).
58. K. Kitamura *et al.*, *Development* **126**, 5749 (Dec, 1999).
59. C. R. Lin *et al.*, *Nature* **401**, 279 (Sep 16, 1999).
60. M. F. Lu, C. Pressman, R. Dyer, R. L. Johnson, J. F. Martin, *Nature* **401**, 276 (Sep 16, 1999).
61. C. T. Basson *et al.*, *Nat Genet* **15**, 30 (Jan, 1997).
62. C. T. Basson *et al.*, *Proc Natl Acad Sci U S A* **96**, 2919 (Mar 16, 1999).
63. Q. Y. Li *et al.*, *Nat Genet* **15**, 21 (Jan, 1997).
64. S. J. Cross *et al.*, *J Med Genet* **37**, 785 (Oct, 2000).
65. N. Fossett, R. A. Schulz, *Trends Cardiovasc Med* **11**, 185 (Jul, 2001).
66. S. G. Tevosian *et al.*, *Cell* **101**, 729 (Jun 23, 2000).
67. A. F. Stewart *et al.*, *J Biol Chem* **269**, 3147 (Feb 4, 1994).
68. Z. Chen, G. A. Friedrich, P. Soriano, *Genes Dev* **8**, 2293 (Oct 1, 1994).
69. C. B. Moens, B. R. Stanton, L. F. Parada, J. Rossant, *Development* **119**, 485 (Oct, 1993).
70. Y. Hiroi *et al.*, *Nat Genet* **28**, 276 (Jul, 2001).

71. H. Kuo *et al.*, *Development* **126**, 4223 (Oct, 1999).
72. H. Shiratori *et al.*, *Mol Cell* **7**, 137 (Jan, 2001).
73. Y. Zou *et al.*, *Development* **124**, 793 (Feb, 1997).
74. L. Li, Z. Liu, B. Mercer, P. Overbeek, E. N. Olson, *Dev Biol* **187**, 311 (Jul 15, 1997).
75. P. S. Chang, L. Li, J. McAnally, E. N. Olson, *J Biol Chem* **276**, 17206 (May 18, 2001).
76. D. Durocher, M. Nemer, *Dev Genet* **22**, 250 (1998).
77. E. C. Svensson *et al.*, *Nat Genet* **25**, 353 (Jul, 2000).
78. C. L. Cai *et al.*, *Dev Cell* **5**, 877 (Dec, 2003).
79. R. G. Kelly, N. A. Brown, M. E. Buckingham, *Dev Cell* **1**, 435 (Sep, 2001).
80. R. G. Kelly, M. E. Buckingham, *Trends Genet* **18**, 210 (Apr, 2002).
81. K. L. Waldo *et al.*, *Development* **128**, 3179 (Aug, 2001).
82. M. D. Schneider, V. Gaussin, K. M. Lyons, *Cytokine Growth Factor Rev* **14**, 1 (Feb, 2003).
83. T. M. Schultheiss, J. B. Burch, A. B. Lassar, *Genes Dev* **11**, 451 (Feb 15, 1997).
84. Y. Shi, S. Katsev, C. Cai, S. Evans, *Dev Biol* **224**, 226 (Aug 15, 2000).
85. E. N. Olson, M. D. Schneider, *Genes Dev* **17**, 1937 (Aug 15, 2003).
86. A. J. Harwood, *Cell* **105**, 821 (Jun 29, 2001).
87. S. Zaffran, M. Frasch, *Circ Res* **91**, 457 (Sep 20, 2002).
88. M. J. Marvin, G. Di Rocco, A. Gardiner, S. M. Bush, A. B. Lassar, *Genes Dev* **15**, 316 (Feb 1, 2001).
89. E. Tzahor, A. B. Lassar, *Genes Dev* **15**, 255 (Feb 1, 2001).
90. V. A. Schneider, M. Mercola, *Genes Dev* **15**, 304 (Feb 1, 2001).
91. P. Pandur, M. Lasche, L. M. Eisenberg, M. Kuhl, *Nature* **418**, 636 (Aug 8, 2002).
92. C. A. Eisenberg, R. G. Gourdie, L. M. Eisenberg, *Development* **124**, 525 (Jan, 1997).
93. C. A. Eisenberg, L. M. Eisenberg, *Dev Dyn* **216**, 45 (Sep, 1999).
94. P. Kastner *et al.*, *Development* **124**, 4749 (Dec, 1997).
95. H. M. Sucov *et al.*, *Genes Dev* **8**, 1007 (May 1, 1994).
96. J. Chen, S. W. Kubalak, K. R. Chien, *Development* **125**, 1943 (May, 1998).

97. C. M. Tran, H. M. Sucov, *Development* **125**, 1951 (May, 1998).
98. J. Xavier-Neto *et al.*, *Development* **126**, 2677 (Jun, 1999).
99. K. Niederreither *et al.*, *Development* **128**, 1019 (Apr, 2001).
100. Y. Y. Zhao *et al.*, *J Biol Chem* **273**, 10261 (Apr 24, 1998).
101. K. F. Lee *et al.*, *Nature* **378**, 394 (Nov 23, 1995).
102. M. Gassmann *et al.*, *Nature* **378**, 390 (Nov 23, 1995).
103. S. A. Crone, K. F. Lee, *Ann N Y Acad Sci* **971**, 547 (Oct, 2002).
104. M. H. Soonpaa, L. J. Field, *Am J Physiol* **272**, H220 (Jan, 1997).
105. F. J. Clubb, Jr., S. P. Bishop, *Lab Invest* **50**, 571 (May, 1984).
106. V. Baldin, J. Lukas, M. J. Marcote, M. Pagano, G. Draetta, *Genes Dev* **7**, 812 (May, 1993).
107. S. X. Skapek, J. Rhee, D. B. Spicer, A. B. Lassar, *Science* **267**, 1022 (Feb 17, 1995).
108. X. Q. Qin *et al.*, *Mol Cell Biol* **15**, 742 (Feb, 1995).
109. M. H. Soonpaa, K. K. Kim, L. Pajak, M. Franklin, L. J. Field, *Am J Physiol* **271**, H2183 (Nov, 1996).
110. E. Zacksenhaus *et al.*, *Genes Dev* **10**, 3051 (Dec 1, 1996).
111. H. L. Weiner, J. L. Swain, *Proc Natl Acad Sci U S A* **86**, 2683 (Apr, 1989).
112. X. Zhu, J. Sasse, D. McAllister, J. Lough, *Dev Dyn* **207**, 429 (Dec, 1996).
113. T. Mima, H. Ueno, D. A. Fischman, L. T. Williams, T. Mikawa, *Proc Natl Acad Sci U S A* **92**, 467 (Jan 17, 1995).
114. Y. Liu *et al.*, *Lab Invest* **73**, 771 (Dec, 1995).
115. P. Anversa, T. Palackal, E. H. Sonnenblick, G. Olivetti, J. M. Capasso, *J Clin Invest* **85**, 994 (Apr, 1990).
116. K. Reiss *et al.*, *Exp Cell Res* **225**, 44 (May 25, 1996).
117. M. A. Pfeffer, C. H. Hennekens, *Am J Cardiol* **75**, 1173 (Jun 1, 1995).
118. J. M. Pfeffer, T. A. Fischer, M. A. Pfeffer, *Annu Rev Physiol* **57**, 805 (1995).
119. N. Frey, E. N. Olson, *Annu Rev Physiol* **65**, 45 (2003).
120. W. R. MacLellan, M. D. Schneider, *Annu Rev Physiol* **62**, 289 (2000).
121. J. D. Molkentin, I. G. Dorn, 2nd, *Annu Rev Physiol* **63**, 391 (2001).
122. S. Miyata, W. Minobe, M. R. Bristow, L. A. Leinwand, *Circ Res* **86**, 386 (Mar 3, 2000).
123. N. Frey, T. A. McKinsey, E. N. Olson, *Nat Med* **6**, 1221 (Nov, 2000).

124. T. Hirano, K. Nakajima, M. Hibi, *Cytokine Growth Factor Rev* **8**, 241 (Dec, 1997).
125. H. Hirota *et al.*, *Cell* **97**, 189 (Apr 16, 1999).
126. Z. Sheng *et al.*, *J Biol Chem* **272**, 5783 (Feb 28, 1997).
127. G. L. Kukielka *et al.*, *Circulation* **92**, 1866 (Oct 1, 1995).
128. H. Hirota, K. Yoshida, T. Kishimoto, T. Taga, *Proc Natl Acad Sci U S A* **92**, 4862 (May 23, 1995).
129. K. Kunisada *et al.*, *Circulation* **98**, 346 (Jul 28, 1998).
130. K. Kunisada *et al.*, *Proc Natl Acad Sci U S A* **97**, 315 (Jan 4, 2000).
131. T. G. Parker, S. E. Packer, M. D. Schneider, *J Clin Invest* **85**, 507 (Feb, 1990).
132. E. Piek, C. H. Heldin, P. Ten Dijke, *Faseb J* **13**, 2105 (Dec, 1999).
133. T. Shioi *et al.*, *Mol Cell Biol* **22**, 2799 (Apr, 2002).
134. D. J. Glass, *Nat Cell Biol* **5**, 87 (Feb, 2003).
135. M. C. Delaughter, G. E. Taffet, M. L. Fiorotto, M. L. Entman, R. J. Schwartz, *Faseb J* **13**, 1923 (Nov, 1999).
136. K. Reiss *et al.*, *Proc Natl Acad Sci U S A* **93**, 8630 (Aug 6, 1996).
137. S. C. Bodine *et al.*, *Nat Cell Biol* **3**, 1014 (Nov, 2001).
138. J. Montagne *et al.*, *Science* **285**, 2126 (Sep 24, 1999).
139. R. Bohni *et al.*, *Cell* **97**, 865 (Jun 25, 1999).
140. T. Shioi *et al.*, *Circulation* **107**, 1664 (Apr 1, 2003).
141. H. Shima *et al.*, *Embo J* **17**, 6649 (Nov 16, 1998).
142. C. B. Klee, H. Ren, X. Wang, *J Biol Chem* **273**, 13367 (May 29, 1998).
143. G. R. Crabtree, *Cell* **96**, 611 (Mar 5, 1999).
144. L. Sun *et al.*, *Immunity* **8**, 703 (Jun, 1998).
145. M. M. Lai, P. E. Burnett, H. Wolosker, S. Blackshaw, S. H. Snyder, *J Biol Chem* **273**, 18325 (Jul 17, 1998).
146. J. D. Molkentin *et al.*, *Cell* **93**, 215 (Apr 17, 1998).
147. O. F. Bueno *et al.*, *Proc Natl Acad Sci U S A* **99**, 4586 (Apr 2, 2002).
148. M. A. Sussman *et al.*, *Science* **281**, 1690 (Sep 11, 1998).
149. B. Ding *et al.*, *Circ Res* **84**, 729 (Apr 2, 1999).
150. W. Zhang *et al.*, *Circ Res* **84**, 722 (Apr 2, 1999).
151. B. Rothermel *et al.*, *J Biol Chem* **275**, 8719 (Mar 24, 2000).
152. T. J. Kingsbury, K. W. Cunningham, *Genes Dev* **14**, 1595 (Jul 1, 2000).

153. J. J. Fuentes *et al.*, *Hum Mol Genet* **9**, 1681 (Jul 1, 2000).
154. B. A. Rothermel *et al.*, *Proc Natl Acad Sci U S A* **98**, 3328 (Mar 13, 2001).
155. H. W. Lim, J. D. Molkentin, *Nat Med* **6**, 3 (Jan, 2000).
156. H. A. Rockman, W. J. Koch, R. J. Lefkowitz, *Nature* **415**, 206 (Jan 10, 2002).
157. R. J. Lefkowitz, H. A. Rockman, W. J. Koch, *Circulation* **101**, 1634 (Apr 11, 2000).
158. S. Engelhardt, L. Hein, U. Keller, K. Klambt, M. J. Lohse, *Circ Res* **90**, 814 (Apr 19, 2002).
159. C. Gaudin *et al.*, *J Clin Invest* **95**, 1676 (Apr, 1995).
160. D. M. Roth *et al.*, *Circulation* **105**, 1989 (Apr 23, 2002).
161. C. L. Antos *et al.*, *Circ Res* **89**, 997 (Nov 23, 2001).
162. G. W. Dorn, 2nd, N. M. Tepe, J. N. Lorenz, W. J. Koch, S. B. Liggett, *Proc Natl Acad Sci U S A* **96**, 6400 (May 25, 1999).
163. W. J. Koch, R. J. Lefkowitz, H. A. Rockman, *Annu Rev Physiol* **62**, 237 (2000).
164. P. Paradis, N. Dali-Youcef, F. W. Paradis, G. Thibault, M. Nemer, *Proc Natl Acad Sci U S A* **97**, 931 (Jan 18, 2000).
165. N. Wettschureck *et al.*, *Nat Med* **7**, 1236 (Nov, 2001).
166. S. Yusuf *et al.*, *N Engl J Med* **342**, 145 (Jan 20, 2000).
167. M. Ichida, T. Finkel, *J Biol Chem* **276**, 3524 (Feb 2, 2001).
168. J. J. Hunter, N. Tanaka, H. A. Rockman, J. Ross, Jr., K. R. Chien, *J Biol Chem* **270**, 23173 (Sep 29, 1995).
169. M. Abdellatif *et al.*, *Mol Cell Biol* **18**, 6729 (Nov, 1998).
170. A. Sotiropoulos, D. Gineitis, J. Copeland, R. Treisman, *Cell* **98**, 159 (Jul 23, 1999).
171. P. H. Sugden, *Circ Res* **84**, 633 (Apr 2, 1999).
172. O. F. Bueno *et al.*, *Circ Res* **88**, 88 (Jan 19, 2001).
173. O. F. Bueno *et al.*, *Embo J* **19**, 6341 (Dec 1, 2000).
174. A. Clerk, A. Michael, P. H. Sugden, *J Cell Biol* **142**, 523 (Jul 27, 1998).
175. J. Gillespie-Brown, S. J. Fuller, M. A. Bogoyevitch, S. Cowley, P. H. Sugden, *J Biol Chem* **270**, 28092 (Nov 24, 1995).
176. G. R. Post, D. Goldstein, D. J. Thuerauf, C. C. Glembotski, J. H. Brown, *J Biol Chem* **271**, 8452 (Apr 5, 1996).

177. J. Thorburn *et al.*, *Mol Biol Cell* **6**, 1479 (Nov, 1995).
178. I. Komuro *et al.*, *Faseb J* **10**, 631 (Apr, 1996).
179. G. Choukroun *et al.*, *J Clin Invest* **102**, 1311 (Oct 1, 1998).
180. M. T. Ramirez *et al.*, *J Biol Chem* **272**, 14057 (May 30, 1997).
181. M. Yano, S. Kim, Y. Izumi, S. Yamanaka, H. Iwao, *Circ Res* **83**, 752 (Oct 5, 1998).
182. Y. Wang *et al.*, *J Biol Chem* **273**, 5423 (Mar 6, 1998).
183. T. Minamino *et al.*, *Proc Natl Acad Sci U S A* **99**, 3866 (Mar 19, 2002).
184. G. Choukroun *et al.*, *J Clin Invest* **104**, 391 (Aug, 1999).
185. T. P. Garrington, G. L. Johnson, *Curr Opin Cell Biol* **11**, 211 (Apr, 1999).
186. J. Han, Y. Jiang, Z. Li, V. V. Kravchenko, R. J. Ulevitch, *Nature* **386**, 296 (Mar 20, 1997).
187. T. T. Yang, Q. Xiong, H. Enslen, R. J. Davis, C. W. Chow, *Mol Cell Biol* **22**, 3892 (Jun, 2002).
188. Y. Jiang *et al.*, *J Biol Chem* **272**, 30122 (Nov 28, 1997).
189. S. A. Cook, P. H. Sugden, A. Clerk, *J Mol Cell Cardiol* **31**, 1429 (Aug, 1999).
190. S. Nemoto, Z. Sheng, A. Lin, *Mol Cell Biol* **18**, 3518 (Jun, 1998).
191. D. Zhang *et al.*, *Nat Med* **6**, 556 (May, 2000).
192. C. L. Zhang *et al.*, *Cell* **110**, 479 (Aug 23, 2002).
193. T. J. Ryan *et al.*, *Circulation* **100**, 1016 (Aug 31, 1999).
194. J. Honold, B. Assmus, R. Lehman, A. M. Zeiher, S. Dimmeler, *Nephrol Dial Transplant* **19**, 1673 (Jul, 2004).
195. Y. Sun, K. T. Weber, *Cardiovasc Res* **46**, 250 (May, 2000).
196. Y. Sun, J. Q. Zhang, J. Zhang, S. Lamparter, *J Lab Clin Med* **135**, 316 (Apr, 2000).
197. A. Desmouliere, A. Geinoz, F. Gabbiani, G. Gabbiani, *J Cell Biol* **122**, 103 (Jul, 1993).
198. Y. Sun, K. T. Weber, *J Mol Cell Cardiol* **28**, 851 (May, 1996).
199. A. Desmouliere, M. Redard, I. Darby, G. Gabbiani, *Am J Pathol* **146**, 56 (Jan, 1995).
200. S. E. Campbell, L. C. Katwa, *J Mol Cell Cardiol* **29**, 1947 (Jul, 1997).
201. D. LeRoith, H. Werner, D. Beitner-Johnson, C. T. Roberts, Jr., *Endocr Rev* **16**, 143 (Apr, 1995).

202. A. A. Butler, D. LeRoith, *Endocrinology* **142**, 1685 (May, 2001).
203. J. Baker, J. P. Liu, E. J. Robertson, A. Efstratiadis, *Cell* **75**, 73 (Oct 8, 1993).
204. J. P. Liu, J. Baker, A. S. Perkins, E. J. Robertson, A. Efstratiadis, *Cell* **75**, 59 (Oct 8, 1993).
205. F. Frasca *et al.*, *Mol Cell Biol* **19**, 3278 (May, 1999).
206. M. Holzenberger *et al.*, *Endocrinology* **141**, 2557 (Jul, 2000).
207. J. L. Liu *et al.*, *Mol Endocrinol* **12**, 1452 (Sep, 1998).
208. J. G. Simmons, J. J. Van Wyk, E. C. Hoyt, P. K. Lund, *Growth Factors* **9**, 205 (1993).
209. E. C. Hoyt, J. E. Hepler, J. J. Van Wyk, P. K. Lund, *DNA Cell Biol* **11**, 433 (Jul-Aug, 1992).
210. A. Shimatsu, P. Rotwein, *Nucleic Acids Res* **15**, 7196 (Sep 11, 1987).
211. P. K. Lund, *Recent Prog Horm Res* **49**, 125 (1994).
212. M. Jansen *et al.*, *Nature* **306**, 609 (Dec 8-14, 1983).
213. E. C. Hoyt, J. J. Van Wyk, P. K. Lund, *Mol Endocrinol* **2**, 1077 (Nov, 1988).
214. M. Adamo, W. L. Lowe, Jr., D. LeRoith, C. T. Roberts, Jr., *Endocrinology* **124**, 2737 (Jun, 1989).
215. J. Shemer, M. L. Adamo, C. T. Roberts, Jr., D. LeRoith, *Endocrinology* **131**, 2793 (Dec, 1992).
216. J. E. Hepler, J. J. Van Wyk, P. K. Lund, *Endocrinology* **127**, 1550 (Sep, 1990).
217. P. Rotwein, K. M. Pollock, D. K. Didier, G. G. Krivi, *J Biol Chem* **261**, 4828 (Apr 15, 1986).
218. L. S. Mathews *et al.*, *Endocrinology* **123**, 2827 (Dec, 1988).
219. W. H. Daughaday *et al.*, *Nature* **235**, 107 (Jan 14, 1972).
220. E. R. Froesch, J. Zapf, *Prog Clin Biol Res* **200**, 75 (1985).
221. A. J. D'Ercole, A. D. Stiles, L. E. Underwood, *Proc Natl Acad Sci U S A* **81**, 935 (Feb, 1984).
222. T. Ludwig *et al.*, *Dev Biol* **177**, 517 (Aug 1, 1996).
223. A. Louvi, D. Accili, A. Efstratiadis, *Dev Biol* **189**, 33 (Sep 1, 1997).
224. S. Yakar *et al.*, *Proc Natl Acad Sci U S A* **96**, 7324 (Jun 22, 1999).
225. F. Lupu, J. D. Terwilliger, K. Lee, G. V. Segre, A. Efstratiadis, *Dev Biol* **229**, 141 (Jan 1, 2001).
226. B. A. Barres *et al.*, *Cell* **70**, 31 (Jul 10, 1992).

227. G. A. Werther, H. Cheesman, V. Russo, *Brain Res* **617**, 339 (Jul 23, 1993).
228. W. Ni, K. Rajkumar, J. I. Nagy, L. J. Murphy, *Brain Res* **769**, 97 (Sep 19, 1997).
229. M. J. Carson, R. R. Behringer, R. L. Brinster, F. A. McMorris, *Neuron* **10**, 729 (Apr, 1993).
230. J. R. O'Kusky, P. Ye, A. J. D'Ercole, *J Neurosci* **20**, 8435 (Nov 15, 2000).
231. D. A. Tiangco, K. C. Papakonstantinou, K. A. Mullinax, J. K. Terzis, *J Reconstr Microsurg* **17**, 247 (May, 2001).
232. S. Yakar, C. J. Rosen, *Exp Biol Med (Maywood)* **228**, 245 (Mar, 2003).
233. C. J. Rosen, L. R. Donahue, *Proc Soc Exp Biol Med* **219**, 1 (Oct, 1998).
234. J. Rubin *et al.*, *J Clin Endocrinol Metab* **87**, 4273 (Sep, 2002).
235. D. Bikle *et al.*, *J Bone Miner Res* **16**, 2320 (Dec, 2001).
236. M. Zhang *et al.*, *J Biol Chem* **277**, 44005 (Nov 15, 2002).
237. A. Musaro, N. Rosenthal, *Mol Cell Biol* **19**, 3115 (Apr, 1999).
238. M. Renganathan, M. L. Messi, O. Delbono, *J Biol Chem* **273**, 28845 (Oct 30, 1998).
239. M. V. Chakravarthy, M. L. Fiorotto, R. J. Schwartz, F. W. Booth, *Mech Ageing Dev* **122**, 1303 (Sep, 2001).
240. D. Dardevet, C. Sornet, D. Attaix, V. E. Baracos, J. Grizard, *Endocrinology* **134**, 1475 (Mar, 1994).
241. P. E. Willis, S. G. Chadan, V. Baracos, W. S. Parkhouse, *Am J Physiol* **275**, E525 (Sep, 1998).
242. A. De Luca, S. Pierno, D. Cocchi, D. Conte Camerino, *Br J Pharmacol* **121**, 369 (Jun, 1997).
243. K. A. Woods, C. Camacho-Hubner, M. O. Savage, A. J. Clark, *N Engl J Med* **335**, 1363 (Oct 31, 1996).
244. H. L. Keller, B. St Pierre Schneider, L. A. Eppihimer, J. G. Cannon, *Muscle Nerve* **22**, 347 (Mar, 1999).
245. K. M. Thrailkill *et al.*, *Diabetes Care* **22**, 585 (Apr, 1999).
246. D. R. Clemmons *et al.*, *J Clin Endocrinol Metab* **85**, 1518 (Apr, 2000).
247. J. I. Jones, D. R. Clemmons, *Endocr Rev* **16**, 3 (Feb, 1995).
248. Y. Oh, *Breast Cancer Res Treat* **47**, 283 (Feb, 1998).

249. L. J. Schedlich, T. F. Young, S. M. Firth, R. C. Baxter, *J Biol Chem* **273**, 18347 (Jul 17, 1998).
250. V. Hwa, Y. Oh, R. G. Rosenfeld, *Endocr Rev* **20**, 761 (Dec, 1999).
251. E. M. Spencer, K. Chan, *Prog Growth Factor Res* **6**, 209 (1995).
252. B. E. Forbes *et al.*, *J Biol Chem* **273**, 4647 (Feb 20, 1998).
253. J. L. Fowlkes, K. M. Thrailkill, C. George-Nascimento, C. K. Rosenberg, D. M. Serra, *Endocrinology* **138**, 2280 (Jun, 1997).
254. S. Rajaram, D. J. Baylink, S. Mohan, *Endocr Rev* **18**, 801 (Dec, 1997).
255. M. R. Schneider, H. Lahm, M. Wu, A. Hoeflich, E. Wolf, *Faseb J* **14**, 629 (Apr, 2000).
256. V. D. Longo, C. E. Finch, *Science* **299**, 1342 (Feb 28, 2003).
257. H. Kato, T. N. Faria, B. Stannard, C. T. Roberts, Jr., D. LeRoith, *Mol Endocrinol* **8**, 40 (Jan, 1994).
258. K. I. Rother *et al.*, *J Biol Chem* **273**, 17491 (Jul 10, 1998).
259. D. Accili, Y. Kido, J. Nakae, D. Lauro, B. C. Park, *Curr Mol Med* **1**, 9 (Mar, 2001).
260. H. Stocker, E. Hafen, *Curr Opin Genet Dev* **10**, 529 (Oct, 2000).
261. S. Tanaka, T. Ito, J. R. Wands, *J Biol Chem* **271**, 14610 (Jun 14, 1996).
262. S. Oldham *et al.*, *Development* **129**, 4103 (Sep, 2002).
263. T. Shioi *et al.*, *Embo J* **19**, 2537 (Jun 1, 2000).
264. D. P. Brazil, B. A. Hemmings, *Trends Biochem Sci* **26**, 657 (Nov, 2001).
265. J. Verdu, M. A. Buratovich, E. L. Wilder, M. J. Birnbaum, *Nat Cell Biol* **1**, 500 (Dec, 1999).
266. T. Schmelzle, M. N. Hall, *Cell* **103**, 253 (Oct 13, 2000).
267. A. Dufner, G. Thomas, *Exp Cell Res* **253**, 100 (Nov 25, 1999).
268. S. Oldham, J. Montagne, T. Radimerski, G. Thomas, E. Hafen, *Genes Dev* **14**, 2689 (Nov 1, 2000).
269. X. Long *et al.*, *Curr Biol* **12**, 1448 (Sep 3, 2002).
270. M. Hertweck, C. Gobel, R. Baumeister, *Dev Cell* **6**, 577 (Apr, 2004).
271. M. L. Leong, A. C. Maiyar, B. Kim, B. A. O'Keeffe, G. L. Firestone, *J Biol Chem* **278**, 5871 (Feb 21, 2003).
272. P. Kermer *et al.*, *Brain Res Mol Brain Res* **85**, 144 (Dec 28, 2000).

273. H. Tran, A. Brunet, E. C. Griffith, M. E. Greenberg, *Sci STKE* **2003**, RE5 (Mar 4, 2003).
274. T. N. Stitt *et al.*, *Mol Cell* **14**, 395 (May 7, 2004).
275. H. Ito *et al.*, *Circulation* **87**, 1715 (May, 1993).
276. R. Foncea *et al.*, *J Biol Chem* **272**, 19115 (Aug 1, 1997).
277. T. Matsui *et al.*, *J Biol Chem* **277**, 22896 (Jun 21, 2002).
278. V. C. Tu, J. J. Bahl, Q. M. Chen, *J Pharmacol Exp Ther* **300**, 1101 (Mar, 2002).
279. M. O. Boluyt *et al.*, *Circ Res* **81**, 176 (Aug, 1997).
280. J. Sadoshima, S. Izumo, *Circ Res* **77**, 1040 (Dec, 1995).
281. T. H. Bark, M. A. McNurlan, C. H. Lang, P. J. Garlick, *Am J Physiol* **275**, E118 (Jul, 1998).
282. A. Cittadini *et al.*, *Circulation* **93**, 800 (Feb 15, 1996).
283. R. L. Duerr *et al.*, *J Clin Invest* **95**, 619 (Feb, 1995).
284. D. Grimm, D. Cameron, D. P. Griese, G. A. Riegger, E. P. Kromer, *Cardiovasc Res* **40**, 297 (Nov, 1998).
285. N. C. Sundgren *et al.*, *Am J Physiol Regul Integr Comp Physiol* **285**, R1481 (Dec, 2003).
286. J. Kajstura, W. Cheng, K. Reiss, P. Anversa, *Exp Cell Res* **215**, 273 (Dec, 1994).
287. Q. Li *et al.*, *J Clin Invest* **100**, 1991 (Oct 15, 1997).
288. M. Buerke *et al.*, *Proc Natl Acad Sci U S A* **92**, 8031 (Aug 15, 1995).
289. R. K. Avramoglu *et al.*, *J Biol Chem* **273**, 6057 (Mar 13, 1998).
290. M. Y. Donath, E. R. Froesch, J. Zapf, *Growth Horm IGF Res* **8 Suppl B**, 167 (Apr, 1998).
291. M. Y. Donath *et al.*, *J Clin Endocrinol Metab* **83**, 3177 (Sep, 1998).
292. D. G. Johnston *et al.*, *Horm Res* **38 Suppl 1**, 68 (1992).
293. A. Cuocolo *et al.*, *Eur J Nucl Med* **23**, 390 (Apr, 1996).
294. R. A. Clark, G. S. Ashcroft, M. J. Spencer, H. Larjava, M. W. Ferguson, *Br J Dermatol* **135**, 46 (Jul, 1996).
295. R. J. Goss, R. Holt, *J Exp Zool* **261**, 451 (Apr 1, 1992).
296. J. P. Brockes, A. Kumar, *Nat Rev Mol Cell Biol* **3**, 566 (Aug, 2002).
297. J. O. Oberpriller, J. C. Oberpriller, *J Exp Zool* **187**, 249 (Feb, 1974).

298. W. S. Kim, D. L. Stocum, *Dev Biol* **114**, 170 (Mar, 1986).
299. E. M. Tanaka, D. N. Drechsel, J. P. Brockes, *Curr Biol* **9**, 792 (Jul 29-Aug 12, 1999).
300. A. Simon, J. P. Brockes, *Exp Cell Res* **281**, 101 (Nov 15, 2002).
301. E. M. Tanaka, *Cell* **113**, 559 (May 30, 2003).
302. G. K. Michalopoulos, M. C. DeFrances, *Science* **276**, 60 (Apr 4, 1997).
303. J. P. Brockes, A. Kumar, C. P. Velloso, *J Anat* **199**, 3 (Jul-Aug, 2001).
304. M. Harty, A. W. Neff, M. W. King, A. L. Mescher, *Dev Dyn* **226**, 268 (Feb, 2003).
305. K. R. Chien, E. N. Olson, *Cell* **110**, 153 (Jul 26, 2002).
306. M. H. Soonpaa, L. J. Field, *Circ Res* **83**, 15 (Jul 13, 1998).
307. A. P. Beltrami *et al.*, *N Engl J Med* **344**, 1750 (Jun 7, 2001).
308. J. Kajstura *et al.*, *Proc Natl Acad Sci U S A* **95**, 8801 (Jul 21, 1998).
309. F. Quaini *et al.*, *N Engl J Med* **346**, 5 (Jan 3, 2002).
310. D. J. Anderson, F. H. Gage, I. L. Weissman, *Nat Med* **7**, 393 (Apr, 2001).
311. D. Orlic *et al.*, *Nature* **410**, 701 (Apr 5, 2001).
312. C. Toma, M. F. Pittenger, K. S. Cahill, B. J. Byrne, P. D. Kessler, *Circulation* **105**, 93 (Jan 1, 2002).
313. C. E. Murry *et al.*, *Nature* **428**, 664 (Apr 8, 2004).
314. P. Seale, M. A. Rudnicki, *Dev Biol* **218**, 115 (Feb 15, 2000).
315. B. Leobon *et al.*, *Proc Natl Acad Sci U S A* **100**, 7808 (Jun 24, 2003).
316. A. P. Beltrami *et al.*, *Cell* **114**, 763 (Sep 19, 2003).
317. H. Oh *et al.*, *Proc Natl Acad Sci U S A* **100**, 12313 (Oct 14, 2003).
318. J. Yamaguchi *et al.*, *Circulation* **107**, 1322 (Mar 11, 2003).
319. J. S. Forrester, M. J. Price, R. R. Makkar, *Circulation* **108**, 1139 (Sep 2, 2003).
320. B. E. Strauer, M. Brehm, T. Zeus, H. W. Muller, P. Wernet, *Med Klin (Munich)* **98 Suppl 2**, 14 (Dec 15, 2003).
321. A. Subramaniam *et al.*, *J Biol Chem* **266**, 24613 (Dec 25, 1991).
322. A. Musaro, K. J. McCullagh, F. J. Naya, E. N. Olson, N. Rosenthal, *Nature* **400**, 581 (Aug 5, 1999).
323. C. Rommel *et al.*, *Nat Cell Biol* **3**, 1009 (Nov, 2001).
324. N. Pullen *et al.*, *Science* **279**, 707 (Jan 30, 1998).

325. G. Ren, O. Dewald, N. G. Frangogiannis, *Curr Drug Targets Inflamm Allergy* **2**, 242 (Sep, 2003).
326. B. Nadal-Ginard, J. Kajstura, P. Anversa, A. Leri, *J Clin Invest* **111**, 1457 (May, 2003).
327. B. Nadal-Ginard, J. Kajstura, A. Leri, P. Anversa, *Circ Res* **92**, 139 (Feb 7, 2003).
328. S. Kim, H. Iwao, *Jpn J Pharmacol* **80**, 97 (Jun, 1999).
329. H. E. Morgan, K. M. Baker, *Circulation* **83**, 13 (Jan, 1991).
330. D. Zechner, D. J. Thuerauf, D. S. Hanford, P. M. McDonough, C. C. Glembotski, *J Cell Biol* **139**, 115 (Oct 6, 1997).
331. S. Kim *et al.*, *Biochem Biophys Res Commun* **236**, 199 (Jul 9, 1997).
332. S. Oldham, E. Hafen, *Trends Cell Biol* **13**, 79 (Feb, 2003).
333. A. F. Shamji, P. Nghiem, S. L. Schreiber, *Mol Cell* **12**, 271 (Aug, 2003).
334. J. B. Harris, M. J. Cullen, *Electron Microsc Rev* **3**, 183 (1990).
335. C. Rajnoch *et al.*, *J Thorac Cardiovasc Surg* **121**, 871 (May, 2001).
336. P. Anversa, B. Nadal-Ginard, *Nature* **415**, 240 (Jan 10, 2002).
337. Y. Jiang *et al.*, *Nature* **418**, 41 (Jul 4, 2002).